PUBLICATIONS OF THE ASTRONOMICAL INSTITUTE OF
THE UNIVERSITY OF AMSTERDAM

No. 7

A. PANNEKOEK

INVESTIGATIONS ON DARK NEBULAE

AMSTERDAM — STADSDRUKKERIJ — 1942

TABLE OF CONTENTS.

I. THE EFFECT OF ABSORBING NEBULÆ.

Introduction.

After the dark patches seen in the Milky Way and shown still more distinctly on photographs of the galactic regions were recognised as dark nebulous matter absorbing the light of the stars behind, various attempts have been made to determine their distance and their opacity. The first and simplest method consists in counting the number of stars of different magnitude in the dark parts, and in comparing it with the number of such stars in adjacent brighter or normal parts of the sky.

DYSON and MELOTTE, delineating (1919) the dark patches in Taurus by means of star counts on the Franklin Adams maps, made an estimate of the distance in their conclusion : "Taking the area as a whole we find the number of stars is about one fifth of the normal number, whether we go down to magnitudes 9.0, 11.0, or 14.0. This would seem to indicate that if the small density is caused by absorbing matter, the screen cannot be at a great distance, say, not more than 200 or 300 parsecs at most". [1])

The present author, by means of the density function and the luminosity curve of KAPTEYN, computed (1920) the theoretical decrease of the number of stars of different magnitudes for different suppositions on distance and opacity of the absorbing screen. In comparing it with the decrease found from counts of stars in the *Bonner Durchmusterung*, the *Carte du Ciel* catalogues and the Franklin-Adams data, the distance of the Taurus nebula was derived to be 140 parsecs, probably between the limits 100 and 200 parsecs. [2])

In some papers (1923-25) MAX WOLF, [3]) who during many years already had studied the dark and bright nebulae by means of star densities on his photographs, gave the results of star counts for a large range of magnitudes in some special regions. He introduced there the lucid method of graphical representation — since then often applied by other investigators and denoted as Wolf-curves — of plotting log $A(m)$, the number of stars per square degree between magnitudes $m \pm 0.5$, (or log $N(m)$, the number of stars down to magn. m) against m, both for the obscured and for a normal adjacent region. The inspection of such a graph shows at once at what magnitude the curves begin to deviate, hence the dark nebula begins to make itself perceptible; how far the deviation goes on increasing, and what is the amount of absorption where for the faintest magnitude-classes the curves are at last parallel and all the stars are situated behind the screen. Thus, for the obscured region near 52 Cygni the curves suddenly begin to deviate at 11^m and reach their constant difference at 12.5^m ; for the dark region about ξ Cygni the effect begins at 9^m and has not yet reached its full amount at 16^m.

WOLF concludes that in the first case the absorbing cloud begins at the mean distance of the 11^m stars and reaches the mean distance of the 12.5^m stars ; and in the second case the nebula, beginning at the 9^m distance, extends to such a large distance that its end is not yet

[1]) Monthly Notices R. A. S. **80**, p. 6.
[2]) Proceedings Amsterdam Academy **23**, p. 707.
[3]) Astron. Nachrichten **219**, 109. **223**, 89, **229**, 1.

reached with the stars of the 16. magnitude. Several critics have since pointed out that it is not correct to derive a large radial extension of the cloud from the large difference between the magnitudes, for which the deviation begins and for which it reaches its full amount. Owing to the large dispersion in distance for the stars of each magnitude class, a consequence of the large dispersion of the stars in absolute magnitude, such a difference must also occur in the case of an absorbing screen of limited radial extension. This method of expressing the results, by the mean distances of very diverging magnitude classes, followed by many later investigators, cannot be said to be in keeping with the care bestowed upon their observational work. The dispersion mentioned, it is true, does not allow a very great precision in the derivation of the distance; and it causes two different clouds situated behind one another to merge in their effects so that they cannot be separated.

To avoid this drawback C. SCHALÉN [1]) made use of the spectra of the stars. For stars of a single spectral class (especially the bright early stars, the B and A classes) the dispersion in absolute magnitude is much smaller than for the totality of the stars. Hence the determination of distance is much sharper by means of such stars, and absorbing nebulae behind one another can now be separated. SCHALÉN applied this method to the study of the dark matter in different parts of the Northern galactic belt. It is restricted, however, in its application because, with moderate instruments, the photographing of spectra is limited to the brighter magnitudes.

Fainter magnitudes can be reached if colour indices are used as a sufficient indication of spectral class. The use of colour indices, however, has led, owing to the high precision of measurements with the photoelectric cell, to a much more accurate method of determination of the distance of absorbing nebulae, by combining them with the knowledge of the spectra. Recent investigations on the nature of the absorbing matter concord in attributing to it a dependence of absorption on wavelength, which seems to be the same everywhere in space. Hence the reddening of a distant star by this matter, measured by its excess of colour over the normal colour of its spectral class, has a fixed proportion to the total absorption. The value of the colour excess, derived from colour index measurement combined with the classification of the spectrum, directly gives the total absorption and the real distance of the star. This method has been applied bij STEBBINS and HUFFER to the B stars of the galactic belt [2]), and by BOK in his study on Galactic Density gradients [3]). If the stars are situated in a small area their arrangement according to distance will show the distribution of the absorbing matter along the line of sight; in this way W. BECKER could determine the distance of the dark nebulae in some of KAPTEYN's Selected Areas [4]).

So the problem of finding the distance of dark nebulae may be considered as fundamentally solved by this method. It involves, however, for each single small region, a great amount of work, exact measurement of colour index as well as spectral classification of all the stars. Moreover, by the necessity of having spectra, it is restricted to a much brighter limit of magnitude than can be used in the simple counting of the number of stars. So B. J. BOK and his coworkers of the Harvard Observatory are certainly right when they say that the old and less refined method of star counts still retains its importance and must be used for the bulk of the stars.

In the present paper only this method will be considered. We will try to examine the method of treating such starcounts somewhat more closely, and apply it to some published star counts.

---

[1]) K. Svensk. Vet. ak., Handl. III S. **6.** No. 6 (Medd. Upsala 37) 1928.
[2]) Aph. Journal **91,** p. 26 (1940).
[3]) Aph. Journal **90,** p. 249 (1939.
[4]) Zschr. f. Astrophysik **17,** p. 285 (1938).

Computations of the number of stars.

For a correct interpretation of the empirical results of the star counts it is necessary to treat first the inverse problem of deriving the number of stars theoretically as a function of magnitude, in the case of absorption by dark matter. In this computation the following assumptions are made :

1. The stars are distributed over a large range of absolute magnitudes, according to some luminosity curve such as derived by KAPTEYN or VAN RHIJN. This is no arbitrary or uncertain assumption ; we know that the bulk of the stars everywhere around us are subject to this wide dispersion. We are not sure, certainly, that the distribution function is the same everywhere in space ; but such differences will produce only minor differences in the effects of obscuration, mostly unimportant as compared to the uncertainties of the observational data of the counts. There is an uncertainty in the ends of the luminosity curve, especially in the number of extreme dwarfs ; but it has hardly any effect on the number of stars derived. Deviating spatial densities, by the smoothing effect of the dispersion in luminosity, also give only small deviations in the absorption effects. The combination of an excess of a special luminosity at one special distance, e.g. a local accumulation of a group of bright stars, would give a perceptible irregularity in the curves. Such a case will then be detected just by its deviation from the normal course.

2. The absorbing nebula has a limited radial extension. When the existence of local dark clouds was first revealed, this assumption was self-evident. Since we cannot admit a radial, conical structure of the dark matter around our sun as centre, the radial extension of the clouds must be comparable to their lateral extension ; in the case of such large dark regions as extending over 30°, this amounts to only $\pm$ 0.25 times their distance. Since the discovery of the general absorption in a galactic layer this argument has lost somewhat of its immediate obviousness. If we may consider the general absorption as the sum total of all the local absorbing clouds, or, conversely, the local dark nebulae as the most strongly condensed part of a general veil which, absent in some parts of space, is more densely spread in other parts, then each special cloud may be said in some way to extend over large distances radially. We may, however, approximate this structure in its total effect by a continuous smaller density with, superimposed upon it, denser local clouds. For these clouds the argument still holds that with a limited lateral they must have a limited radial extension ; so the former treatment may still be used here.

In practical computation this roundish mass may, of course, be replaced by an absorbing screen of negligible thickness, at the distance of its centre, in consequence of the large dispersion of the luminosity function.

The formulas for the number of stars of a certain magnitude, normally without absorption as well as changed by absorption, have been treated by different authors emphasizing different sides of the problem. We repeat them here in short for a general survey.

The un obscured number of stars $A(m)$ per square degree between magnitudes $m \pm 0.5$ is given by

$$A(m) = C \int_{-\infty}^{+\infty} D(\varrho)\ \Phi(M)\ 10^{0.6\varrho}\ d\varrho$$

where $\varrho = 5 \log r$, M is the absolute magnitude (at 1 parsec) $= m - \varrho$, $\Phi(M)$ is the luminosity function, $D(\varrho)$ is the density (number of stars per cubic parsec) taken 1 near to the sun, $10^{0.6\varrho}$ is the volume between $\varrho \pm 0.5$, $C = 0.2/(57.3^2 \times 0.43)$. Putting for these functions regular Gaussian probability functions :

$$\log\ \Phi(M)\ = \text{Const.} - {}^1/\alpha^2\ (M - M_0)^2\ ;\ \log\ D\ (\varrho) = \text{Const.} - {}^1/\beta^2\ (\varrho - \varrho_0)^2$$

we have

$$A(m) = \text{Const.} \int_{-\infty}^{+\infty} 10^{-1/\beta^2\,(\varrho-\varrho_0)^2 - 1/\alpha^2\,(m-\varrho-M_0)^2 + 0.6\varrho}$$

$$= \text{Const.}\ 10^{-1/\gamma^2\,(m-\varrho_0-M_0-0.3\beta^2)^2} \int_{-\infty}^{+\infty} 10^{-\gamma^2/\alpha^2\beta^2\,(\varrho-\varrho_m)^2}\, d\varrho$$

where $\gamma^2 = \alpha^2 + \beta^2$; $\varrho_m = \beta^2/\gamma^2\ m - M_0 + \alpha^2/\gamma^2\ m_0$. So we find

$$\log A(m) = \text{Const.} - 1/\gamma^2\ (m - m_0)^2 \text{ with } m_0 = \varrho_0 + M_0 + 0.3\beta^2.$$

In the case of a screen at distance ϱ_1 absorbing ε magnitudes the stars of magnitude m behind the screen will be dimmed to magnitude $m + \varepsilon$. In their stead the stars of normal magnitude $m - \varepsilon$ behind the screen will now appear and be counted as m-magnitude stars. Then the number of stars $A^1(m)$ of magnitude m will be :

$$A^1(m) = C \int_{-\infty}^{\varrho_1} D(\varrho)\ \Phi(m-\varrho)\ 10^{0.6\varrho}\, d\varrho + C \int_{\varrho_1}^{\infty} D(\varrho)\ \Phi\,(m-\varrho-\varepsilon)\ 10^{0.6\varrho} d\varrho,$$

which by the substitutions

$$x_1 = \frac{\gamma}{\alpha\beta}\,\varrho_1 - \frac{\beta}{\alpha\gamma}\,(m - M_0) - \frac{\alpha}{\beta\gamma}\,(m_0 - M_0)$$

$$x_2 = \frac{\gamma}{\alpha\beta}\,\varrho_1 - \frac{\beta}{\alpha\gamma}\,(m - \varepsilon - M_0) - \frac{\alpha}{\beta\gamma}\,(m_0 - M_0) = x_1 + \frac{\beta}{\alpha\gamma}\,\varepsilon$$

$$\frac{1}{\sqrt{0.43\pi}} \int_{-\infty}^{x_1} 10^{-t^2}\, dt = F_1\ ;\ \frac{1}{\sqrt{0.43\pi}} \int_{x_2}^{\infty} 10^{-t^2}\, dt = F_2$$

takes the form

$$A^1(m) = F_1\, A(m) + F_2\, A(m - \varepsilon).$$

The number of stars of magnitude m in an obscured region consists of two parts, first the stars before the screen being the fraction F_1 of the normal number, secondly the stars behind the screen, being the fraction F_2 (less than $1 - F_1$) of the normal number of the brighter magnitude $m - \varepsilon$.

For the galactic equator and the Kapteyn-Van Rhijn luminosity curve we have $M_0 = 2.7$, $\varrho_0 = 10.4$, $m_0 = 25.7$, $\alpha^2 = 29$, $\beta^2 = 42$, $\gamma^2 = 71$, hence $\gamma/\alpha\beta = 0.241$, $\beta/\alpha\gamma = 0.142$, $\alpha/\beta\gamma = 0.099$; $x_1 = 0.241\varrho_1 - 0.142m - 1.894$, $x_2 = x_1 + 0.142\varepsilon$.

Methods of practical computation.

Two different ways can be followed in the practical computation. The first is by making use of the analytical expressions, as shown above. Then results may be derived for arbitrary small and large values of the absorption ε as well as for arbitrary values of m. It is, however, bound to the validity of the Gaussian functions, or other analogous, analytically integrable functions. Corrections are needed in any case, because a Gaussian function for the density $D(\varrho)$ implies a decrease of the density to zero for $r = 0$, whereas in reality the density must be taken constant for the surroundings of the sun, say to $r = 100$ parsecs.

In the other, the numerical method, the conical space covering one square degree is divided into a number of space cells each extending one unit in the modulus of distance ϱ. For each cell the number of stars of magnitude m is found by multiplying volume and density $CD(\varrho)\ 10^{0.6\varrho}$ by $\Phi(m-\varrho)$, m, ϱ and M always varying by steps of one unit; $\log C = 0.147 - 4$.

By writing the logarithms of the two factors on two vertical slips of paper and sliding them along one another, the products are easily written down. These tables of the numbers of stars of each magnitude class in each space cell form the basis of all further computations. The sum total of all values belonging to m gives $A(m)$. For the case of an absorbing screen on the border between two cells, say at $\varrho = 13.5$, we have to add all the cell values from below to $\varrho = 13$ incl. from the table for m and the values from $\varrho = 14$ upward from the table for $m - \varepsilon$. Figure 1 illustrates the procedure, showing the distribution of the magnitude classes 9—14 over the distances, in such a way that the number of stars in each cell is given by the surface between its limiting ordinates.

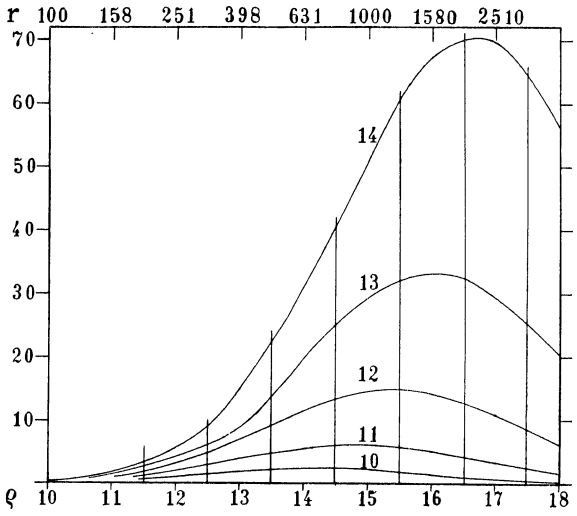

Fig. 1. Distribution of magnitude classes.

In this method of numerical summation we are not bound to any regular analytical function. For $D(\varrho)$, values constant below a certain distance and then decreasing in some way, may be used, and also for the luminosity curve empirical data deviating from a Gaussian curve may be assumed. These advantages and the easy practicability of the method of numerical summation have been emphasized by Bok and applied in his studies of the structure of the galactic system. Of course we are now bound to special distances for the absorbing screen, at the limits between the cells, entire numbers + 0.5 for ϱ_1, and to entire numbers of magnitudes for the absorption ε. As a rule this will be sufficient for interpolation purposes.

Table 1. Density and luminosity curve adopted.

ϱ	$\log CD(\varrho)\,10^{0.6\varrho}$	M	log Φ vis.	v. Rhijn	log Φ phgr.	c
20	6.040	— 10	2.298		2.513	(— 0.26)
19	5.850	— 9	3.139	(3.64)	3.274	— .26
18	5.616	— 8	3.912	(4.25)	3.974	— .20
17	5.338	— 7	4.615	4.60	4.612	— .19
16	5.017	— 6	5.249	5.05	5.186	— .13
15	4.655	— 5	5.815	5.58	5.694	+ .16
14	4.251	— 4	6.311	6.19	6.134	+ .35
13	3.796	— 3	6.738	6.71	6.506	+ .43
12	3.289	— 2	7.096	6.88	6.812	+ .40
11	2.730	— 1	7.386	7.13	7.054	+ .58
10	2.148	0	7.606	7.35	7.238	+ .80
9	1.550	+ 1	7.757	7.61	7.378	+ 1.00
8	0.950	+ 2	7.840	7.53	7.480	+ 1.14
7	0.350	+ 3	7.853	7.40	7.556	+ 1.26
6	9.750	+ 4	7.797	7.39	7.615	+ 1.34
5	9.150	+ 5	7.673	7.55	7.663	+ 1.47
4	8.550	+ 6	7.479	7.61	7.704	(+ 1.6)
		+ 7	7.216	7.71	7.744	(+ 1.7)
		+ 8	6.884	7.95	7.784	(+ 1.7)

The computations were made first by making use of the luminosity curve for visual magnitudes, given by KAPTEYN and VAN RHIJN 1917 [1]) and conforming to the Gaussian formula $\log \Phi = -2.934 + 0.1858\, M - 0.0345\, M^2$. Afterwards, in view of the many starcounts by photographic magnitudes the computations were repeated with a luminosity curve for photographic magnitudes. Its basis was the curve deduced by VAN RHIJN 1925 [2]), which was smoothed to remove the irregularities and get a continuous course. In Table 1. the data for the curves are given as they have been used. The density was taken as given in Publ. Amsterdam 1, in Table 4 p. 14, for galactic latitude 5°. The third decimal in these tables has no real meaning; it is added only to have a control in the smooth course of the results.

Table 2. Number of stars (vis.).

The table gives the logarithmic deficiency of stars log $A(m)$ — log $A^1(m)$ in 0.001.

m	log $A(m)$	9.5	10.5	11.5	12.5	13.5	14.5	15.5	16.5	17.5	9.5	10.5	11.5	12.5	13.5	14.5	15.5	16.5	17.5
		$\varepsilon = 1^m$									$\varepsilon = 3^m$								
5	8.722	329	225	133	069	027	009	003	001										
6	9.273	399	299	194	107	049	018	006	001										
7	804	448	364	259	157	080	034	012	003		866	597	373	206	099	041	014		
8	0.312	479	412	320	214	121	058	023	008		1069	779	514	304	158	071	028	009	
9	795	468	435	369	272	170	090	041	015	005	1236	967	676	424	237	117	050	018	
10	1.251	451	436	395	320	221	131	066	027	009	1327	1127	847	565	337	181	085	034	011
11	681	429	423	403	353	271	178	100	047	018	1332	1219	1004	722	461	266	137	061	023
12	2.083	402	401	392	366	307	225	141	074	033	1281	1239	1110	873	602	373	207	101	042
13	458	375	375	373	361	327	264	184	109	054	1207	1197	1143	990	746	499	299	159	073
14	807	349	349	349	345	330	290	225	149	083	1127	1126	1112	1041	869	635	411	237	120
15	3.128	321	322	322	322	317	297	253	187	117	1046	1047	1046	1024	937	757	535	333	184
16	423	295	295	296	296	296	289	265	218	153	965	966	968	966	938	837	654	446	267
17	691	268	268	269	269	270	269	261	233	184	885	885	887	889	890	851	704	558	366
		$\varepsilon = 2^m$									$\varepsilon = 4^m$								
6	9.273	602	410	247	129	057	021	006											
7	804	745	543	351	198	096	043	014	004		898	609	377	208	099	041	014	004	001
8	0.312	853	674	470	287	152	069	027	009		1044	807	524	307	159	072	028	009	003
9	795	908	781	591	390	224	113	049	018	005	1399	1031	699	432	239	118	050	018	005
10	1.251	910	832	694	499	312	171	082	033	011	1516	1264	898	583	343	182	085	034	011
11	681	879	848	761	602	412	247	130	058	022	1735	1475	1115	761	474	270	138	061	023
12	2.083	831	821	781	676	510	335	193	096	040	1734	1602	1317	959	631	383	210	102	042
13	458	778	776	762	709	590	428	270	148	070	1660	1617	1458	1155	811	521	306	161	074
14	807	724	724	722	702	637	511	356	215	112	1558	1550	1493	1306	998	685	428	243	122
15	3.128	670	670	671	667	640	565	436	291	168	1449	1450	1439	1365	1156	859	573	347	188
16	423	617	617	618	619	616	580	496	368	235	1341	1343	1345	1330	1237	1017	735	476	278
17	691	563	563	564	566	567	559	519	429	305	1233	1234	1239	1239	1219	1111	888	622	390

Table 2 gives the results for the visual and Table 3 for the photographic magnitudes. They contain log $A(m)$ for normal regions, and for the case of absorption, instead of log $A^1(m)$ itself the logarithmic deficiency of stars log $A(m)$ — log $A^1(m)$. The computations have been made for distances of the absorbing screen $\varrho_1 = 9.5, 10.5 \ldots\ldots 17.5$, corresponding to $r = 79, 126, 200, 316, 501, 794, 1260, 2000, 3160$ parsecs, and for an absorption of 1, 2, 3 and 4 magnitudes.

[1]) Astrophysical Journal **52**. 300.

[2]) Publ. Groningen **38**, p. 74 (Table 71).

Table 3. Number of stars (photogr.).

The table gives the logarithmic deficiency of stars log $A(m)$ — log $A^1(m)$ in 0.001.

m	log $A(m)$	9.5	10.5	11.5	12.5	13.5	14.5	15.5	16.5	17.5	9.5	10.5	11.5	12.5	13.5	14.5	15.5	16.5	17.5
		$\varepsilon = 1^m$									$\varepsilon = 3^m$								
4	8.099	315	215	128	065	027	009	003	001										
5	.650	385	285	184	102	047	015	006	001										
6	9.183	437	351	247	149	076	033	012	003	001	824	565	353	196	095	040	014	004	001
7	.694	463	401	309	204	115	055	022	007	002	1021	739	487	287	150	068	026	009	002
8	0.180	466	429	359	260	162	085	038	014	004	1196	923	643	401	224	110	047	017	005
9	.642	454	435	390	310	212	124	062	026	009	1295	1083	807	535	319	169	079	032	010
10	1.077	432	423	399	344	260	169	093	043	016	1316	1188	960	683	435	248	126	055	020
11	.487	408	405	394	362	299	215	133	070	031	1282	1220	1071	830	568	349	192	093	039
12	.869	382	381	376	360	321	255	174	102	050	1219	1193	1115	944	703	466	276	146	067
13	2.225	356	355	353	347	326	281	213	139	076	1146	1137	1102	1004	820	590	378	216	108
14	.555	330	330	329	326	315	289	241	175	107	1068	1064	1051	1002	888	700	488	302	165
15	.861	306	306	305	304	299	285	255	204	141	992	991	985	965	904	776	593	400	239
16	3.141	280	280	280	280	278	271	254	220	169	916	916	913	905	878	805	670	495	322
17	.397	256	256	256	256	255	251	243	223	186	842	842	842	838	824	787	705	570	406
		$\varepsilon = 2^m$									$\varepsilon = 4^m$								
5	8.650	574	388	235	123	055	021	006	002										
6	9.183	715	517	333	188	092	039	014	004	001	852	575	357	197	096	040	014	004	001
7	.694	828	646	447	271	144	066	026	009	002	1084	764	496	290	151	068	027	010	002
8	0.180	894	757	567	370	207	106	046	016	005	1334	978	663	408	226	111	047	017	006
9	.642	905	822	671	477	296	161	076	031	010	1543	1199	851	551	324	171	080	032	010
10	1.077	880	840	742	577	391	231	120	053	020	1674	1399	1053	717	447	252	127	056	020
11	.487	839	822	770	655	487	316	180	089	038	1705	1533	1242	900	593	358	195	094	039
12	.869	790	783	760	694	567	404	251	136	063	1659	1577	1382	1079	757	484	283	148	067
13	2.225	738	735	726	694	615	483	331	197	102	1577	1544	1440	1222	924	630	393	221	110
14	.555	686	685	681	667	625	537	405	267	151	1474	1462	1419	1292	1061	780	520	314	169
15	.861	636	636	634	628	608	557	462	336	211	1374	1370	1353	1292	1146	913	655	424	247
16	3.141	586	586	585	583	574	548	489	392	273	1273	1271	1264	1239	1165	1004	778	543	341
17	.397	536	536	536	535	531	519	486	422	325	1172	1172	1171	1160	1122	1031	867	654	442

The Wolf-curves.

By means of log $A^1(m)$, easily derived from the values in Tables 2 and 3, theoretical Wolf-curves have been drawn. Figure 2 gives these curves after Table 2, for visual magnitudes, first for $\varepsilon = 1$ and $\varepsilon = 2$, and for alternate distance values $\varrho_1 = 9.5$ 11.5 13.5 15.5 17.5, and then, at the right hand side, for $\varepsilon = 3$ for all the distances; Fig. 3 gives them for photographic magnitudes. These figures, as well as the table values, may be used to study the general character and the properties of the curves.

We see that the log $A^1(m)$ curves for the brighter magnitudes gradually deviate from the log $A(m)$ curve; a beginning of the deviation can, of course, not be indicated. No more than a magnitude can be ascertained where at last the curves become parallel and the obscured curve merges into the ε magn. displaced normal curve. The increase of deviation extends over a large range of magnitudes, larger than is usually assumed after the results of star counts over small areas. If we assume 0.1 and 0.9 ε to be the limits of the discernible change, the range is still more than 5 magnitudes.

The gradient of the log $A^1(m)$ curves has an irregular course. For small absorption ($\varepsilon = 1$)

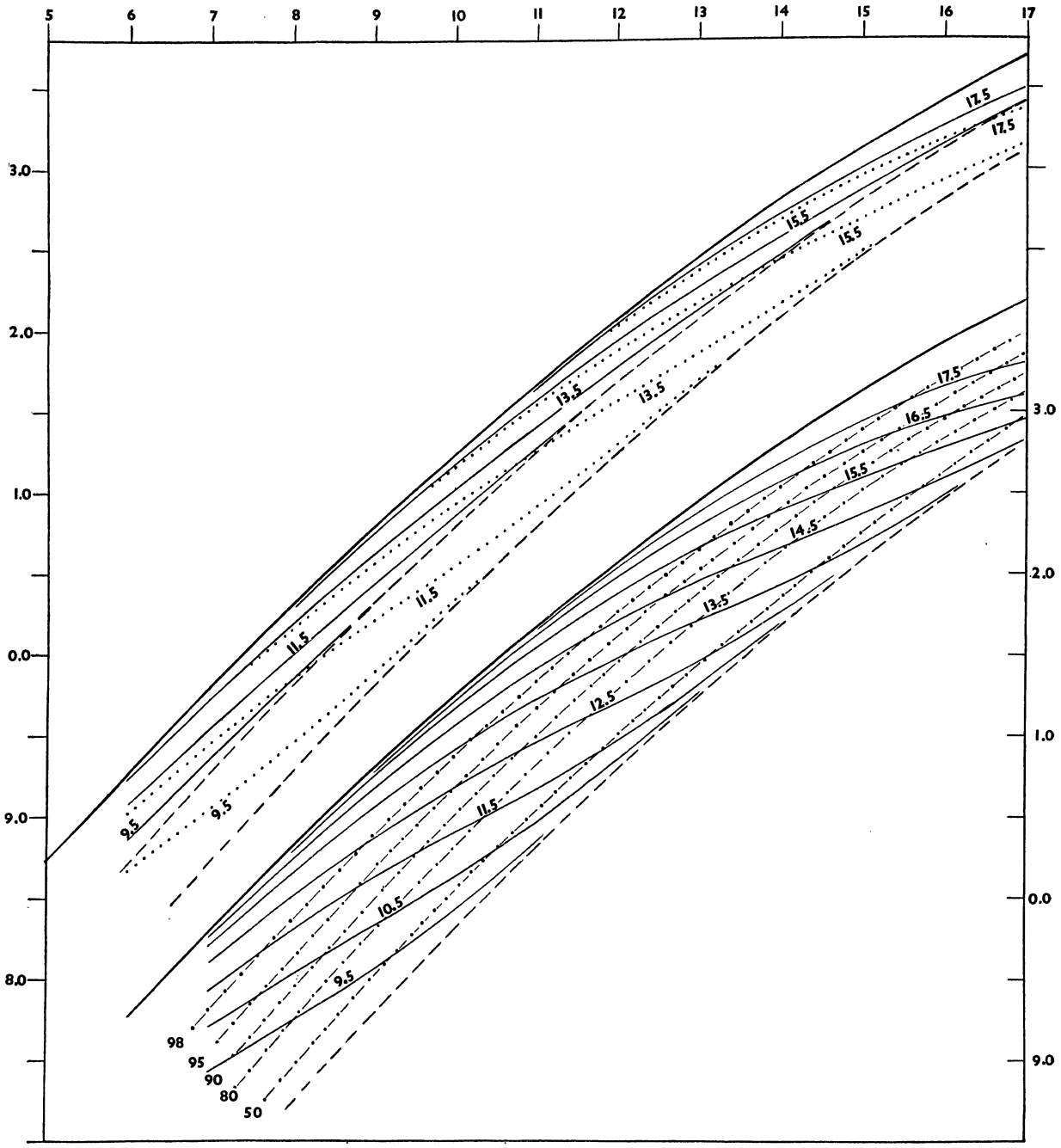

Fig. 2. Theoretcial Wolf-curves (vis. magn.) for absorption 1^m, 2^m, 3^m.

it decreases steadily, as the gradient of log A(m), but with a retardation and an acceleration; for stronger absorption the decrease is interrupted by a wave. After the slow and steady change, where the curves deviate only slightly, the gradient begins to decrease rapidly, reaches a minimum,

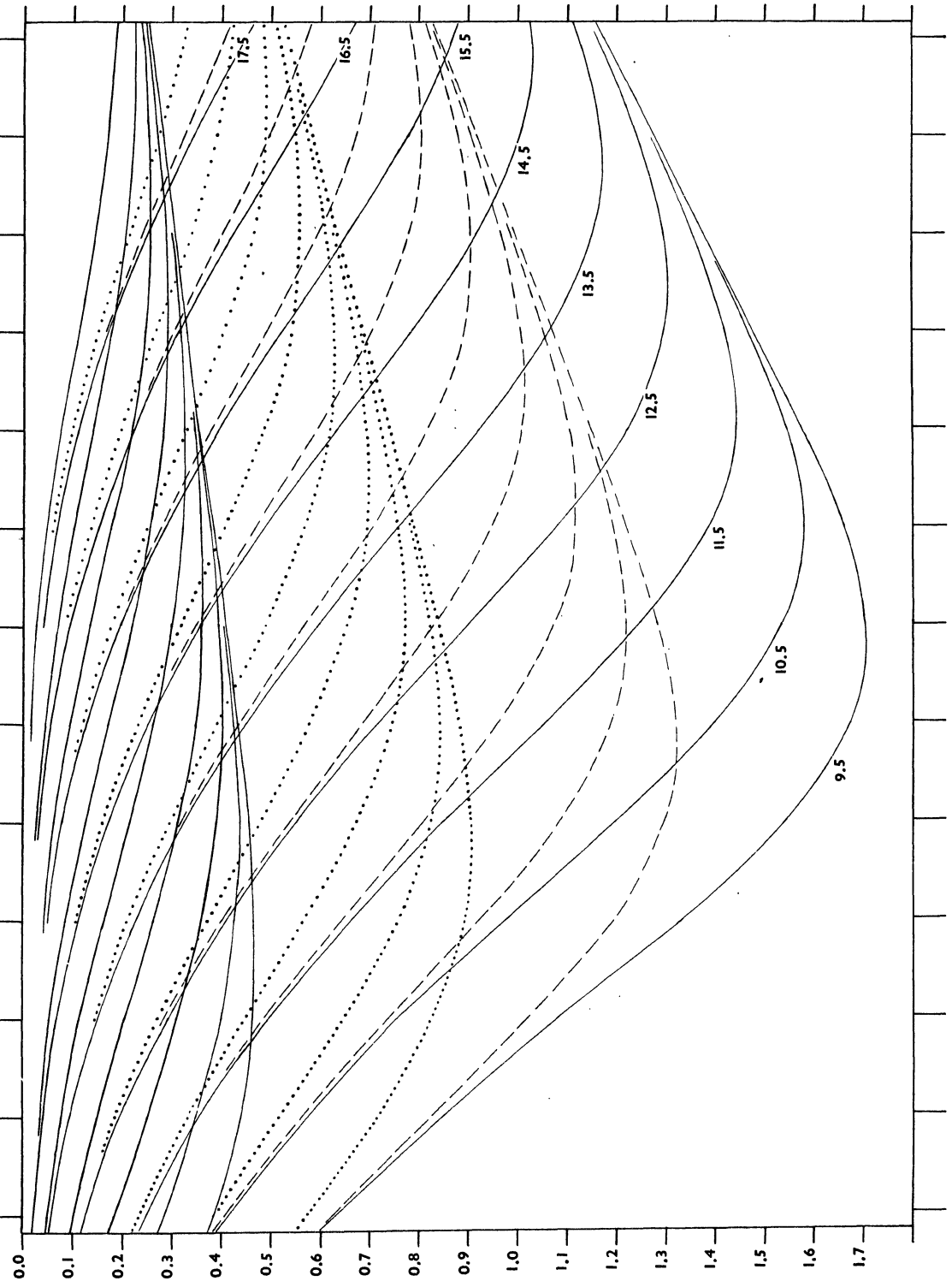

Fig. 3. Deviations Δ log A (vis. magn.) for absorption 1^m, 2^m, 3^m, 4^m.

increases, and has a maximum shortly before the curve merges into the parallel log $A(m - \varepsilon)$ curve, with which the gradient further on slowly decreases.

The effect of absorption can be more clearly seen in graphs of Δ log A, the logarithmic deficiency. In Fig. 4 they are represented for photographic magnitudes.

Sometimes the beginning of the deviation of the curves is spoken of as a partial dimming of the stars. So it is worth while remarking that the first decrease of the number of stars is entirely due to the removal of stars of magnitude m behind the screen; their diminished number consists

Table 4. Percentage of foreground stars.

m	9.5	10.5	11.5	12.5	13.5	14.5	15.5	16.5	17.5	9.5	10.5	11.5	12.5	13.5	14.5	15.5	16.5	17.5
	$\varepsilon = 1^m$									$\varepsilon = 3^m$								
5	69	83	92	97	99	100												
6	52	72	86	95	98	99	100											
7	35	57	76	89	96	98	100			91	97	99	100					
8	20	40	62	81	92	97	99			80	92	97	99	100				
9	10	24	46	69	85	94	98	99		59	82	94	98	99	100			
10	5	13	30	54	75	89	96	98	100	34	64	85	95	98	100			
11	2	6	17	38	62	81	92	97	99	14	39	70	89	96	99	100		
12	1	3	9	24	46	69	85	94	98	5	19	47	76	91	97	99	100	
13	0	1	4	13	31	54	75	89	96	1	7	24	55	81	93	98	99	100
14		0	2	6	18	38	62	80	91	0	2	10	32	63	85	95	98	99
15			1	3	10	24	46	68	85		1	3	14	40	70	88	96	99
16				1	6	13	31	54	74			1	5	20	48	75	91	97
17				0	2	7	18	38	61			0	2	8	26	55	80	93
	$\varepsilon = 2^m$									$\varepsilon = 4^m$								
6	84	93	97	99	100													
7	69	85	94	98	99	100				98	99	100						
8	48	72	88	95	98	99	100			95	98	100						
9	28	54	77	89	97	99	100			85	96	99	100					
10	13	32	60	82	93	97	99	100		66	88	96	99	100				
11	5	17	40	67	86	95	98	99	100	37	70	90	97	99	100			
12	2	7	22	48	74	89	96	99	100	14	43	75	92	98	99	100		
13	1	3	10	29	57	79	92	97	99	4	18	50	80	94	98	99	100	
14	0	1	4	14	37	64	83	93	98	1	6	24	58	85	95	99	100	
15		0	1	6	20	45	70	87	95	0	2	9	31	67	88	97	99	100
16			0	2	9	26	52	76	90		0	2	12	39	72	90	97	99
17				1	4	13	33	59	80			1	4	17	47	81	92	98

entirely of foreground stars. Only when the decrease in number has gone very far already do the dimmed stars behind the screen begin to occur in larger numbers. In Table 4 the percentage of foreground stars is given for the cases corresponding to Table 2. As an illustration in Fig 2 for one case ($\varepsilon = 3$) the points of all the log $A^1(m)$ curves for which 98, 95, 90, 80 and 50 percent are foreground stars, are connected by special curves. They show how the removing of the background stars is the dominant feature for the larger part of the curves. This is important in the discussion of mean values or properties in obscured regions ; we might be inclined wrongly to ascribe to the physical effect of absorption what is chiefly an effect of selection and singling out of nearby foreground stars out of the normal totality.

In the Wolf curves attention is mainly directed to the horizontal deviation between the curves, because it tends to a constant final value equal to ε. For other points of the curves we

can, for different log A(m), compute their horizontal distances from the normal curve by a somewhat laborious process of interpolation from Table 2. For the case of $\varepsilon = 3$ Table 5 gives as the result of this computation, for a number of values of log $A(m_0)$ = log $A^1(m)$ the normal m_0 and the differences $\Delta m = m - m_0$. In representing these Δm as a function of log A or of m it appears

Table 5. Horizontal distance of the Wolf-curves $\Delta m = m - m_0$, for $\varepsilon = 3^m$.

log A	m_0	9.5	10.5	11.5	12.5	13.5	14.5	15.5	16.5	17.5
8.95	5.40	1.63								
9.15	5.77	1.92								
9.35	6.14	2.20	1.27							
9.55	6.51	2.46	1.54	0.79						
9.75	6.89	2.64	1.83	.96	0.46	0.20	0.08			
9.95	7.28	2.78	2.13	1.17	.57	.25	.10	0.03		
0.15	7.67	2.87	2.40	1.43	.69	.31	.13	.05		
0.35	8.07	2.93	2.61	1.72	.86	.39	.17	.06	0.02	
0.55	8.48	2.96	2.76	2.05	1.06	.49	.21	.08	.03	
0.75	8.90	2.98	2.86	2.35	1.31	.62	.27	.10	.04	
0.95	9.33	2.99	2.93	2.59	1.63	.77	.35	.14	.05	
1.15	9.77	3.00	2.96	2.76	1.98	.97	.44	.19	.07	
1.35	10.22		2.98	2.87	2.32	1.25	.57	.24	.10	0.03
1.55	10.68		3.00	2.94	2.60	1.59	.75	.33	.13	.05
1.75	11.16			2.97	2.78	2.00	.98	.44	.18	.07
1.95	11.65			2.99	2.89	2.39	1.30	.58	.24	.09
2.15	12.17					2.67	1.71	.79	.34	.13
2.35	12.70						2.19	1.08	.47	.19
2.55	13.25						2.58	1.50	.66	.27
2.75	13.82						2.83	2.05	.95	.40
2.95	14.43							2.55	1.39	.58
3.15	15.06								2.03	.89

that for all the distances ϱ_1 the curves are nearly parallel and only displaced ; solely the extreme cases are somewhat deviating in form, 16.5 and 17.5 being somewhat steeper, 9.5 and 10.5 somewhat flatter. Practically they can be represented by the same curve ; for smaller ε the differences are hardly perceptible. The shape of this curve characterizes the Wolf curves ; it differs for different amounts of absorption. It is represented by the small tables 6 and 7. Table 6 gives the unobscured magnitude m_0 for which the horizontal distance of the curves is equal to $^1/_2\ \varepsilon$:

$$\log A(m_0) = \log A^1(m_0 + 0.5\,\varepsilon).$$

Table 6. Argument for horizontal distance. Value of m_0 for which $\Delta m = 0.5\ \varepsilon$.

ϱ_1	r	$\varepsilon = 1$	$\varepsilon = 2$	$\varepsilon = 3$
9.5	79	3.9	4.8	5.4
10.5	126	5.2	6.0	6.6
11.5	200	6.6	7.3	7.9
12.5	316	8.0	8.7	9.3
13.5	501	9.5	10.2	10.7
14.5	794	11.0	11.6	12.0
15.5	1260	12.5	13.0	13.3
16.5	2000	13.9	14.3	14.5
17.5	3160	15.3	15.6	15.8

Table 7. Differences in m_0 for Δm other fractions of ε.

Δm	$\varepsilon = 1$	$\varepsilon = 2$	$\varepsilon = 3$
0.1ε	— 3.4	— 3.0	— 2.7
0.2ε	— 2.1	— 1.9	— 1.5
0.3ε	— 1.3	— 1.1	— 0.9
0.4ε	— 0.6	— 0.5	— 0.4
0.5ε	0.0	0.0	0.0
0.6ε	+ 0.6	+ 0.4	+ 0.3
0.7ε	+ 1.2	+ 0.9	+ 0.6
0.8ε	+ 1.9	+ 1.4	+ 1.0
0.9ε	+ 2.9	+ 2.0	+ 1.7

Table 7 gives the change of m_0, if in this equation for 0.5ε we substitute 0.1ε, 0.2ε .... 0.9ε. These tables may serve to utilize the Wolf curves, constructed from starcounts, for a direct computation of distance and opacity of the absorbing nebula. First the final constant horizontal distance ε is ascertained. Then in the deviating part of the curves some values of the horizontal distance are measured and expressed in fractions of ε. Then for the reading of their termini on the normal curve m_0 the tables give ϱ_1, the modulus of distance. In different parts of the galactic belt, especially for different latitudes, in consequence of the different normal densities the log A corresponding to a certain Δm will be different, but the relation between Δm and m_0 is changed only by minor amounts.

It may be remarked that it is inappropriate in this case to speak of an absorption of 0.5ε or another fractional amount of magnitudes. For the final parallel parts of the curves the expression is right; two points at equal height represent the same stars, in one case undimmed, in the other case obscured by the nebula and displaced in the diagram ε magnitudes to the right hand side. But for points on the diverging part of the curves this is not true. The equality of the numbers $A(m_0) = A^1(m_0 + {}^1/_2\,\varepsilon)$ is a result of entirely dropping the m_0 stars — partly cut off, transferred to a ε magn. fainter apparent magnitude and replaced by a smaller number of obscured stars, hence reduced in number — and looking among a fainter more numerous class till we find there a number equal to the original $A(m_0)$.

Combined and composite effects.

The above mentioned tables of the numbers of stars of each magnitude in each space cell may be used to investigate the combined effect of two absorbing nebulae at different distances. Table 8 gives the values of log $A(m)$ — log $A^1(m)$ for the case of two absorbing screens, first each absorbing 1^m and sitated one at $\varrho_1 = 10.5$, the other at $\varrho_2 = 11.5$ .... 17.5; and then each absorbing 2^m at the same distances. These computations have been made for photographic magnitudes only, hence must be compared with Table 3. Since an absorbing screen at one distance, say $\varrho_1 = 10.5$ may be considered as a nebulous cloud filling an entire space cell from $\varrho_1 = 10$

Table 8. Two absorbing nebulae, log $A(m)$ — $A^1(m)$ in 0.001.

m	$\varepsilon_1 = \varepsilon_2 = 1^m$							$\varepsilon_1 = \varepsilon_2 = 2^m$						
	10.5 11.5	10.5 12.5	10.5 13.5	10.5 14.5	10.5 15.5	10.5 16.5	10.5 17.5	10.5 11.5	10.5 12.5	10.5 13.5	10.5 14.5	10.5 15.5	10.5 16.5	10.5 17.5
5	349	319	299	290	286	285								
6	463	415	382	363	355	352	351	554	536	525	519	517		
7	580	513	460	427	410	404	402	726	692	668	655	649	647	
8	686	603	528	477	449	436	431	916	855	807	778	764	759	757
9	762	675	585	514	472	448	439	1107	1008	925	871	842	829	824
10	798	723	629	544	484	449	432	1283	1144	1020	931	880	855	844
11	798	745	662	572	497	448	422	1417	1256	1096	973	894	851	832
12	772	740	679	595	513	450	411	1491	1339	1161	1009	901	836	803
13	731	715	676	610	530	457	405	1494	1382	1218	1049	914	824	773
14	683	676	655	610	543	468	406	1439	1374	1249	1087	935	821	748
15	635	632	621	595	547	480	413	1360	1329	1250	1118	966	833	737
16	585	584	579	565	536	484	421	1268	1253	1212	1122	992	853	738
17	537	536	534	528	511	477	425	1172	1166	1146	1094	1000	873	748

to 11, the first of each of these cases represents an absorbing cloud extending over a larger distance in the line of sight (here from $r = 100$ to 250).

The results are represented in the usual form of Wolf-curves in Fig. 4. We see that now the divergence of the curves is slower and extends over a larger range of magnitudes. This still

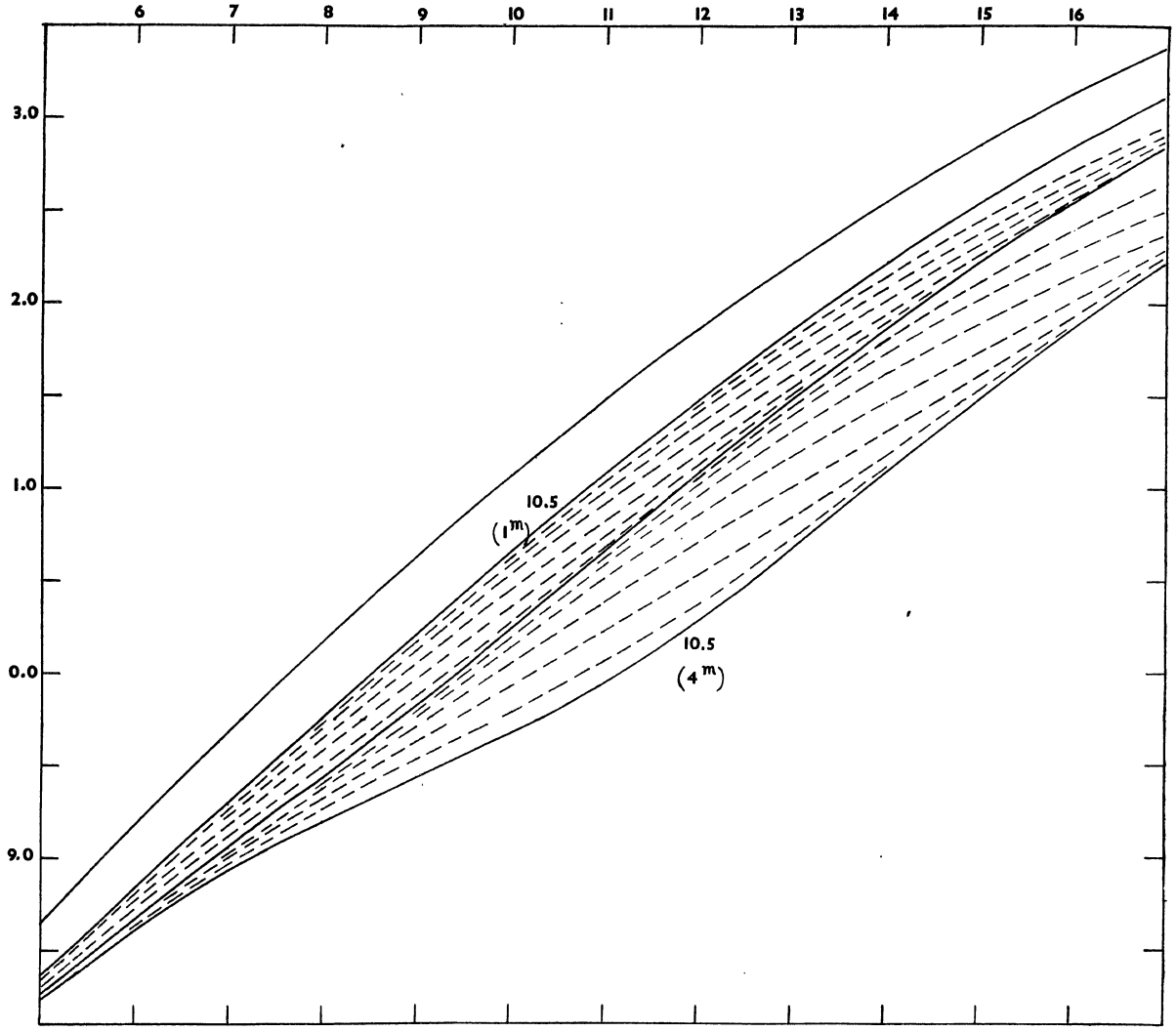

Fig. 4. Wolf-curves for two absorbing nebulae.

holds when the screens are more widely separated; even with 10.5 and 14.5 (126 and 793 parsecs) we see the divergence increase continuously and rather regularly from the 5th to the 17th magnitude. A double hump in the curve, such as was sometimes drawn in graphs of starcounts and considered as a clear indication of two clouds one behind the other, can hardly be detected here. Only with still greater separation a direct indication of a double origin can be seen in the form of a double wave in the log $A^1(m)$ curve. This irregularity presents itself more clearly if, instead of log $A^1(m)$, we represent the differences log $A(m)$ — log $A^1(m)$ as given in the table;

then we get rid of the original curvature of the log A curve. They are represented for the same cases in Fig. 5. Now the double origin of the deficiency of stars is already visible as a trace of a double wave in the case of 10.5 and 14.5. For smaller separation of the screens their combined presence must be concluded, if the data of the star counts are sufficiently reliable, from the slower increase of the logarithmic deficiency.

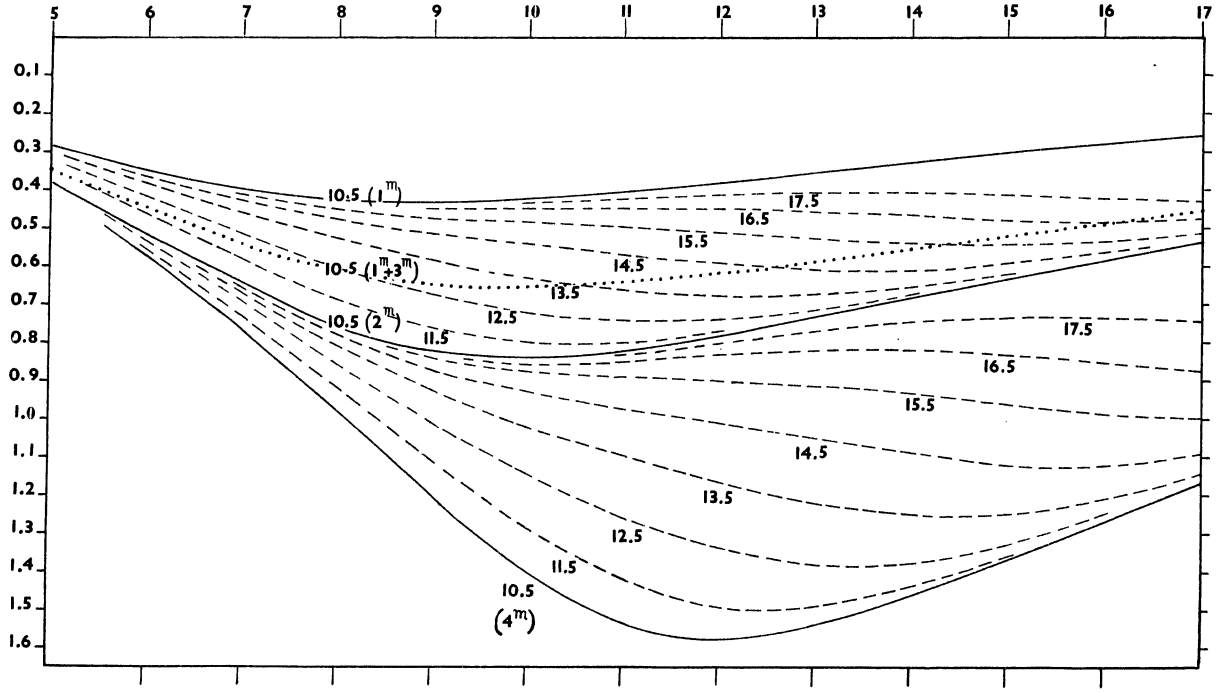

Fig. 5. Δ log A for two absorbing nebulae.

So far we have considered well detached absorption screens, which over a large area weaken the stars behind them by a constant definite amount. In reality we have seldom to do with this ideal case, because the density of the dark matter varies rather rapidly from place to place. Though as a rule observers try to delineate and separate the darkest patches carefully and keep and treat the half obscured parts separately, still it can never be entirely avoided that each dark region contains a mixture of different degrees of absorption. By inspection of photographs of the Milky Way we find many regions where rather dense masses of stars are furrowed by a large number of dark streaks (e.g. the surroundings of 58 Ophiuchi) or a complicated network of patches, so that in the mean they may appear as half obscured areas.

The effect on the number of stars in such a case is different from that of homogeneous absorption. For a mixture of two different degrees of absorption ε the effect can easily be computed, by averaging the numbers $A^1(m)$ with weights proportional to the surface occupied by each. Since the logarithm of the mean is larger than the mean of the logarithms, the logarithmic deficiency is smaller than corresponds to a homogeneous absorption by the average ε, the more so the more the separate values are different. Where for bright magnitudes the effect of absorption begins to appear, the composite effect is nearly equal to that of the average absorption coefficient. For larger deficiencies, however, it is smaller and increases more slowly than in the

case of homogeneous absorption. As an instance the effect was computed for half the area having $\varepsilon = 1$, half having $\varepsilon = 3$; the results for 4 different distances are given in Table 9, and for one of them ($\varrho_1 = 10.5$) a dotted line in Fig. 5 shows the course of the variation.

Table 9. Logarithmic deficiency for composite fields ($\varepsilon = 1^m$ and 3^m).

	10.5	12.5	14.5	16.5
5	344	114	020	002
6	445	172	036	004
7	538	243	061	008
8	610	325	097	014
9	648	409	146	029
10	656	482	207	049
11	644	536	277	081
12	620	560	347	123
13	590	561	408	176
14	557	544	448	234
15	525	519	465	291
16	491	488	461	336
17	457	456	442	362

Assuming a random fluctuation of the absorption coefficient ε around a mean value, with a standard deviation σ, then putting for a certain m the ratio $d \log A^1(m)/d\varepsilon = g$, the standard deviation in the logarithmic deficiencies for m in the separate parts will be $g\sigma$, and the systematic decrease of the result of $\log A(m) - \log A^1(m)$ will be $1.15\,(g\sigma)^2$.

Mean parallax and proper motion.

As an additional datum for studying the absorbing nebulae proper motions sometimes have been used. DYSON and MELOTTE in their paper on the Taurus nebulosity tried to find an increase of the mean proper motion in the darkened regions, but owing to the smallness of the motions and the small number of stars they failed to find any. In later years HIEMSTRA measured the proper motions in the dark parts of some of KAPTEYN's Special Selected Areas, giving a statistical discussion of the results.[1]) Our method of computation makes it easy to derive the change which an absorbing screen brings about in the mean parallax of the stars, hence also in their mean proper motion.

For a star at distance r the parallax $1/r = 10^{-0.2\varrho}$; it is assumed to be the same for all the stars of a space cell. For the stars of magnitude m, the mean parallax, then, is given, for the normal case, by

$$\bar{\pi} = 1/A^1(m) \int_{-\infty}^{+\infty} D(\varrho)\, \Phi(m - \varrho)\, 10^{0.4\varrho}\, d\varrho$$

and for an obscured region by

$$\bar{\pi} = 1/A^1(m) \left\{ \int_{-\infty}^{\varrho_1} D(\varrho)\, \Phi(m - \varrho)\, 10^{0.4\varrho}\, d\varrho + \int_{\varrho_1}^{\infty} D(\varrho)\, \Phi(m - \varrho - \varepsilon)\, 10^{0.4\varrho}\, d\varrho \right\},$$

the exponent 0.6ϱ in the integrals for the number of stars being replaced by 0.4ϱ.

[1]) Publ. Groningen, 48 (1938).

The results of the computations, made for photographic magnitudes, are contained in Table 10. First the logarithm of the mean parallax $\bar{\pi}$ for each magnitude in the normal case is given, followed by the logarithm of the ratio of the increased parallax in the obscured region to the normal one, log $\bar{\pi}^1/\bar{\pi}$. Reading the results for a certain m from the last column back to the first, we begin with the stars all unobscured, because the screen is behind them; then the screen is placed nearer and nearer, step by step, till at last all the stars are behind the screen. Then we see that at first the mean parallax is the normal; then increases because always more background stars are removed and only the foreground stars remain; when dimmed stars appear the mean parallax decreases, but not to the first value, because finally the stars, all of them obscured, belong to a brighter class and have the smaller mean distance and the larger mean parallax of that class.

Table 10. Increase of mean parallax log $\bar{\pi}^1$ — log $\bar{\pi}$ in 0.001.

		9.5	10.5	11.5	12.5	13.5	14.5	15.5	16.5	17.5	9.5	10.5	11.5	12.5	13.5	14.5	15.5	16.5	17.5
m	log $\bar{\pi}$	$\varepsilon = 1^m$									$\varepsilon = 3^m$								
5	8.024	247	204	143	085	041	016	005	001										
6	7.871	245	227	178	117	064	030	011	003										
7	729	221	227	202	149	092	047	020	006		591	466	333	213	120	058	023	008	
8	596	187	210	209	174	122	069	033	012	003	627	536	409	279	170	090	041	015	004
9	468	159	183	200	189	148	096	052	023	008	597	573	476	393	228	132	066	029	009
10	346	139	156	179	188	167	123	075	037	015	527	564	522	415	293	184	101	047	018
11	226	128	139	158	177	176	147	101	058	028	455	513	531	472	361	245	148	077	034
12	111	119	125	139	157	170	160	124	080	042	400	447	498	495	419	309	201	115	056
13	6.996	116	119	126	142	159	164	143	105	063	371	402	448	485	460	372	264	165	089
14	885	112	114	118	128	142	154	150	125	084	352	367	402	446	464	417	324	220	131
15	775	111	112	114	120	130	142	148	136	105	341	350	369	405	441	436	375	278	181
16	669	107	107	109	113	120	130	139	139	121	331	336	347	371	406	429	404	331	235
17	566	103	104	105	107	112	119	128	134	126	321	324	336	346	371	400	406	367	287
		$\varepsilon = 2^m$									$\varepsilon = 4^m$								
6	7.871	439	350	245	149	078	035	013	004										
7	7.729	451	397	303	201	115	056	023	008										
8	596	422	418	354	256	156	087	040	014	004	729	573	423	284	171	091	041	015	
9	468	364	398	380	306	211	126	064	028	009	770	657	508	360	232	134	067	029	009
10	346	310	354	376	341	261	169	097	046	018	753	710	588	440	302	187	102	048	018
11	226	274	308	346	353	303	221	138	074	034	679	711	649	521	378	252	150	078	034
12	111	250	271	307	337	332	264	182	107	053	590	657	670	589	457	321	206	117	056
13	6.996	237	248	272	307	325	297	229	150	084	529	588	640	628	532	401	274	168	093
14	885	230	235	249	276	304	307	264	194	119	487	524	583	619	580	474	347	229	134
15	775	223	227	235	252	277	297	283	231	159	465	486	528	579	592	531	419	296	188
16	669	218	220	224	235	254	276	283	257	198	451	461	486	530	572	559	480	366	250
17	566	210	211	214	221	234	253	267	264	226	434	441	464	486	525	549	516	427	314

For a definite distance of the screen the mean parallax in the obscured case still decreases with increasing m, but more irregularly than in the normal regions, being always larger, and most so when nearly 60 or 70 percent of the stars are foreground stars.

The same holds for the mean proper motion in obscured and normal regions, as well as for average values of one component of the proper motion, because they vary proportionally to the parallax. This effect has been perceived by HELMUT MÜLLER [1]) who in comparing the proper

[1]) Untersuchungen über absorbierende Wolken. Zschr. f. Astrophysik **2**, p. 285.

motions in obscured Taurus regions found them for 11^m stars larger, relative of normal regions, than for 13^m stars.

The mean colour.

The mean colour of the stars in dark regions has sometimes been determined, by measuring their photographic and photovisual magnitudes, in order to prove the existence of absorbing matter by means of its colouring effect. The existence of such absorbing matter can indeed be proved in this way, but not necessarily by that it colours the remoter stars. For without such a reddening property, the absorption must change the mean colour already by cutting off the most distant, *i. e.* the intrinsically brightest and whitest stars, while the redder dwarf stars before the screen remain. If the determination of the mean colour has to serve to find the reddening effect of the nebula, it has first to be corrected to eliminate this effect of selection.

To find the amount of this effect quantitatively, the results of VAN RHIJN and SCHWASSMANN for the luminosity curves for each spectral class were used [1]). For each of the main spectral classes they give the number of stars between $M \pm 0.5$ per cubic parsec in the surroundings of the sun. Thus for each class of absolute magnitude we know the spectral composition, the percentage of stars contributed by each of the spectral classes. Assuming the mean colour indices -0.3, $+0.1$, $+0.5$, $+0.9$, $+1.3$ and $+1.8$ for the B, A, F, G, K, M stars, we can compute the mean colour index for every luminosity class. The results are given in Table 1, in the last column headed c. They show a rather irregular course, a consequence of the rather irregular way in which, with decreasing luminosity, now this, then another spectrum jumps into prominence and then falls back. It was not deemed advisable to smooth the values into a more regular course, because we cannot maintain that these are not real irregularities.

The mean colour of all stars of magnitude m, in a normal region and in the case of an absorbing screen, is given by

$$\bar{c} = 1/A(m) \int_{-\infty}^{+\infty} D(\varrho)\, \Phi(M)\, c(M)\, 10^{0.6\varrho}\, d\varrho, \quad (M = m - \varrho), \text{ and}$$

$$\bar{c}^1 = 1/A^1(m) \left\{ \int_{-\infty}^{\varrho_1} D(\varrho)\, \Phi(M)\, c(M)\, 10^{0.6\varrho}\, d\varrho + \int_{\varrho_1}^{\infty} D(\varrho)\, \Phi(M-\varepsilon)\, c(M-\varepsilon)\, 10^{0.6\varrho}\, d\varrho \right\}.$$

The computation is easy if in the method used formerly for the number of stars, for the slip of paper with values $\Phi(M)$ we substitute a slip with values $\Phi(M)\, c(M)$. The results are given in the left hand part of Table 11., in such a form that for each magnitude first the normal mean colour is given, and then the increase of colour index for different distances of an absorbing screen.

Though of course there are now irregularities in the sequence of the values and their differences, a general behaviour is clearly shown. Looking along a horizontal line, i. e. considering a certain magnitude with the screen set first far away and then gradually nearer, we see the colour reddening by the removal of the white remote stars. Then, however, when the foreground stars diminish and are exhausted and all the stars are behind the screen, the mean colour decreases and falls below the original value, because now the stars belong to a brighter class, which has a lower mean colour. Looking along a vertical line, representing for a certain distance of the screen the colour as function of the magnitude, we see it for the brighter magnitudes rise above the normal curve and for the fainter magnitudes fall below it.

[1]) Zschr. f. Astrophysik, **10**, p. 174.

Table 11. Variation of mean colour index $\bar{c}^1 - \bar{c}$ in 0.01.

m	$\bar{c}$	By selection									Bij colouring								
		9.5	10.5	11.5	12.5	13.5	14.5	15.5	16.5	17.5	9.5	10.5	11.5	12.5	13.5	14.5	15.5	16.5	17.5
								$\varepsilon = 1m$											
6	0.01	+ 09	+ 11	+ 14	+ 09	+ 05	+ 02	+ 01	+ 00	+ 00	12	08	04	02	01	00			
7	.05	+ 01	08	10	13	08	04	02	01	00	15	11	07	04	02	01			
8	.10	— 00	02	09	10	12	07	03	01	00	18	15	10	06	03	01	00		
9	.15	03	+ 00	02	09	09	10	05	02	01	19	17	13	09	05	02	01	00	
10	.20	04	— 02	+ 01	03	09	09	08	04	02	19	18	16	12	07	04	02	01	
11	.25	05	04	— 01	03	04	04	08	07	03	20	19	18	15	10	06	03	01	00
12	.30	06	05	03	+ 00	05	04	08	06	05	20	20	19	17	13	08	04	02	01
13	.36	06	05	05	— 03	+ 02	06	05	08	05	20	20	19	18	16	11	07	03	01
14	.42	07	06	06	05	— 02	+ 03	07	05	06	20	20	20	19	17	14	10	06	03
15	.47	05	05	05	04	03	— 00	+ 05	08	05	20	20	20	19	18	16	13	08	04
16	.54	07	07	07	06	06	04	— 00	05	08	20	20	20	20	19	18	15	11	07
17	.60	— 06	— 06	— 06	— 06	— 06	— 05	— 02	+ 02	+ 07	20	20	20	20	19	19	17	13	09
								$\varepsilon = 2m$											
6	0.01	+ 26	+ 26	+ 22	+ 12	+ 06	+ 03	+ 01	00	00	11	05	02	01	00				
7	.05	15	25	23	17	10	05	02	+ 01	00	19	10	04	03	01				
8	.10	09	16	24	21	16	08	03	01	+ 01	27	17	08	04	01	00			
9	.15	+ 01	09	15	22	18	14	07	03	01	31	25	14	06	03	01	00		
10	.20	— 05	+ 03	11	15	20	15	11	05	02	37	32	22	12	05	02	01		
11	.25	08	— 03	+ 06	14	15	18	13	09	04	39	36	29	18	09	04	02	00	
12	.30	10	08	— 02	09	15	14	15	10	07	40	38	34	26	16	10	03	01	00
13	.36	11	10	07	+ 01	12	16	13	13	09	40	39	37	32	22	12	06	02	01
14	.42	12	12	11	— 06	+ 03	14	16	12	10	40	40	38	36	29	19	10	04	02
15	.47	12	12	11	09	— 03	+ 08	17	16	12	40	40	39	38	34	26	16	08	03
16	.54	12	12	12	11	08	— 01	09	17	15	40	40	40	39	36	31	22	13	06
17	.60	— 13	— 13	— 13	— 12	— 12	— 08	+ 00	+ 11	+ 18	40	40	40	39	38	35	28	20	11
								$\varepsilon = 3m$											
7	0.50	+ 31	+ 35	+ 28	+ 21	+ 11	+ 05	+ 02	+ 01	+ 00	11	04	01	01	00				
8	.10	32	31	34	24	17	09	04	02	00	22	09	04	01	01				
9	.15	17	30	28	29	21	15	07	03	01	35	19	08	02	01	00			
10	.20	+ 03	20	29	25	26	17	12	05	02	47	32	16	06	02	01	00		
11	.25	— 08	+ 06	22	29	23	22	15	10	04	55	44	28	12	04	02	01	00	
12	.30	14	— 06	+ 10	26	29	21	19	12	08	58	52	40	23	10	04	01	01	
13	.36	15	12	— 02	+ 16	29	27	18	16	10	59	57	50	35	18	07	02	01	00
14	.42	18	17	12	— 00	19	29	25	16	13	59	58	55	46	29	14	06	02	01
15	.47	18	17	15	08	+ 07	24	30	24	15	60	59	58	52	41	25	11	04	02
16	.54	19	18	17	14	— 06	+ 10	25	28	22	60	60	59	56	49	36	22	09	04
17	.60	— 19	— 19	— 18	— 16	— 13	— 04	+ 13	+ 26	+ 27	60	60	59	58	54	45	31	17	07
								$\varepsilon = 4m$											
8	0.10	+ 51	+ 39	+ 36	+ 25	+ 19	+ 09	+ 04	+ 02	+ 00	10	03	01	00					
9	.15	44	46	34	32	22	15	07	03	01	22	08	02	01	00				
10	.20	27	45	42	30	28	18	12	06	02	42	19	06	02	01	00			
11	.25	+ 03	30	43	39	27	24	15	10	04	60	37	15	05	02	01			
12	.30	— 14	+ 07	33	44	36	24	20	12	08	72	55	31	12	04	01	00		
13	.36	17	— 07	+ 14	38	42	33	21	17	10	77	69	49	25	10	03	01	00	
14	.42	24	20	— 07	18	39	41	30	18	14	78	75	64	42	20	07	02	01	00
15	.47	24	22	16	+ 01	28	41	39	28	16	79	78	73	58	35	15	06	02	01
16	.54	24	24	21	— 13	+ 08	30	39	36	25	80	79	77	69	52	30	12	04	02
17	.60	— 25	— 25	— 24	— 20	— 10	+ 10	+ 32	+ 38	+ 23	80	80	78	74	64	45	24	10	03

This is the mere effect of selection, without taking account of the physical reddening effect of the absorbing matter; hence applicable to the imagined case of gray absorption. To take the colouring of the background stars by the absorbing matter into account we have to increase for each of them its proper colour index by a constant amount. Since the absorption coefficient of interstellar matter has been found to be proportional to the inverse first power of the wavelength, the colour excess (as determined by λ 5500 and 4400) is one fifth of the photographic absorption coefficient. So the constant increase of colour index of the background stars is $0.2\ \varepsilon$, and the mean colour of all the stars is increased by $0.2\ \varepsilon \times$ the percentage of the stars $A^1(m)$ that is situated behind the screen. Table 11 in its right hand part gives this part of the colouring effect. Though a graphical representation shows irregularities it is seen that now for all magnitudes we have an increase of colour; for the brighter magnitudes it is an effect of selection by screening, for the fainter classes of colouring by absorption.

II. DISCUSSION OF STAR COUNTS.

Comparison tables.

The amount of labour spent by different astronomers on star counting, using well standardized plates taken especially for this purpose and often based on accurate measurements of the magnitude of a great number of stars, makes it worth while to submit their results to a more exact discussion. Especially the vague and inaccurate indication that the absorption sets in at the mean distance of one and extends to the mean distance of another magnitude has to be replaced by a computation of the distance at which absorbing masses have to be placed to produce the observed deficiency of stars. It will be necessary, first, to construct some auxiliary tables.

The computations in the preceding section, made some years ago to establish general relations and effects, were based on the mean distribution of star density $D(\varrho, \beta)$ as given in *Amsterdam Public.* **1.** for the schematical universe, corresponding to the mean distribution of magnitudes $A(m, \beta)$ derived from *Groningen Publ.* **27,** For the fainter magnitude classes this shows an appreciable and increasing difference from the distribution given in *Groningen Publ.* **43,** which is based on the International Scale of magnitudes. Since all modern star counts are based on the same scale their results had to be compared with normal numbers taken from the latter source. So the values of log $N(m, \beta)$ of Table V, *Gron. Publ.* **43** were combined into zones of 5° width and smoothed, and from these the values of log $A(m, \beta)$ of Table 12 were derived. We cannot pretend, of course, that they represent the normal number of stars in the absence of any absorption. They represent averages taken over the entire zone of lalitude, including many absorption areas. Our knowledge of absorption effects is not yet sufficient to free stellar statistics from the effect of absorbing nebulae. We therefore have to compare the obscured regions with ,,normal'' distributions, which are themselves affected by a certain amount of absorption.

With these $A(m)$ the decrease of density with distance must be less than has been assumed in the preceding section, and the logarithmic deficiency due to single absorbing screens at certain distances must be larger. To compute the distribution of density corresponding to this $A(m)$ first quadratic exponential expressions were used for $D(\varrho)$ and $A(m)$, as well as for the smoothed photographic luminosity curve $\Phi(M)$ from Table 1. Corresponding to the greater straightness of log $A(m)$ a smaller curvature for log $D(\varrho)$ was found (i. e. smaller coefficients c and l in the expressions p. 4 of *Amsterdam Publ.* 1). The values of D between $\varrho = 10$ and 15 (density between 100 and 1000 parsecs) were depressed, above $\varrho = 15$ and below 10 they were enhanced, so that between 10 and 100 parsecs they far surpassed the value unity, which must be assumed for the surroundings of the sun. So a distribution had to be sought for, by trial and error, that left D unity in the central parts and that below 1000 parsecs had a smaller, and at a larger distance a greater density than in the former solutions. It was unavoidable that the resulting log $D(\varrho)$ curve, represented by Table 13, showed rather sudden changes in curvature. Even so a complete adaptation to the observed $A(m)$, as shown by a comparison of Tables 12 and 13, could not be reached. The computations were made for two galactic latitudes, 5° and 15°.

From these data the absorption effects were derived by the same numerical method (with

Table 12. Normal log $A(m)$ (photogr. magn.)

m	0°—5°	5°—10°	10°—15°	15°—20°	m	0°—5°	5°—10°	10°—15°	15°—20°
5.0	8.75	8.66	8.57	8.51	5.5	8.97	8.89	8.79	8.73
6.0	9.20	9.11	9.02	8.95	6.5	9.43	9.34	9.24	9.17
7.0	9.66	9.57	9.46	9.39	7.5	9.88	9.79	9.68	9.62
8.0	0.11	0.02	9.90	9.84	8.5	0.33	0.24	0.12	0.06
9.0	0.56	0.46	0.34	0.27	9.5	0.78	0.68	0.56	0.50
10.0	1.00	0.91	0.78	0.71	10.5	1.22	1.13	1.00	0.92
11.0	1.45	1.34	1.21	1.13	11.5	1.67	1.56	1.43	1.34
12.0	1.89	1.77	1.64	1.55	12.5	2.11	1.98	1.84	1.75
13.0	2.32	2.19	2.05	1.95	13.5	2.53	2.40	2.25	2.14
14.0	2.73	2.60	2.45	2.33	14.5	2.93	2.80	2.65	2.52
15.0	3.12	2.99	2.84	2.70	15.5	3.31	3.18	3.03	2.87
16.0	3.49	3.36	3.20	3.04	16.5	3.67	3.54	3.37	3.20
17.0	3.84	3.71	3.54	3.35	17.5	4.01	3.87	3.69	3.49
18.0	4.17	4.03	3.84	3.63					

Table 13. Density and Number of stars.

log $D(\varrho)$			log $A(m)$		
ϱ	$\beta = 5°$	$\beta = 15°$	m	$\beta = 5°$	$\beta = 15°$
7	0.00	0.00	3	7.50	7.46
8	00	00	4	8.06	8.00
9	00	9.97	5	8.60	8.52
10	9.98	.93	6	9.12	9.03
11	.94	.88	7	9.62	9.51
12	.85	.74	8	0.11	9.98
13	.72	.57	9	0.58	0.43
14	.57	.40	10	1.03	0.86
15	.40	.22	11	1.47	1.28
16	.25	.05	12	1.90	1.68
17	.09	8.87	13	2.31	2.06
18	8.91	.63	14	2.69	2.42
19	.67	.31	15	3.06	2.76
20	.36	7.93	16	3.40	3.06
21	7.98	.46	17	3.71	3.34
22	.52	6.90			
23	6.98	.24			

photographic log $\Phi(M)$ of Table 1) as those in the first section. They are given in Table 14, in two decimals, for absorption screens at distances ϱ_1, $= 9{,}5 \ldots . 15.5$ and magnitudes $m = 7$ to 17, which may cover the extent of most of these investigations.

Probability of numbers of stars.

The number of stars counted in a field for a certain magnitude does not coincide, generally, with the number that should be present according to computation under the assumed values of distance and absorption of the nebula. In order to judge whether the deviations may be due to chance and whether the values assumed may be considered probable, Von der Pahlen has given a method

Table 14. Logarithmic deficiency Δ log A in 0.01 for $\beta = 5°$ and 15°.

ϱ_1	ε	$m = 7$		8		9		10		11		12		13		14		15		16		17	
9.5	1	45	42	46	44	46	44	45	43	44	42	42	40	41	38	39	36	36	34	34	31	31	28
	2	79	72	87	81	90	85	91	86	89	84	86	82	83	78	80	74	75	70	70	64	65	58
	3	96	87	104	105	127	118	134	125	134	127	131	124	127	120	122	114	116	108	109	100	101	92
	4	101	92	126	115	150	138	167	155	176	164	175	166	172	162	166	156	159	148	150	138	140	128
	∞	103	94	131	119	162	148	195	169	232	212	264	245										
10.5	1	38	34	42	39	44	41	44	42	44	41	42	40	41	38	39	36	36	34	34	31	31	28
	2	60	53	72	65	81	75	86	80	87	82	86	81	83	78	80	74	75	69	70	64	65	58
	3	68	60	87	77	105	95	120	110	127	118	128	120	126	119	122	114	116	108	109	100	101	92
	4	70	62	92	81	115	103	139	126	157	144	166	155	168	158	164	154	158	147	150	138	140	128
	∞	71	62	93	82	119	106	149	134	181	163	213	194	247	226	281	257						
11.5	1	29	25	35	31	39	36	42	39	42	40	42	39	41	38	39	36	36	33	34	31	31	28
	2	41	35	53	46	66	59	76	69	82	76	83	78	82	77	79	74	75	69	70	64	65	58
	3	44	37	60	52	78	68	96	86	112	101	120	111	122	114	120	112	116	107	109	100	101	92
	4	45	38	62	53	82	72	105	93	127	114	145	133	157	145	160	149	156	145	149	137	140	127
	∞	„	„	„	„	83	72	108	95	136	121	165	149	196	177	228	208	263	236				
12.5	1	19	16	25	22	32	28	37	33	40	36	40	38	40	37	38	36	36	33	34	30	31	28
	2	25	21	36	30	48	42	60	54	71	64	77	71	79	74	78	72	75	69	70	64	65	58
	3	26	22	38	32	53	46	71	62	89	79	104	94	113	104	116	107	114	105	108	99	101	91
	4	26	22	39	33	54	47	74	65	96	85	118	106	137	124	148	136	151	139	147	135	139	126
	∞	„	„	„	„	55	47	75	66	98	87	124	111	153	138	184	165	213	192	241	218	267	231
13.5	1	11	09	17	14	23	20	29	26	34	31	38	34	38	35	38	35	36	33	34	30	31	28
	2	14	12	22	18	32	27	44	38	56	50	66	60	73	67	75	69	74	67	70	63	65	58
	3	15	12	23	19	34	29	48	42	65	58	82	74	98	88	107	98	110	100	106	97	100	90
	4	„	„	„	„	35	30	50	43	68	60	89	79	110	99	128	116	140	126	141	128	137	123
	∞	„	„	„	„	„	„	„	„	69	61	91	81	116	104	143	129	172	153	197	177	223	199
14.5	1	06	05	10	08	15	13	21	18	27	24	32	29	35	32	36	33	35	32	33	30	31	27
	2	07	06	12	10	19	16	29	25	40	35	52	46	62	56	68	62	70	63	68	61	64	57
	3	„	„	13	11	20	17	31	27	44	39	60	53	77	68	91	82	100	90	102	91	98	88
	4	„	„	„	„	20	18	32	27	46	40	63	55	82	73	102	91	119	106	129	115	131	116
	∞	„	„	„	„	„	„	„	„	„	„	64	56	84	75	108	96	133	118	157	139	181	160
15.5	1	03	02	05	04	09	07	14	12	19	17	25	22	30	26	33	29	34	30	32	29	30	27
	2	03	03	06	05	11	09	18	15	27	23	37	32	48	42	58	50	63	56	64	57	62	55
	3	04	03	07	05	11	09	18	16	28	25	41	35	56	48	71	62	84	73	92	80	93	82
	4	„	„	„	„	11	10	19	16	29	25	42	36	58	50	76	66	94	82	109	95	118	110
	∞	„	„	„	„	„	„	„	„	„	„	„	„	59	51	78	68	99	86	121	105	144	124
16.5	1	01	01	02	02	05	04	08	06	12	10	17	14	23	19	27	23	30	25	30	26	29	25
	2	01	01	03	02	06	04	10	08	16	13	24	19	34	28	43	36	52	44	57	48	58	50
	3	02	01	„	„	06	05	„	„	17	14	26	21	37	30	50	41	64	53	75	63	82	69
	4	„	„	„	„	„	„	„	„	„	„	„	„	38	31	52	43	68	56	84	70	97	81
	∞	„	„	„	„	„	„	„	„	„	„	„	„	„	„	53	44	70	58	88	73	108	90

of computation [1]) based on his former studies on the probability of star distributions, which has been applied by several astronomers in their researches on dark nebulae.[2]) From a large number n of such fields (usually an entire zone of the same galactic latitude) with, in total, N stars of this kind he computes the mean or most probable number of stars N/n that may be expected in this field. Then the comparison of the probability W of this mean number and the probability of the counted number of stars i is presented in such a form that instead of the probability itself he derives how many fields (t) with the one, and how many with the other number of stars must occur among the total number of fields in the zone. From these number of fields t certain quantities χ^2 and P may be derived which are a direct measure of the probability of this system of observed data. In the papers mentioned this computation of the total probability is omitted, probably owing to its greater complication, and only the values t are computed.

The probability that in a chance distribution of N stars over n fields there are i stars in a field is given by

$$W = \frac{N!}{i!\,(N-i)!}\left(\frac{1}{n}\right)^i (1 - 1/n)^{N-i}.$$

For N and n very large (which is always the case here, with some 1000 fields in a zone) this may be replaced by

$$W = \frac{1}{i!}\left(\frac{N}{n}\right)^i e^{-N/n},$$

where, besides the number counted, only the mean number N/n appears. It is easier, then, to discard this total number of fields, which is rather an arbitrary quantity, and to work only with the mean or expected number of stars $N/n = a$ and the observed number i. It is also more appropriate, to use the probabilities W themselves instead of the products $t = nW$, the probable number of fields. In this case we have

$$W = \frac{1}{i!}\, a^i\, e^{-a}.$$

This probability is maximum for $i = a$ (and $a - 1$). Dividing other values by this maximum we find the relative probability as a fraction of the maximum. For large a this relative probability approaches to a Gaussian distribution with a mean error $\sqrt{a}$

$$W_i/W_m = \frac{a!}{i!}\, a^{a-i} \sim e^{-(i-a)^2/2a}.$$

In the case of large a the treatment is the obvious, ordinary one. The deviations $i - a$ for a number of n cases are used to derive the mean error μ by $\mu^2 = \Sigma(i-a)^2/n$. If no other sources of error are present and if we have a purely chance distribution, we must find $\mu^2 = a$ or $\Sigma(i-a)^2/a = n$. If we call $((i-a)/\sqrt{a})^2 = E$, the relative error square, then the sum total of all relative error squares should be equal to the number of independent data (or as much less as there have been unknowns deduced from them).

Our case is different, inasmuch as we have not n data belonging to the same a, but n counts belonging to n different a. In one darkened field we have a counted number of stars for each magnitude; we represent them by a curve of a values, leaving differences $i-a$, each standing for another magnitude with another a. Then the same expression holds ; and the quantity

[1]) E. v. D. Pahlen, Astron. Nachr., **238**, 271 (1930). Lehrbuch der Stellarstatistik (1937), p. 128 *sqq*, p. 650.

[2]) R. Müller, Zs. f. Astroph. **3**, 265, **4**, 367 (1931—'32); H. von Klüber, ibidem **6**, 268 (1933); G. Hartwig. ibidem **17**, 224 (1938).

$$\frac{1}{n}\Sigma E = \frac{1}{n}\Sigma\frac{(i-a)^2}{a},$$

now with a different for each term, should be in the neighbourhood of unity. It will be superfluous, in this kind of investigation, to derive a value for the probability that a mean error, derived from this limited set of data, is found to be so and so much different from its *a priori* value (or that in this notation ΣE is found to be so and so much different from n). Every scientist will be able to judge of the character of a representation of data by theory and the presence of unknown systematic errors from the mere inspection of the quantities E and their sum total.

When a and i are small the Gaussian probability function cannot be used. The treatment of large a and i may be extended to this case by substituting for $(\imath-a)^2/a$ its equivalent for small values, *viz*

$$E = \frac{(\imath-a)^2}{a} = -2\ln(W_i/W_m).$$

For values of i and a below 10 this quantity may be taken from Table 15; i is always assumed to be entire, but a may be fractional. Though in E no more than one decimal is needed, the table gives two decimals for interpolation. By means of this table a counted number 0 may be included as a datum of observation.

When a and i are large the computations are better founded on the residuals in log A — because the entire discussion deals with log A —, instead of using $A \times$ surface of the area = the number of stars itself. The mean error μ_n in log A, corresponding to $\sqrt{a}$ in the number of stars, is found from

$$\mu_n = {}^1/_2 \log\frac{a+\sqrt{a}}{a-\sqrt{a}}.$$

Then, if A_{obs} and A_{cp} are the observed and computed values of A, and in the same way $\Delta \log A_{obs}$ and $\Delta \log A_{cp}$ are the observed and computed values of the logarithmic deficiency the former expression for ΣE may be replaced by

$$\Sigma E = \Sigma\left(\frac{\log A_{obs} - \log A_{cp}}{\mu_n}\right)^2 = \Sigma\left(\frac{\Delta \log A_{obs} - \Delta \log A_{cp}}{\mu_n}\right)^2.$$

The values of μ_n and $\mu_n{}^2$ as functions of a, the computed number of stars, are given by Table 16.

In graphs of log A^1 or Δ log A it is often useful to indicate its reliability by a vertical line through each point. When extending the line to an amount μ, the mean error, above and below the point, we may say that a curve adequately represents the data if for ${}^2/_3$ of the cases it cuts these lines, and for ${}^1/_3$ runs outside them. For large numbers of stars this mean error μ_n may be taken from Table 16 ; for small numbers it may be derived from Table 15. When the counted number is i it is not right to say that the mean uncertainty is $\sqrt{i}$. It is determined by such a value of a, the mean or expected number, that the observed value i is just the limit of the natural uncertainty of a. For large i and a the difference of $\sqrt{a}$ and $\sqrt{i}$ is unimportant. For small i and a we have to look into Table 15 for what values of a above and below i in each column E reaches the value 1. The results have been collected in the little Table 17. For $i = 0$ the limiting $a = 1.65$ $(= \sqrt{e})$, hence in a graph of log A the line extends from $-\infty$ to (0.22 — log surface), in a graph of Δ log A from $-\infty$ to (0.22 — log surf. — log A). In some of our graphs these lines are inserted.

In comparing the counted with the computed number of stars we have not to deal solely with the chance deviations in distribution. The errors of the magnitudes of the stars also play their part.

Table 15. Relative error square $E = 2\ln W_m/W$ for small numbers.

a \ i	0	1	2	3	4	5	6	7	8	9	10
0.1	0.00	4.61	10.60	17.40							
.2	0.	3.22	7.82	13.24							
.3	0.	2.41	6.20	10.81	15.99						
.4	0.	1.83	5.05	9.08	13.68						
.5	0.	1.39	4.16	7.74	11.90	16.50					
.6	0.	1.02	3.43	6.65	10.44	14.68					
.7	0.	0.71	2.81	5.72	9.21	13.14	17.44				
.8	0.	0.45	2.28	4.92	8.14	11.81	15.83				
.9	0.	0.21	1.81	4.22	7.20	10.63	14.42				
1.0	0.	0.00	1.39	3.58	6.36	9.57	13.16	17.05			
1.1	0.19	0.	1.20	3.20	5.78	8.81	12.21	15.91			
1.2	36	0.	1.02	2.85	5.26	8.12	11.34	14.86			
1.3	52	0.	0.86	2.53	4.78	7.48	10.54	13.90	17.54		
1.4	.67	0.	.71	2.24	4.34	6.88	9.79	13.01	16.50		
1.5	.81	0.	.58	1.96	3.92	6.33	9.10	12.19	15.53		
1.6	.94	0.	.45	1.70	3.54	5.81	8.46	11.41	14.63		
1.7	1.06	0.	.32	1.46	3.17	5.33	7.85	10.68	13.78	17.11	
1.8	1.18	0.	.21	1.23	2.83	4.87	7.28	10.00	12.98	16.20	
1.9	1.28	0.	.10	1.02	2.51	4.44	6.74	9.35	12.22	15.33	
2.0	1.39	0.	0.00	0.81	2.20	4.03	6.23	8.73	11.51	14.51	17.73
2.1	1.58	0.10	0.	.71	2.00	3.74	5.84	8.25	10.92	13.83	16.95
2.2	1.77	.19	0.	.62	1.82	3.46	5.46	7.78	10.36	13.18	16.21
2.3	1.95	.28	0.	.53	1.64	3.19	5.11	7.34	9.83	12.56	15.50
2.4	2.12	.36	0.	.45	1.47	2.94	4.77	6.91	9.32	11.96	14.82
2.5	2.28	.45	0.	.36	1.30	2.69	4.44	6.50	8.83	11.39	14.16
2.6	2.44	.52	0.	.29	1.15	2.46	4.13	6.11	8.36	10.84	13.53
2.7	2.59	.60	0.	.21	1.00	2.23	3.83	5.73	7.90	10.31	12.93
2.8	2.73	.67	0.	.14	0.85	2.01	3.53	5.37	7.47	9.80	12.35
2.9	2.87	.74	0.	.06	.71	1.80	3.25	5.02	7.05	9.31	11.79
3.0	3.01	.81	0.	0.00	.58	1.60	2.98	4.68	6.64	8.84	11.24
3.2	3.40	1.07	0.13	0.	.45	1.34	2.60	4.16	5.99	8.06	10.34
3.4	3.76	1.31	.25	0.	.32	1.10	2.23	3.68	5.39	7.33	9.49
3.6	4.10	1.54	.36	0.	.21	0.87	1.89	3.22	4.82	6.65	8.69
3.8	4.43	1.76	.47	0.	.10	.65	1.56	2.79	4.28	6.00	7.94
4.0	4.73	1.96	.58	0.	0.00	.45	1.26	2.38	3.76	5.38	7.22
4.2	5.12	2.25	.77	0.10	0.	.35	1.06	2.08	3.37	4.90	6.63
4.4	5.50	2.53	.96	.19	0.	.26	0.88	1.80	3.00	4.43	6.07
4.6	5.85	2.80	1.13	.28	0.	.17	.70	1.54	2.64	3.99	5.54
4.8	6.19	3.06	1.30	.36	0.	0.08	.53	1.28	2.30	3.56	5.03
5.0	6.52	3.30	1.47	.45	0.	0.	.36	1.04	1.98	3.15	4.54
5.5	7.47	4.06	2.04	.83	0.19	0.	.17	0.66	1.41	2.39	3.59
6.0	8.34	4.76	2.56	1.18	.36	0.	0.	.31	0.88	1.69	2.72
6.5	9.30	5.56	3.20	1.66	.68	0.16	0.	.15	.56	1.21	2.08
7.0	10.19	6.30	3.80	2.10	.98	.31	0.	0.	.27	0.77	1.48
7.5	11.16	7.13	4.48	2.65	1.40	.58	0.14	0.	.13	.49	1.07
8.0	12.06	7.90	5.13	3.17	1.78	.84	.27	0.	0.	.23	0.68
8.5	13.03	8.75	5.86	3.78	2.27	1.21	.51	0.12	0.	.11	.44
9.0	13.95	9.55	6.54	4.35	2.72	1.55	.74	.24	0.	0.	.21
9.5		10.42	7.30	5.00	3.27	1.98	1.06	.45	0.11	0.	.10
10.0		11.24	8.02	5.61	3.78	2.39	1.37	.66	.21	0.	0.

Table 16. Mean error in log A.
μ in 0.001 ; μ^2 in 0.0001.

a	μ	μ^2	a	μ	μ^2	a	μ	μ^2	a	μ	μ^2
4	239	569	20	99	98	100	44	19.0	500	19.5	3.8
5	209	437	22	94	88	110	42	17.3	600	17.7	3.1
6	188	354	24	90	81	120	40	15.8	700	16.4	2.7
7	173	299	26	86	74	130	38	14.5	800	15.4	2.4
8	160	257	28	83	69	140	37	13.5	900	14.5	2.1
9	150	226	30	80	64	150	35	12.5	1000	13.7	1.9
10	142	202	35	74	55	160	34	11.8	1500	11.2	1.3
11	135	182	40	69	48	170	33	11.1	2000	9.7	0.9
12	129	166	45	65	42	180	32	10.6	3000	7.9	0.6
13	124	154	50	62	38	190	32	10.0	4000	6.8	0.5
14	119	142	60	56	32	200	31	9.5	6000	5.6	0.3
15	115	132	70	52	27	250	28	7.6			
16	111	123	80	49	24	300	25	6.3			
17	107	115	90	46	21	350	23	5.4			
18	104	109	100	44	19	400	22	4.7			
19	101	103				450	20	4.2			
20	99	98				500	19	3.8			

Table 17. Limits of mean error in log A.

i	$-\mu$	$+\mu$
1	— 0.22	+ 0.50
2	— .22	+ .35
3	— .20	+ .28
4	— .17	+ .24
5	— .16	+ .22
6	— .15	+ .20
7	— .14	+ .18
8	— .13	+ .17
9	— .13	+ .16
10	— .12	+ .15

The influence of magnitude errors.

In comparing the counted with the computed number of stars we have not to deal solely with the chance deviations in distribution. The errors of the magnitudes of the stars also play their part. When the number of stars is small the magnitude errors are quite negligible beside the natural chance errors of distribution ; so the use of Table 15 remains unimpaired. When the number of stars is large, however, the distribution errors are very small and the magnitude errors are dominant. We can take them into account by computing their effect on log A ; the mean error μ_s in log A arising from this source is added to the μ_n, so that in the former expressions the denominater μ_n^2 must be replaced by $\mu_n^2 + \mu_s^2$.

These magnitude errors are of two kinds : systematic errors of the photometric scale, and accidental errors in the magnitudes of the separate stars. An error Δm in the scale produces an error $b\,\Delta m$ in log A, because log $A = a + bm$ for small ranges ($b = 0.5$ to 0.3 for normal fields, but may go outside these limits for darkened fields). If by μ_1 we denote the mean amount of systematic scale error, then a corresponding mean error $b\mu_1$ will occur in log A. Moreover the interval between two succeeding magnitude limits may be changed by a mean amount $\mu_1/\sqrt{2}$; the number of stars changes proportionally to the width of the interval, hence A varies by a factor $(1 + \mu_1/\sqrt{2})$, and log A changes by a mean amount of log $(1 + \mu_1/\sqrt{2}) = 0{,}60\ \mu_1$ (for not too large μ_1). The average contribution of these effects to the mean error square in the denominater of E may be put $\mu_s^2 = 0.50\ \mu_1^2$.

Accidental errors in the magnitudes of the stars, with the mean value μ_2, have the effect that at the limits of each interval stars are thrown across the border and are either lost or gained to this interval. Putting

$$\frac{1}{\sqrt{\pi}}\int_x^\infty e^{-z}\,dz = F(x),$$

$F\left(\frac{\Delta m}{\mu_2\sqrt{2}}\right)$ denotes the fraction of the stars of magnitude m, Δm different from the limit,

which are thrown across the border. From all the magnitudes m above the limit the total number of transgressions is

$$\int_0^\infty A(m)\, F\left(\frac{\Delta m}{\mu_1 \sqrt{2}}\right) d\,\Delta m.$$

If for $A(m)$ we take the value of A for the limit, which is allowed in this problem, the integral can be computed, and so the number is found to be $0.564\ \mu_2 \sqrt{2}\ A = 0.797\ \mu_2\ A(m)$. This is the number of one-sided transgressions of the limit according to theory, if they should follow the Gaussian formula exactly ; the four transgressions from and to this interval across two limits produce a systematic change in the number of stars, which is a second order effect, that is negligible in our case. The chance variations, however, of these transferred numbers of stars may be of interest ; their mean value is given by the square root of the transferred numbers $\sqrt{4 \times 0.797\ \mu_2\ A(m)} = \sqrt{3.19\ \mu_2\ A}$. This mean error is added to those from the other sources ; its effect on log A is given by the same kind of expressions as the chance error of distribution $\sqrt{A}$. So it can be accounted for by multiplying $\mu_n{}^2$ in the denominator by the factor $f = 1 + 3{,}19\ \mu_2$. So we have

$$\Sigma\, E = \Sigma \frac{(\Delta \log A_{obs} - \Delta \log A_{cp})^2}{f\,\mu_n{}^2 + \mu_s{}^2}.$$

The evaluation of these mean errors presents some dififculties. Two methods are used in starcounts. One consists in determining the individual magnitudes of all the stars by estimating them in a series of artificial star images (usually with steps of about 0.25^m), and then afterwards, after various reductions, counting in the catalogue the stars between definite limits of magnitude. The other consists in counting direct on the plate all the stars which are brighter than certain members of a comparison scale of artificial images. In both cases the comparison scale images are standardized by means of Selected Area or Polar Sequence exposures on the same plate. The first method is more laborious, but more accurate, while it may also yield data, in the form of mean errors, concerning the degree of accuracy reached. With the second method we may expect larger individual errors, but it admits of the inclusion of more and wider fields to be counted in the available time.

The mean error of one magnitude determination was found by Von Klüber to be 0.08^m (from estimates of the same standard stars at different times); by G. Hartwig to be 0.07^m (from partly overlapping plates, after systematic reductions), and by H. Müller, $0{,}10^m$; the latter, however, found larger differences, whose source could not be found, by comparing different plates, which leads him to think that the m.e. of one determination may reach 0.15^m. Doubtless accidental plate differences play an important role, so that the accuracy of magnitudes derived from one or a few plates is less than it may seem to be from the results of one plate. Thus, for magnitudes from a single plate μ_2 will not be less than $0{,}10^m$, perhaps larger, up to $0{,}15^m$, whereas for results based on more plates smaller errors, down to 0.07 or 0.06 may be assumed. This means values of 1.32 up to 1.48 in the first case, down to 1.20 in the second case, for the factor f.

By careful standardization of the magnitudes by means of Selected Areas and the Polar Sequence we may expect the mean scale errors μ_1 to be small. Yet Hartwig's graph of the comparison of Yerkes and Mt Wilson magnitudes in one of his standard fields shows differences increasing for fainter magnitudes to 0.1 and $0{,}2^m$. Moreover one of his plates shows a systematic difference of 0.25^m as compared to the other two plates, which difference, between 12.5 and 13.5 decreases to 0. H. Muller also finds unaccountable systematic plate differences, especially in their zero point, which sometimes run up to 0.10 and in one case even to 0.20^m. Thus, scale errors represented by $\mu_1 = 0.10$ may easily occur, or perhaps even larger ones, corresponding to $\mu_s{}^2 = 50$; only where the magnitudes rest on more plates may smaller values, such as $\mu_1 = 0.06$ and $\mu_s{}^2 = 20$, be assumed.

In the case where stars are counted directly on the plate we have some data by Mc CUSKEY, who found the m. e. of one scale magnitude determination to be 0.20^m, with systematic differences between the plates of 0.12^m. By comparison of counts on overlapping plates the m.e. in log $N(m)$ was found to be 0.05 for the faint, and up to 0.12 for the bright classes, corresponding to 0.15 to 0,36 in m ; the systematic and accidental counting errors were estimated at less than 0,07 in log N and 0.22 in m. Generally, therefore, the errors are here larger than with the other method ; by assuming $\mu_1 = 0.15$ and $\mu_2 = 0.20$ we have $f = 1.6$, $\mu_s^2 = 100$.

The Taurus-Auriga nebulae.

The regions of greatest absorption in Taurus, revealing themselves by a scarcity of stars on the Franklin Adams maps, were depicted in 1919 by DYSON and MELOTTE [1]). In the following year the present author [2]) derived the logarithmic deficiency of stars of different magnitude from different sources (*BDM*, Harvard Map, Carte du Ciel, Franklin Adams maps) for some fields, covering the darkest and less dark fields. Although the fixing of the limiting photometric magnitudes left considerable uncertainty it appeared that the derivation of the distance of the dark nebula depended almost exclusively on the brighter stars, i.e. those of the Bonner Durchmusterum. The stars below 11^m were situated almost completely behind the screen and showed little difference in absorption. For the distance $\varrho_1 = 10.7$ was found, or $r = 140$ parsecs.

H. VON KLÜBER [3]) has discussed counts of stars derived from magnitude determinations on a plate 6° square, that covers the densest parts of the nebulae. ($4^h\ 18^m + 28°$, $\beta = -12°$). Two poor fields and 3 other surrounding fields were treated separately ; by drawing Wolf curves they were found to run nearly parallel with the normal log A curve for that latitude and might well be represented by a constant absorption of 2.3^m for the darkest and $0.6 - 1.0^m$ for the surrounding fields.

Since the numbers counted are not themselves stated in the paper we had to recompute them from the values A^m (called N^m in the paper) and from the surfaces of the areas. Then we combined them into one strongly obscured and one less obscured area (A and B). The discussion is contained in Table 18; the comparison data are taken from Tables 12 and 14. For each of the different assumptions

Table 18. H. von Klüber, Taurus-field ($\beta = -14°$). *A*, dark field 6.92 sqd., *B*, surr. fields 9.50 sq.d.

m	Counted		log A^1		log A	Δ log A		Δ log A comp.				Number of stars Comp.				Deviations Obs.—Comp.				E			
	A	B	A	B		A	B	Aa	Ab	Ba	Bb												
8.0	0	4	—	9.61	9.90	—	— 29	53	34	33	24	1.6	2.5	3.6	4.5	—	—	+ 04	— 05	0.9	2.2	0.3	0
9.0	3	4	9.64	9.61	0.34	— 70	— 73	69	48	37	31	3.1	5.0	9.1	10.5	— 01	— 22	— 36	— 42	0	0.4	2.8	4.4
10.0	9	22	0.11	0.35	0.78	— 67	— 43	84	64	40	37	6.0	9.6	23	25	+ 17	— 03	— 03	— 06	1.7	0.0	0.1	0.2
11.0	13	80	0.30	0.91	1.21	— 91	— 30	96	81	40	41	12	17	63	62	+ 05	— 10	+ 10	+ 11	0.1	0.5	1.2	1.5
12.0	31	201	0.65	1.31	1.64	— 90	— 33	101	95	40	42	30	34	170	160	+ 11	+ 05	+ 07	+ 09	0.9	0.2	0.8	1.4
13.0	71	420	1.00	1.63	2.05	— 105	— 42	102	104	39	42	74	71	450	420	— 03	— 01	— 03	00	0.1	0.0	0.2	0.0
14.0	160	1064	1.36	2.05	2.45	— 109	— 40	99	107	37	41	200	166	1180	1070	— 10	— 02	— 03	+ 01	1.9	0.1	0.2	0.0
log surf. 0.84 and 0.99. Abs. screen *a* $\varrho_1 = 11.5$, $\varepsilon = 2.6$ and 1.0; *b* $\varrho_1 = 12.5$, $\varepsilon = 2.9$ and 1.1																				5.6	3.4	5.6	7.5

[1]) Monthly Notices R. A. S. **80,** p. 6 (Nov. 1919).
[2]) Proceedings Amsterdam Ac. Vol. **23,** 707 (1920).
[3]) Zschr. f. Astrophysik **6,** p. 259 (1933).

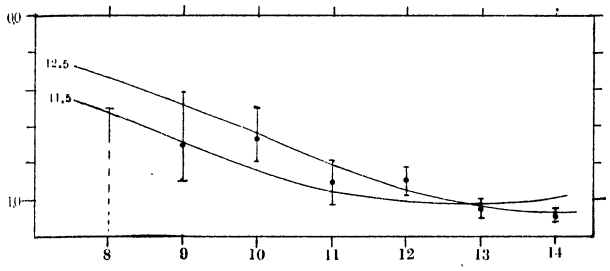

Fig. 6. Δ log A in Taurus field, v. Klüber.

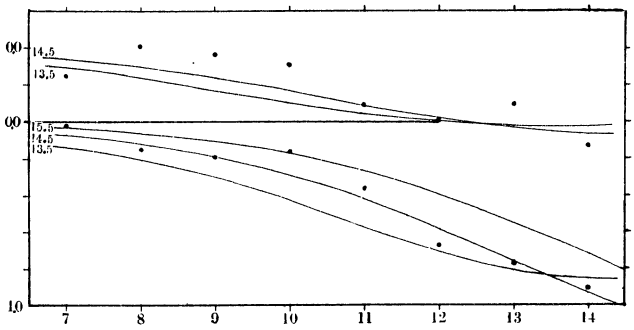

Fig. 9. Δ log A in ξ Persei field, Lehmann-Balanovskaja.

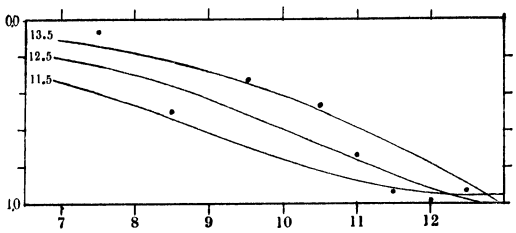

Fig. 7. Δ log A in o Persei field, Reimer.

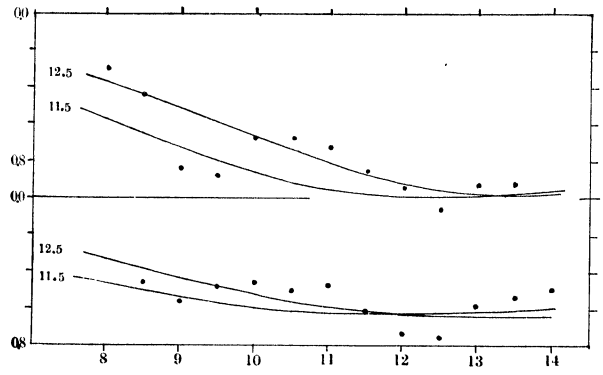

Fig. 8. Δ log A in Auriga fields, Hartwig.

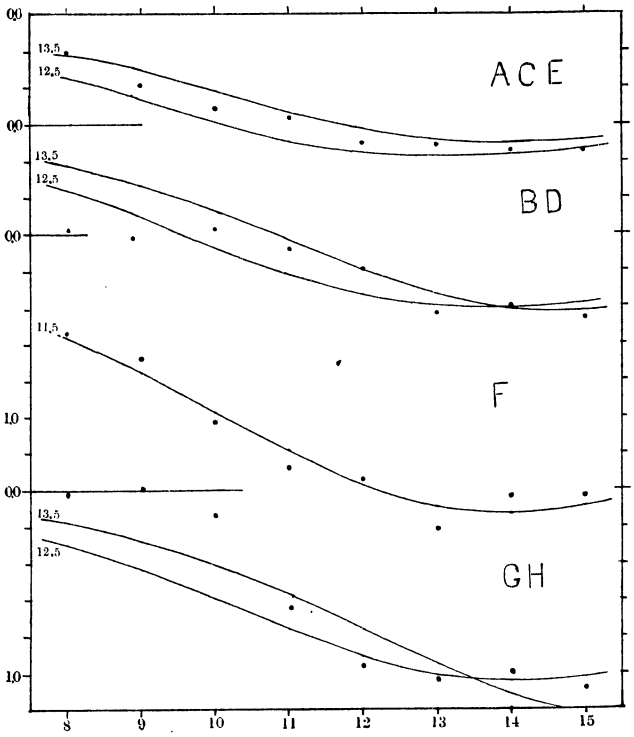

Fig. 10. Δ log A in Taurus fields, Mc Cuskey.

on distance ($\varrho_1 = 10.5 \ldots . 13.5$) a value of ε was computed which should represent the observed values of Δ log A for the faintest magnitude classes, and with this combination (ϱ_1, ε) the values of Δ log A were interpolated from Table 14. In Fig. 6 we may see that the curves for $\varrho_1 = 10{,}5$ and 13.5 run far outside the points observed ; hence in Table 18. only the computations for $\varrho_1 = 11{,}5$ and 12.5 are given. The values of E for small numbers (above the dotted lines) were taken from Table 15 ; for the larger numbers they were computed from the ,,Deviations Obs-Comp'' wth the μ_n^2 of Table 16, assuming $f = 1{,}40$ and $\mu_s^2 = 40$. The most probable value of ϱ_1, seems to be slightly below 12.5; say 12.3 ($r = 290$ parsecs). The total ΣE for 7 data with two unknowns are very satisfactory.

J. P. REIMER [1]) investigated the dark area near o Persei ($3^h40^m + 31°$, $\beta = -18°$), which doubtless belongs to the Taurus complex and nearly corresponds to the dark area A in my first study. Each of the three partly overlapping fields $2° \times 2°$ and a fourth, more remote, ware taken on two plates with different exposure times. The standards of magnitude were taken from exposures of the Pleiades on the same plates. Special areas (one darkest I, three adjacent less dark parts II—IV, and the remote field, supposed to be outside the obscured region) were counted. In each, the number of stars brighter than the round limits 7.0 8.0 .... 11.5 12.0 12.5 13.0 was counted directly on the plate. We combined II—IV and deiived the (partly overlapping) numbers of stars $A(m)$ between $m \pm 0.5$. The results are given and discussed in Table 19, and are represented in Fig. 7. For the dark

Table 19. J. P. Reimer, o Persei-field ($\beta = -18°$). A dark field I, 2.78 sq.d., B adj. fields II-IV 8.37 sq.d.

m	Counted		log A^1		log A	Δ log A		Δ log A comp.				Number of stars Comp.		Deviations Obs.—Comp.				E			
	A	B	A	B		A	B	Aa	Ab	Bb	Bc										
7.5	1	5	9.56	9.78	9.62	— 06	+ 16	40	25	19	12	0.5	0.6	2.2	2.6	+ 34	+ 19	+ 35	+ 28	1.4	1.0	3.5	2.5
8.5	1	7	9.56	9.92	0.06	— 50	— 14	54	36	26	18	0.9	1.4	5.3	6.3	+ 04	— 14	+ 12	+ 04	0.2	0.0	0.6	0.2
9.5	4	27	0.16	0.51	0.49	— 33	+ 02	69	51	32	26	1.7	2.6	12	14	+ 36	+ 18	+ 34	+ 28	3.2	1.1	3.7	1.8
10.5	8	45	0.46	0.73	0.92	— 46	— 19	82	68	37	35	3.5	4.8	30	31	+ 36	+ 22	+ 18	+ 16	5.1	2.3	2.1	1.7
11.0	7	51	0.40	0.79	1.13	— 73	— 34	87	76	38	38	5.0	6.5	47	47	+ 14	+ 03	+ 04	+ 04	1.0	0.1	0.1	0.1
11.5	7	75	0.40	0.95	1.34	— 94	— 39	91	84	39	41	7.4	8.7	74	71	— 03	— 10	00	+ 02	0	0.1	0	0.0
12.0	10	108	0.56	1.11	1.55	— 99	— 44	94	91	40	43	11	12	118	110	— 05	— 08	— 04	— 01	0.1	0.2	0.2	0
12.5	18	166	0.82	1.30	1.75	— 93	— 45	95	97	40	45	17	16	190	170	+ 02	+ 04	— 05	00	0	0.1	0.4	0
																				11.0	4.9	10.6	7.3

log surf. 0.44 and 0.92. Abs. screen a $\varrho_1 = 11.5$, $\varepsilon = 2.5$; b $\varrho_1 = 12.5$, $\varepsilon = 3.0$ and 1.1; c $\varrho_1 = 13.5$. $\varepsilon = 1.4$

field the curve for $\varrho_1 = 11.5$ is too low; $\varrho_1 = 12.5$ is quite satisfactory; $\varrho_1 = 13.5$ even with $\varepsilon = \infty$ is too high for the faint classes. For the less dark areas the deviations show a continusus positive sign, and even $\varrho_1 = 13.5$ gives a smaller number of stars than is counted. The number of brighter stars is here larger than normal ; this may be due to an agglomoration of bright stars, which on photograph 3 of BARNARD'S Atlas is visible around, and W of o Persei. The author himself draws attention to the surplus of stars of $10m$ which appears in both areas. The number of stars, however, is rather too small to allow of drawing definite conclusions. The values of E were computed with $f = 1{,}6$, $\mu_s^2 = 50$.

GEORG HARTWIG has made an investigation of a dark region in Auriga [2]) ($4^h\,32^m + 36°$, $\beta = -6°$), which belongs to the Taurus complex and is connected with its densest parts. Not only photographic, but also photovisual magnitudes were measured, so that for each star the colour could be determined. The plates were standardized by means of the Parkhurst standard fields at $\delta = +45°$. The numbers of stars were couuted in the catalogue in groups of half magnitudes, which were combined into overlapping entire magnitude intervals. Two darkest areas, 1 and 2 (6.19 and 10.75 sq. d) combined, and a less dark area 3 (4.42 sq. d.) were compared by the author with an area 4 in an apparently normal region near the gelactic circle. In our Table 20 we have omitted the latter and given only the data and discussion for area 1—2 combined (A) and area 3(B).

In the deviations Δ log A in the table, as well as in Fig. 8 a strong fluctuation is visible, so that after a maximum deficiency at $9m$ it decreases for 10^m—10.5^m and then reaches again a stronger maximum for 12^m—12.5^m. The author explains this according to the usual interpretation of the Wolf curves, by two separate absorptions, one of 1.4^m below 150 parsecs, the other of 0.7^m beginning at 250—350 parsecs. It is clear, however, after our computations of the effect of two absorbing clouds

[1]) Mitth. d. Wiener Sternwarte Nr. 4, p. 237 (1935).
[2]) Zschr. f. Astrophysik **17**, p. 191—245 (1938).

Table 20. G. Hartwig, Auriga-field ($\beta = -5°$). *A* dark fields (1 + 2), 16.94 sq.d.; *B* less dark field (3), 4.42 sq.d.

m	Counted A	Counted B	log A^1	log A	Δ log A	Δ log A comp. Aa Ab	Δ log A comp. Ba Bb	Number of stars Comp.		Deviations Obs.—Comp.		E	
8.0	10	0	9.77 —	0.06	— 29 —	57 37	46 33	5.3 8.3	1.8 2.4	+ 28 + 08	— —	4.1 0.5	1.2 2.1
8.5	12	3	9.85 9.83	0.28	— 43 — 45	65 44	50 38	7.3 11.8	2.7 3.6	+ 22 + 01	+ 05 — 07	3.0 0	0.2 0
9.0	8	4	9.67 9.95	0.51	— 84 — 56	73 51	54 43	10 17	4.2 5.4	— 11 — 33	— 02 — 13	0.4 5.5	0 0.2
9.5	12	8	9.85 0.25	0.73	— 88 — 48	80 59	57 48	14 23	6.5 7.9	— 08 — 29	+ 09 00	0.3 5.0	0.6 0
10.0	32	14	0.28 0.50	0.95	— 67 — 45	86 67	60 52	21 32	10 12	+ 19 00	+ 15 + 07	2.1 0	0.7 0.2
10.5	54	21	0.50 0.67	1.17	— 67 — 50	92 74	62 56	30 46	16 18	+ 25 + 07	+ 12 + 06	4.7 0.5	0.7 0.2
11.0	80	37	0.67 0.92	1.39	— 72 — 47	96 81	63 59	46 65	26 28	+ 24 + 09	+ 16 + 12	5.6 0.9	1.8 1.0
11.5	97	45	0.76 1.00	1.61	— 85 — 61	97 87	63 62	75 93	43 44	+ 12 + 02	+ 02 + 01	1.7 0.1	0 0
12.0	27	56	0.87 1.10	1.83	— 94 — 73	98 92	63 63	120 138	71 71	+ 04 — 02	— 10 — 10	0.2 0.1	1.2 1.2
12.5	167	87	0.99 1.29	2.04	— 105 — 75	98 95	62 64	195 210	118 112	— 07 — 10	— 13 — 11	0.8 1.6	2.4 1.7
13.0	360	211	1.33 1.67	2.25	— 92 — 58	98 97	61 64	320 320	195 180	+ 06 + 05	+ 03 + 06	0.6 0.4	0.1 0.6
13.5	583	377	1.54 1.93	2.46	— 92 — 53	97 98	60 63	520 510	320 300	+ 05 + 06	+ 07 + 10	0.4 0.6	0.8 1.8
14.0		668	2.17	2.66	— 49	96 97	59 62		525 490		+ 10 + 13		1.9 3.1
												23.9 15.2	11.6 12.1

log surf. 1.23 and 0.65. Abs. screen *a* $\varrho_1 = 11.5$, $\varepsilon = 2.4$ and 1.5; *b* $\varrho_1 = 12.5$, $\varepsilon = 2.5$ and 1.6.

behind each other (cf. p . . . .), that such strong fluctuations cannot be explained in this way. Their combined effect, even with wider separation than the author assumes, will hardly be distinguishable from that of a single cloud at intermediate distance. To get a curve as represented by HARTWIG's results, a very small dispersion of the stars in luminosity would be required. We cannot admit that everywhere a long the line of sight in this direction only stars with a small range of luminosity should occur, and the evidence of these counts does not seem large enough to outweigh all other data. Since magnitude errors of this amount must be excluded — though the fluctuation appears in both areas and even, to a lesser degree, in the normal area 4 — we can describe his result only as the local occurrence of a group of stars of limited range of luminosity in a limited part of space, producing a surplus of 10^m stars, or as a defect of such stars at some other distance.

Table 21. Colour Indices in the Auriga cloud.

m	(1 + 2)	(3)	(4)	(4) smoothed	(1 + 2) — (4) *sm*	(3) — (4) *sm*
7.5			— .23	— .11		
8.0	+ 08			— 05	+ 13	
8.2			+ 06	— 03		
		+ 18				+ 18
8.7	29		22	+ 03	+ 26	
9.2	38	12	01	+ 08	+ 30	+ 04
9.7	39	38	04	+ 14	+ 25	+ 24
10.2	64	19	23	+ 20	+ 44	— 01
10.7	55	44	10	+ 25	+ 30	+ 19
11.2	55	50	33	+ 31	+ 24	+ 19
11.7	66	57	32	+ 37	+ 29	+ 20
12.2	71	57	38	+ 42	+ 29	+ 15
12.7	82	74	53	+ 48	+ 34	+ 26
13.2	84	84		(+ 54)	(+ 39)	(+ 30)
13.7	86			(+ 59)	(+ 27)	
14.2	93			(+ 65)	(+ 28)	

Computed from Table 11.

	$\frac{-}{c}$	11.5	12.5	11.5	12.5
		2.4	2.5	1.5	1.6
8.0	0.10	35	25	26	21
9.0	.15	32	30	23	24
10.0	.20	38	29	25	22
11.0	.25	41	37	26	26
12.0	.30	39	42	27	28
13.0	.36	37	41	27	26
14.0	.42	33	38	26	24

This irregularity produces, of course, a considerable uncertainty in the distance of the absorbing matter. The curves in Fig. 8 and the computations in Table 20 show that a distance between $\varrho_1 = 11.5$ and 12.5 (200 and 320 parsecs) will best fit the data. The values for the sum total of the relative error squares, derived by means of $f = 1.30$ and $\mu_s^2 = 50$, are too large (as might now be expected) to be consistent with merely accidental errors ; they put the most probable distance nearer to the upper limit, say, $\varrho_1 = 12.2$ (280 parsecs).

The colour indices derived by HARTWIG for these stars have been reduced in our Table 21 to the international scale by multiplying the differences between photographic and photovisual magnitude by 0.54 (*cf.* p. 203 *l.c.*). The results for field 4, which the author considers as a field without absorption, run up a little more steeply than the normal values in our Table 11, p. 22, for which admittedly an exact concordance with the international system is not warranted. So we took the differences of field 1 + 2 and field 3 with smoothed values of field 4 as the effect of the absorbing screen. When compared with the mean colours computed from table 11, they are seen to be of the same order of magnitude, mostly somewhat lower, and especially for the brightest classes they have lower values, as if there were more white stars before the screen. Since the colours in Table 11 have been computed with a slightly different distribution of density, complete concordance cannot be expected.

A study of the dark nebula near ξ Persei ($3^h\ 56^m + 37.5°$, $\beta = -10°$) was made by J. N. LEHMANN-BALANOVSKAJA [1]). It was based on determinations of magnitude on three photographic and two photovisual plates. Moreover, the spectrum was determined from other plates, so that the chief purpose of the paper consists in finding the space colouring in relation to absorption. We are here considering the star counts from the photographic plates. They were standardized by the N. Polar Sequence ; the mean error of one magnitude was found to be 0.12^m (not including the effect of reduction to centre), and the systematic differences between the plates reach 0.11^m. The region is divided into a poor northern and a richer southern half ; part of the latter being covered by the well known luminous nebula of ζ Persei, which, however, was hardly visible on these plates. In Table 22 the numbers counted, and the reductions for both parts (*N* and *S*) are given ; the values for 15.0, being doubtless incomplate, are omitted. Comparison with the normal numbers shows that the southern

Table 22. I. N. Lehmann—Balanovskaja, ξ Persei-field ($\beta = -10°$). *N* dark northern field, 3.1 1sq.d.; *S* southern field 4.24 sq.d.

m	Counted *N*	Counted *S*	log A^1		log *A*	Δ log *A*	Δ log *A* comp. *Na*	*Nb*	*Sa*	*Sb*	Number of stars Comp.				Deviations Obs.—Comp.				*E*			
7.0	1	1	9.51	9.37	9.52	— 01	— 15	14	07	10	06	0.7	0.9	1.1	1.2	+ 13	+ 06	— 05	— 09	0.7	0.0	0	0
8.0	2	4	9.81	9.97	9.96	— 15	+ 01	21	12	16	10	1.7	2.1	2.7	3.1	+ 06	— 03	+ 17	+ 11	0.3	0.0	1.3	0.5
9.0	5	10	0.21	0.37	0.40	— 19	— 03	30	19	23	16	3.9	5.0	6.3	7.4	+ 11	00	+ 20	+ 13	0.5	0	2.3	1.1
10.0	15	25	0.69	0.77	0.85	— 16	— 08	43	29	29	23	8.1	11.2	15	18	+ 27	+ 13	+ 21	+ 15	1.9	0.6	2.1	1.2
11.0	26	41	0.92	0.98	1.28	— 36	— 30	57	42	35	31	16	22	36	40	+ 21	+ 06	+ 05	+ 01	2.2	0.2	0.2	0.0
12.0	34	89	1.04	1.32	1.71	— 67	— 39	71	58	39	38	31	42	89	91	+ 04	— 09	00	— 01	0.1	0.9	0	0
13.0	69	287	1.35	1.83	2.12	— 77	— 29	81	76	41	42	63	71	220	210	+ 04	— 01	+ 12	+ 13	0.2	0	3.4	4.0
14.0	129	433	1.62	2.01	2.53	— 91	— 52	85	93	41	45	148	123	560	510	— 06	+ 02	— 11	— 07	0.8	0.1	3.5	1.4
	log surf. 0.49 and 0.63. Abs. screen *a* $\varrho_1 = 13.5$, $\varepsilon = 2.4$ and 1.1 ; *b* $\varrho_1 = 14.5$, $\varepsilon = 3.5$ and 1.3.																			6.7	2.0	12.8	8.2

half also is slightly obscured. The curves in Fig. 9 indicate that the distance of the matter obscuring the dark field must be nearly 800 parsecs ($\varrho_1 = 14.5$) — the curve for $\varrho_2 = 13.5$ is certainly too low,

[1]) Pulkowo Bulletin **14**, Nr. 118 (1935).

while that for $\varrho_1 = 15{,}5$ is too high and cannot represent, even with $\varepsilon = \infty$, the deficiency of the lowest classes. For the southern, less obscured field a curve for 15.5 would fit better than 14.5. The residuals and the values of E, computed with $f = 1.40$ $\mu_s{}^2 = 30$ are, with distance 14.5, for the dark field quite, for the brighter field less satisfactory. The large distance found for this nebula, far behind the other dark nebulae treated here makes it doubtful whether it has any real connection with the Taurus complex of absorbing matter.

A study of the galactic structure in Taurus by S. W. Mc CUSKEY [1]) is part of a large investigation on galactic structure by means of star counts, taken up at Harvard Observatory by B. J. BOK and his coworkers. The method followed consists in counting directly on the plate all stars brighter than certain limiting magnitudes, fixed by artificial scales of images, which are looked at repeatedly during counting. In this way log N down to m 8.0 9.0 ... 15.0 was determined for a large number of areas. The chief object of this study was the distribution of stellar density. As to the absorbing matter results are given for eight strongly obscured areas designated $A - H$. Only the values of the resulting distances (ranging from 80 to 200 parsecs) and absorptions are given ; the original data of the counts and the values of log A were not communicated by the author. They had to be reconstructed by the somewhat uncertain reading of the coordinates from the small scale reproductions of the Wolf curves (Fig. 5, p. 584 *l.c.*) representing them. They were compared with the normal log A of Table 12, and combined into groups according to the amount of absorption for the lowest classes ; the areas $G - H$ near o Persei kept separate from the low latitude areas B and D. The data and discussion are given in Table 23, and are represented in the graphs Fig. 10. It appears that ACE can be well represented

Table 23. Mc Cuskey, Taurus-fields.

m	Areas A, C, E (14.4 sq.d.)					Areas B, D (10.3 sq.d.)					Area F (3.5 sq.d.)				Areas G, H (16.9 sq.d.)				
	$\Delta \log A$	a	b	$O-C$	E	$\Delta \log A$	c	d	$O-C$	E	$\Delta \log A$	e	$O-C$	E	$\Delta \log A$	f	g	$O-C$	E
8	— 20	34	21	+ 14 + 01	1.4 0.1	— 56	36	22	— 20 — 34	0.3 1.6	— 53	56	+ 03	0.0	— 02	30	18	+ 28 + 16	2.1 0.9
9	— 38	46	30	+ 08 — 08	0.2 0.3	— 60	50	33	— 10 — 27	0.1 2.5	— 67	75	+ 08	0.0	+ 01	44	28	+ 45 + 29	2.8 1.6
10	— 51	58	41	+ 07 — 10	0.3 0.6	— 57	67	47	+ 10 — 10	0.4 0.5	— 102	97	— 05	0.0	— 15	59	41	+ 44 + 26	4.8 2.3
11	— 56	69	53	+ 13 — 03	1.2 0.1	— 68	82	63	+ 14 — 05	1.1 0.2	— 127	118	— 09	0.0	— 64	76	57	+ 12 — 07	0.5 0.2
12	— 70	75	62	+ 05 — 08	0.2 0.6	— 79	93	80	+ 14 + 01	1.4 0.0	— 134	137	+ 03	0.1	— 96	91	76	— 05 — 20	0.1 2.6
13	— 71	77	68	+ 06 — 03	0.3 0.1	— 103	99	93	— 04 — 10	0.1 0.9	— 161	149	— 12	0.5	— 103	101	95	— 02 — 08	0.0 0.5
14	— 74	76	70	+ 02 — 04	0 0.1	— 100	100	101	00 + 01	0 0	— 143	153	+ 10	0.5	— 99	104	112	+ 05 + 13	0.2 1.4
15	— 74	73	68	— 01 — 06	0 0.4	— 106	98	102	— 08 — 04	0.6 0.2	— 143	149	+ 06	0.3	— 108	102	122	— 06 + 14	0.3 1.8

Abs. screens a $\varrho_1 = 12.5$, $\varepsilon = 2.0$; b $\varrho_1 = 13.5$, $\varepsilon = 1.9$; c $\varrho_1 = 12.5$, $\varepsilon = 2.6$; d $\varrho_1 = 13.5$, $\varepsilon = 2.8$; e $\varrho_1 = 11.5$, $\varepsilon = 4.0$; f $\varrho_1 = 12.5$, $\varepsilon = 3.0$; g $\varrho_1 = 13.5$, $\varepsilon = 4.0$.

by $\varrho_1 = 13$ ($r = 400$), $\varepsilon = 2.0^m$, both $\varrho_1 = 12{,}5$ and 13.5 leaving slight errors. The areas BD are best represented by $\varrho_1 = 12.5$ $\varepsilon = 2.5$ ($r = 320$ *ps*) ; $\varrho_1 = 11.5$ and 13.5 are both too far outside the points. For the darkest area F an absorbing screen at $\varrho_1 = 11.5$ (200 parsecs) with $\varepsilon = 4^m$ fits the counted numbers far better than would be expected. For the areas G-H there is an excess of bright stars, just as was found from REIMER'S counts, so that here larger values of the relative error square E remain. The general smallness of the E values here (computed by $f = 1.3$, $\mu_s{}^2 = 100$) may be seen as an indication that in this work the errors are smaller than had been presumed *a priori*.

[1]) Astrophys. Journal 88, 209 (1938); 89, 568 (1939).

The Taurus-Auriga nebula after the bright star classes.

Since the determination of the distance of an absorbing nebula depends on the brightest star classes, where the Wolf curves begin to diverge, we have to look in the first place, in the case of such near dark matter, at the stars brighter than 9^m. For these brightest classes the decrease in log A is very insensitive to variations in the amount of absorption ε; for this part of the curves, therefore, large areas with different values of ε may be taken together, whereas for fainter stars they must be kept separate.

Hence, for the Taurus nebulosities, one large continuous area, where the number of *DM* stars falls below $^2/_3$ of the normal number, was treated as a whole. It is delineated in Fig 11 ; outlying

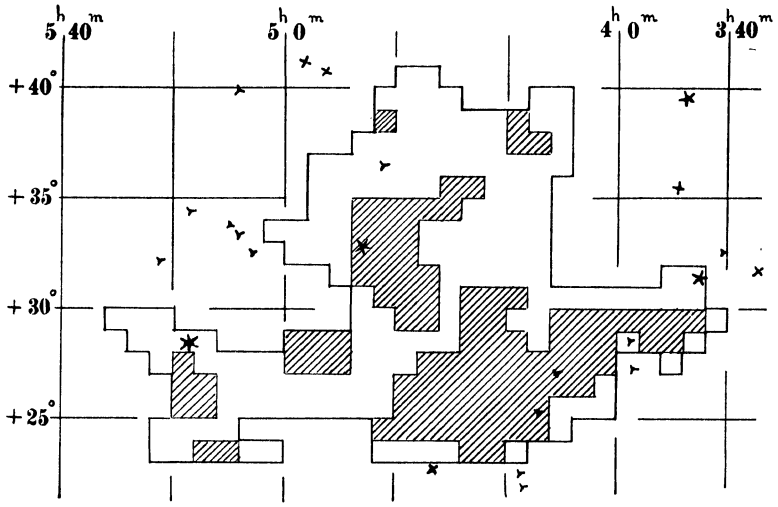

Fig. 11. Dark region counted in Taurus-Auriga.

poor parts (e.g. the dark area near o Persei) were not included. For this region, comprising 210.6 sq.d. counts were made in the *B.D.M.*, and in the Harvard Photometry (*H.C.O. Annals* Vol 50). For the *D.M.* stars a division was made between the darker parts (number of stars smaller than 0,4 times the normal), measuring 82.2 sq. d. and the remaining, less obscured 128.4 sq.d. The Harvard stars were counted over half magnitudes and combined into overlapping magnitudes 2.50—3.49, 3.00—3.99 etc. The *BDM* stars were counted between the limits 6.55, 7.05, ... 9.05, and also combined into overlapping magnitude intervals. These limits were reduced to photometric magnitude by means of the reduction tables in *Publ. Amsterdam* 1 (Tables 16, 26, 29, 30). Stars belonging to the Hyades, after the list of W. Chr. Martin [1]), were excluded ; for the same reason the zones south of + 23° were omitted. The results of the counts are given in Table 24. For the *BDM* stars under log A the number per square degree is given ; not for the interval of one magnitude, but for the larger intervals in the first column. The normal number of stars has been taken from Van Rhijn, *Groningen Publ.* 27 Table V, giving log $N(m)$ for visual magnitudes. The mean latitude was taken — 10°.

For the brightest magnitude classes the small number of stars counted, sometimes zero, makes it difficult to derive Δ log A. That there is already a decided shortage of stars here is shown by comparing the normal numbers computed for such an area : 1.1, 2.0, 3.8, 6.8, 12 with the counted numbers 1, 1, 0, 0, 6.

[1]) B. A. N. **256**, Vol **7**, p. 170.

Table 24. Bright stars in the Taurus-Auriga region ($\beta = 10°$) 210.6 sq.d.

	m	n	log A^1	log A	Δ log A	Δ log A comp. a b c	n comp. a b c	$O-C$	E
	3.0	1	7.68 (7.47)	7.73	—05 (— 26)	17 09 06	0.8 0.9 1.0		0.4 0.2 0
	3.5	1	7.68 (7.47)	7.99	—31 (— 52)	21 12 07	1.3 1.5 1.7		0 0 0
	4.0	0	— (7.16)	8.26	— (—110)	24 15 09	2.2 2.7 3.1		1.8 2.5 3.4
	4.5	0	— (7.95)	8.51	— (— 56)	28 19 11	3.6 4.4 5.2		4.1 5.5 6.9
	5.0	6	8.46 (8.51)	8.77	—31 (— 26)	32 22 14	5.9 7.4 9.0	+ 01 — 09 — 17	0.0 0.2 0.8
	5.5	16	8.88 (8.89)	9.03	—15 (— 14)	36 26 17	10 12 15	+ 21 + 11 + 02	1.7 0.6 0.0
	6.0	30	9.16	9.29	—13	39 30 21	17 20 25	+ 26 + 17 + 08	4.3 2.3 0.6
> 6.53		41	9.29	9.46	—17				
6.53 — 7.63	7.08	85	9.61	9.87	—26	44 38 31	56 65 76	+ 18 + 12 + 05	2.7 1.1 0.3
7.06 — 8.19	7.62	123	9.77	0.16	—39	45 41 35	107 118 135	+ 06 + 02 — 04	0.4 0.0 0.2
7.63 — 8.78	8.20	221	0.02	0.46	—44	46 43 40	210 224 240	+ 02 — 01 — 04	0.1 0 0.2
8.19 — 9.46	8.82	483	0.36	0.81	—45	46 45 45	470 480 480	+ 01 00 00	0 0 0
	log surf. 2.32. Abs. screens a $\varrho_1 = 9.5$, $\varepsilon = 1.0$; b $\varrho_1 = 10.5$, $\varepsilon = 1.1$; c $\varrho_1 = 11.5$, $\varepsilon = 1.5$.								15.5 12.4 12.4
	Darkest part 82.2 sq.d.								
> 6.53	13	9.20		—26					
7.08	24	9.47		—40	66 54 36	14 18 27	+ 26 + 14 — 04		2.0 0.7 0.1
7.62	32	9.59		—57	72 63 45	22 28 42	+ 15 + 07 — 12		1.0 0.3 1.0
8.20	44	9.73		—73	75 70 53	42 47 69	+ 02 — 03 — 15		0.0 0.1 2.1
8.82	93	0.05		—76	76 77 63	91 89 123	.00 + 01 — 13		0 0 2.1
	log surf. 1.92. Abs. screens $\varepsilon = 1.7$, 2.2, 4.0.								
	Less obscured 128.4 sq.d.								
> 6.53	28	9.34		—12					
7.08	61	9.68		—19	29 26 25	49 52 54	+ 10 + 07 + 06		0.8 0.4 0.3
7.62	91	9.85		—31	29 28 28	96 98 98	— 02 — 03 — 03		0.0 0.1 0.1
8.20	177	0.14		—32	29 30 31	190 186 182	— 03 — 02 — 01		0.1 0.1 0
8.82	390	0.48		—33	28 30 34	440 420 380	— 05 — 03 + 01		0.4 0.2 0
	log surf. 2.11. Abs. screens $\varepsilon = 0.6$, 0.7, 1.0.								

The latter have therefore been smoothed into averages of 3 consecutive values. It should be remarked that corrections are then necessary, because, if log $A(m)$ can be represented by $a + bm$, the mean of A_{m-1}, A_m and A_{m+1} is larger than $A(m)$; so that a negative correction depending on b should be applied to log $^1/_3$ $(A_{m-1} + A_m + A_{m+1})$. For

$b =$ 0.20 0.25 0.30 0.35 0.40 0.45 0.50

this correction is 0.030 0.047 0.066 0.089 0.114 0.143 0.173

In smoothing, as in this case, A for $m - 0.5$, m, $m + 0.5$ the correction must be read for $^1/_2\, b$.

The smoothed values of log A and Δ log A, corrected in this way, have been added in parentheses. For each of the distance moduli 9.5 10.5 11.5 the value of the absorption ε was derived by fitting Δ log A for the lowest classes. In Fig 12 the curves are represented with the points of the Δ log A. The m.e. of a magnitude in *Harvard* **50** was taken $0{,}10^m$, of a reduced magnitude from the *BDM* 0.30^m after the data *Publ. Amsterdam* **1**, p. 24 and 33; so for f 1.3 and 2.0 is taken. If the systematic scale errors of *Harvard* **50** are estimated at, at most, 0.05^m they are entirely negligible beside the large natural uncertainties of the small counted numbers. For the *BDM* we assume that the systematic scale errors, by the uncertainty of the reduction for density, for decimal width and for

Rectascension, have a mean value of 0.10 ; then $\mu_s^2 = 50$ here. So the values of E have been computed.

From ΣE for the three assumptions we may infer that the most probable distance of the absorbing screen is $\varrho_1 = 11.0$, $r = 160$ parsecs. Representing ΣE by $12.0 + 1.52\ (\varrho_1 - 11.0)^2$, derived from 11 data, a m.e. in ϱ_1 of 0.9 is found. The value of ΣE is somewhat larger than would correspond to merely chance errors for 11 data with 2 unknowns.

There are reasons, however, to assume for the Taurus nebulosities a more complex structure than a mere veil at 160 parsecs distance, of a thickness of, say, one unit in ϱ_1 with denser and less dense parts. The computed numbers of the brightest stars above 5^m come nearest to the observed small number in the case of the lowest distance $\varrho_1 = 9.5$ — a still smaller distance would fit still better —, whereas $\varrho_1 = 10.5$ and 11.5 leave greater errors. On the other hand, for the fainter stars 5^m — 8^m the largest distance 11.5 fits better. The empirical $\Delta \log A$ seems to stretch more gradually over a larger range of m than the computed values for one definite distance. So these data indicate that the absorbing matter begins at smaller distances , perhaps 40 or 60 parsecs ($\varrho_1 = 8$ or 9) and extends to larger distances than the mean value found here, say to $\varrho_1 = 12$, $r = 250$ parsecs.

The discrepancy between the smaller distance found from the bright stars in this large area and the larger distances derived above from the counts of faint photographic magnitudes in the densest parts (290, 320, 280, 400 parsecs) points in the same direction. These distances derived from a continuation of the increase of $\Delta \log A$ from 9^m to 12^m, give the impression that in the darkest places the absorbing matter protrudes at the remote side of the nebula. It must be remarked here that Mc Cuskey, for his 8 darkest areas, derives smaller distances, from 80 to 200, in the mean 142 parsecs. The difference from our result from the same counts is due to a difference in assumptions on the ,,normal'' distribution. Mc Cuskey takes as the normal distribution in this region the average of a number of ,,apparently unobscured areas'' ; his average $N(m)$ shows a marked decrease with increasing m as compared to the values of *Groningen Publ* **43**. This decrease is represented by a

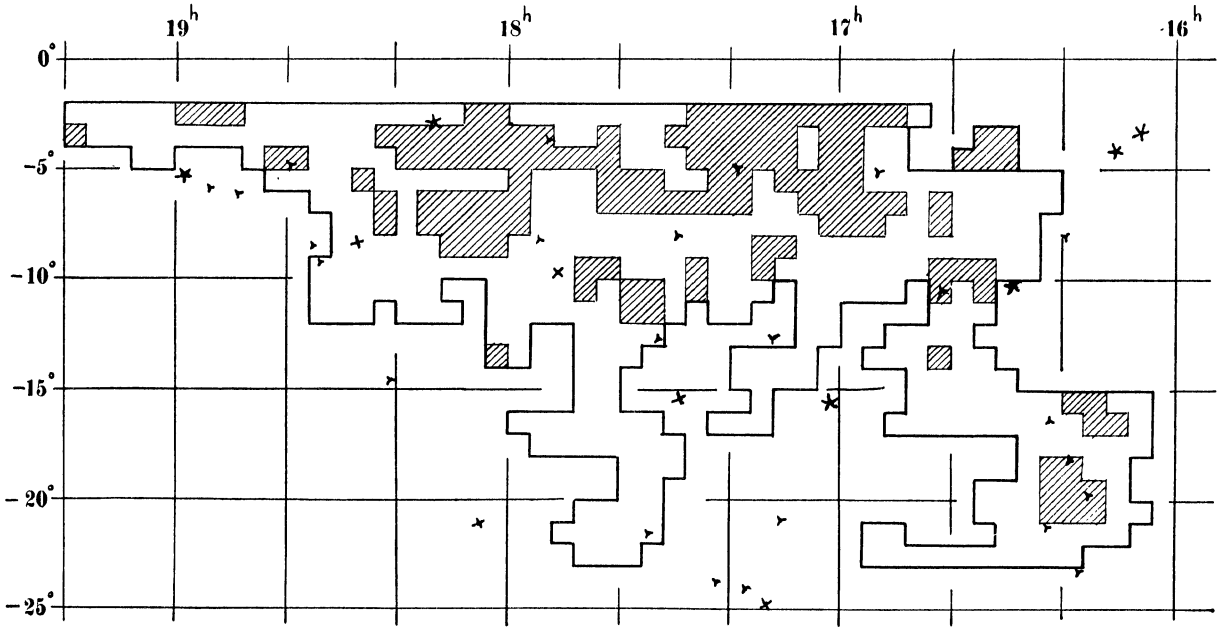

Fig. 13. Dark region counted in Ophiuchus.

general absorption of 0.5^m per kiloparsec in this direction. It is clear that comparison with such more rapidly decreasing normal $A(m)$ must give values of $\Delta \log A$ which, for faint magnitudes, are smaller and reach their maximum earlier, and are therefore interpreted as absorption at a smaller distance. This smaller distance is then chiefly due to the assumption that, behind the Taurus nebula, space is filled everywhere with this continuous absorption, in addition to the general space structure as represented by the mean $A(m)$ of the Groningen tables.

The problems, here encountered, of the real spatial distribution of the absorbing matter of the Taurus nebulosities can be studied more thoroughly only by means of colour excesses and spectra.

The Ophiuchus nebulae.

A large region of absorption stretches over the constellation Ophiuchus. The shortage of stars shows itself already in the naked-eye stars, and in the *DM* stars its outlying parts extend to within Aquila and Scorpio. Since the distance of these nebulosities must be small, it has to be studied chiefly

Table 25. Bright stars in the Ophiuchus region ($\beta = +12°$) 456.8 sq.d.

m	n	log A^1	log A	Δ log A	Δ log A comp. a	b	c	d	n comp.				$O-C$				E			
3.0	1	7.34	7.72	— 38	23	15	09	05	1.4	1.7	2.0	2.1	— 15	— 23	— 29	— 33	0	0	0	0.2
3.5	2	7.64 (7.67)	7.98	— 34 (— 31)	26	19	12	07	2.5	2.8	3.3	3.7	— 08	— 15	— 22	— 27	0	0	0.2	0.4
4.0	5	8.04 (8.13)	8.24	— 20 (— 11)	29	22	15	09	4.0	4.8	5.6	6.5	+ 09	+ 02	— 05	— 11	0.4	0.1	0	0.2
4.5	14	8.49 (8.34)	8.50	— 01 (— 16)	32	26	18	11	6.9	7.9	9.6	11.2	+ 31	+ 25	+ 17	+ 10	2.4	1.8	1.0	0.4
5.0	13	8.45 (8.44)	8.75	— 30 (— 31)	35	30	21	14	12	13	16	19	+ 05	00	— 09	— 16	0.1	0	0.5	1.8
5.5	13	8.45 (8.67)	9.01	— 56 (— 34)	37	32	25	17	20	22	26	32	— 19	— 24	— 30	— 39	2.7	4.7	8.5	17.3
6.0	44	8.98	9.26	— 28	38	35	28	21	35	37	44	51	+ 10	+ 07	00	— 07	1.2	0.6	0	0.8
> 6.60	67	9.17	9.45	— 28																
7.17	183	9.60	9.92	— 32	40	38	36	30	152	159	166	190	+ 08	+ 06	+ 04	— 02	0.9	0.5	0.2	0.1
7.80	301	9.82	0.21	— 39	39	40	38	36	303	295	310	320	.00	+ 01	— 01	— 03	0	0	0	0.1
8.33	577	0.10	0.50	— 40	39	41	40	41	590	560	590	560	— 01	+ 01	00	+ 01	0	0	0	0
9.00	1234	0.43	0.84	— 41	37	40	42	47	1350	1260	1200	1070	— 04	— 01	+ 01	+ 06	0.3	0	0	0.6
log surf. 2.66. Abs. screens a $\varrho_1 = 8.5$, $\varepsilon = 0.8$; b $\varrho_1 = 9.5$, $\varepsilon = 9.0$; c $\varrho = 10.5$, $\varepsilon = 1.0$; d $\varrho_1 = 11.5$, $\varepsilon = 1.5$.																	8.0	7.7	10.4	21.9
Darkest part 134.7 sq.d.					a	b														
> 6.60	14	9.03		— 42																
7.17	35	9.43		— 49	62	57			27	30			+ 13	+ 08			0.9	0.4		
7.80	55	9.63		— 58	62	61			52	54			+ 04	+ 03			0.1	0.1		
8.33	98	9.88		— 62	62	62			102	102			00	00			0	0		
9.00	198	0.18		— 66	61	63			230	220			— 05	— 03			0.4	0.1		
log surf. 2.13. Abs. screens a $\varrho_1 = 8.5$, $\varepsilon = 1.3$; b $\varrho_1 = 9.5$, $\varepsilon = 1.4$.																				
Less obscured part 322.1 sq.d.					a	b														
> 6.60	53	9.22		— 23																
7.17	148	9.66		— 26	35	31			120	132			+ 09	+ 05			1.0	0.3		
7.80	246	9.88		— 33	34	33			240	245			+ 01	00			0	0		
8.33	479	0.17		— 33	34	33			470	480			+ 01	00			0	0		
9.00	1036	0.50		— 34	33	32			1050	1070			— 01	— 02			0	0.1		
log surf. 2.51. Abs. screens a $\varrho_1 = 8.5$, $\varepsilon = 0.7$; b $\varrho_1 = 9.5$, $\varepsilon = 0.7$.																				

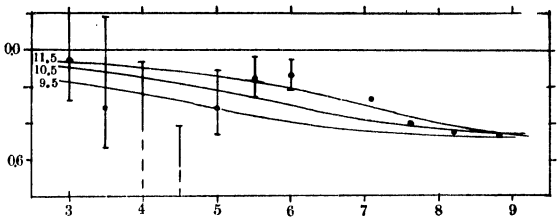

Fig. 12. Δ log A **in Taurus-Auriga, bright stars.**

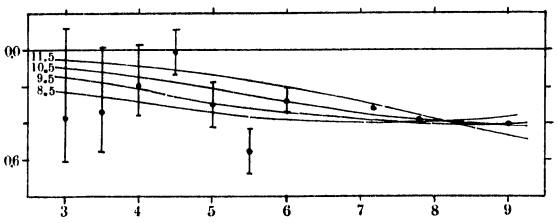

Fig. 14. Δ log A **in Ophiuches, bright stars.**

by means of the brighter magnitude classes. This has been done in the same way as was done in the Taurus region.

An area was delineated (*cf.* Fig. 13) where the number of *DM* stars was less than $^2/_3$ of the normal number. To ensure reduction elements for the magnitudes as homogeneous as possible the area was restricted to the realm of the „*Südliche Bonner Durchmusterung*", between — 2° and — 23° Decl.; moreover the most Western parts with high galactic latitude were omitted. Outlying separate areas, such as *S* of ϑ Ophiuchi, were not included; the parts *N* of α Scorpii, however, were. Within this coherent area, measuring 456.8 sq.d., a group of smaller parts, in which the density fell below 40 perc. of normal, was treated separately (surface 134.7 sq.d.). The stars of the *SDM* were counted between the limits 6.55 7.05....9.05; these were reduced to photometric scale by means of the Tables in *Publ. Amsterdam* **1** (Tables 33, 40, 41). The resulting photometric limits are 6.60, 7.24, 7.74, 8.36, 8.93 and 9.63; the counted numbers and also log A^1 and log A in Table 25 hold for the overlapping intervals 6.60—7.74, 7.24—8.36, 7.74—8.93, 8.36—9.63, with central magnitudes 7.17 7.80 8.33 and 9.00. The brighter stars were counted from *Harvard Annals* **50.**

From a Wolf curve drawn through the counted and the smoothed values of log A^1 it was seen that the most probable value for ϱ_1 must be lower than 10. So the computations and comparisons were made with $\varrho_1 = 8.5\ 9.5\ 10.5\ 11.5$, each combined with an absorption ε satisfying the lowest magnitude classes. In Fig. 14 these curves are represented in a graph of the data observed. In the computation of *E*, in view of the larger numbers counted for the lower classes, a value $\mu_s^2 = 10$ was assumed for the Harvard results.

The results for ΣE show that $\varrho_1 = 11.5$ would be far too large, and that the most probable value for ϱ_1 is 9,1, corresponding to a distance of 65 parsecs. The minimum value of ΣE being 7,4 is smaller than would be expected for 11 data with 2 unknowns. This small distance chiefly depends on the conspicuous lack of bright naked-eye stars in this region. The increase of Δ log A from 6^m to $9m$ in the most obscured part, however, indicates that here more remote parts also take part in the obscuration.

On the southern side of the Ophiuchus region a great number of larger and smaller dark markings are visible both on Milky Way photographs and visually, which, in these southern constellations, partly constitute a rift between the galactic branches. From the photographs it cannot be discerned whether they are outlying parts of this Ophiuchus nebula or independent absorbing masses at greater distance. This may be decided by star counts, at least for the larger among these markings.

Three such areas have been investigated by ROLF MÜLLER, by means of exposures made on the German astronomical Station at La Paz (Bolivia).[1]) The dark nebula *S* of ϑ Ophiuchi ($17^h\ 24^m$ — 26°, β = + 3°) is visible to the eye as the blackest part of the entire galactic zone and

[1]) Zschr. f. Astrophysik **3**, p. 261, 369; **4**, p. 365.

appears on the photographs of the Milky Way as a most conspicuous irregular dark region almost entirely devoid of stars. The nebulous region around ϱ Ophiuchi ($16^h\ 20^m$ $-24°$, $\beta = +16°$) is remarkable for the luminous nebulosities surrounding the brightest stars. The region SW of ξ Ophiuchi ($17^h\ 8^m$ $-22°$, $\beta = +8°$) has a much more complex structure; a small curved dark marking standing out between much less obscured parts.

The magnitude of each star in the dark fields was determined by estimating it within an artificial scale which was standardized by Selected Area exposures on the same plate. The results of the counts and reductions are given in Table 26, 27, 28. For the ϑ Oph. region the small blackest part of 1.90 sq.d. has been kept separate from the remaining 4.53 sq.d. In the same way, the darkest part of the ξ Oph. region, 3.09 sq.d. has been treated separately from the richer part, 3.38 sq.d. For the larger ϱ Oph. area (15.70 sq.d.) the counts are given from the 5 th to the 15 th magnitude. In all these regions we have compared them with absorbing screens at $\varrho_1 = 10.5,\ 11.5,\ 12.5$; for the computation of E we took $= 1.3\ \mu_s{}^2 = 40$.

The figures 15, 16, 17 with the curves, as well as the tables show that the representation of the data generally is not at all satisfactory. Large jumps occur in the points and make it difficult to choose the best curve. From three ΣE the most probable value for ϱ_2 may be derived by a parabolic formula; from ϑ Oph., the darkest part, we find 11.3, $r = 180$, (ΣE min. $= 4.4$), from the other part 11.7, $r = 220$, (ΣE min $= 13.8$), from ϱ Oph. 11.4, $r = 190$, (ΣE min $= 12.3$); ξ Oph., the darkest part A gives a highly uncertain indication of a

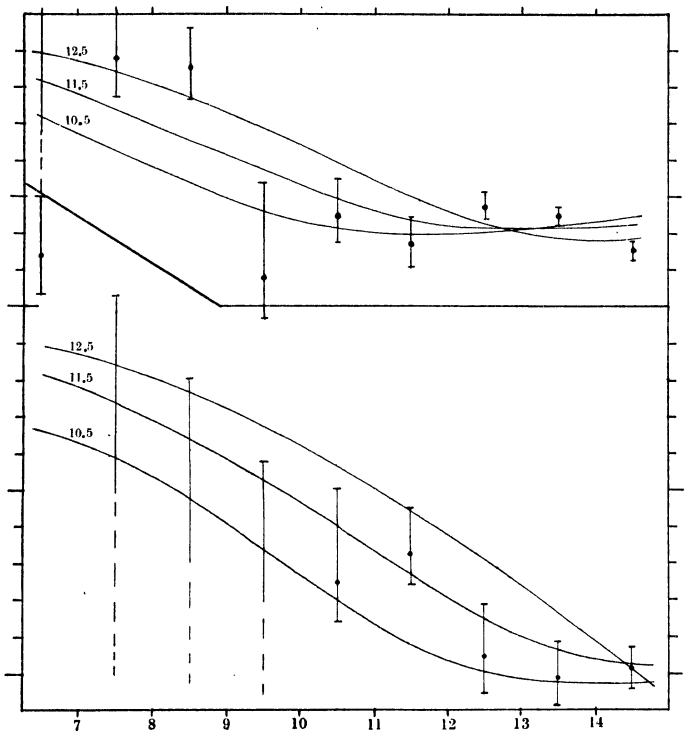

Fig. 15. Δ log A in ϑ Oph. field, R. Müller.

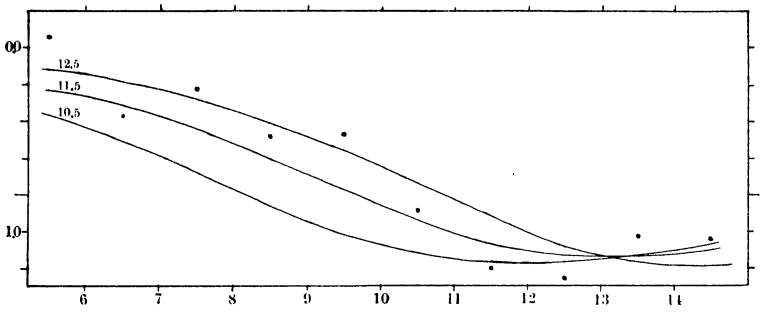

Fig. 16. Δ log A in ϱ Ophiuchus field, R. Müller.

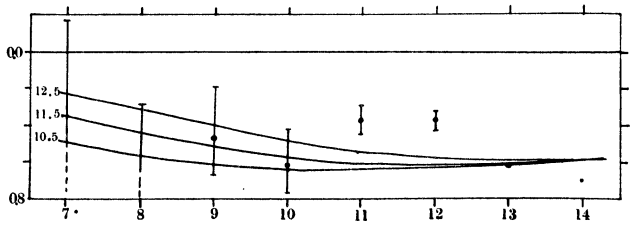

Fig. 17. Δ log A in ξ Ophiuchus field, R. Müller.

larger distance, and the other part B leaves such large residuals that it is not worth while giving computations in full. In both parts of this field there is a considerable excess of 11^m and 12^m stars.

For all these fields we find distances certainly greater than those found from the bright stars, though they doubtless belong to the Ophiuchus complex and are connected with it. So the same phenomenon presents itself here that in the case of the Taurus nebula was expressed as an apparent protruding of the darkest parts on the remote side.

Table 26. R. Müller, ϑ Oph. field ($\beta = +3°$).
Less dark part 4.53 sq.d. in the first, darkest part 1.90 sq.d. in the second table.

m	n	log A^1	log A	Δ log A	Δ log A comp. a	b	c	n comp.			$C-O$			E		
6.5	0	—	9.43	—	57	36	21	0.3	0.5	0.8				0	0	0
7.5	2	9.64	9.88	— 24	76	52	32	0.6	1.0	1.7	+ 52	+ 28	+ 08	3.4	1.4	0.3
8.5	5	0.04	0.33	— 29	93	69	45	1.1	2.0	3.5	+ 64	+ 40	+ 16	8.8	4.0	1.0
9.5	1	9.34	0.78	— 144	108	86	62	2.3	3.8	6.6	— 36	— 58	— 82	0.3	1.7	5.7
10.5	6	0.12	1.22	— 110	118	102	82	5.0	7.3	11.5	+ 08	— 08	— 28	0.4	0.1	2.6
11.5	12	0.42	1.67	— 125	120	113	100	13	16	21	— 05	— 12	— 25	0.1	0.7	3.9
12.5	52	1.06	2.11	— 105	119	117	115	38	40	42	+ 14	+ 12	+ 10	1.8	1.4	1.0
13.5	121	1.43	2.53	— 110	116	117	122	107	105	93	+ 06	+ 07	+ 12	0.6	0.8	2.2
14.5	199	1.64	2.93	— 129	111	115	123	300	280	230	— 18	— 14	— 06	6.8	4.0	0.7
														22.2	14.1	17.4
6.5	1	9.72		+ 29	68	37	21	0.1	0.2	0.3	—	—	—	4.6	3.2	2.4
7.5	0	—		—	82	53	32	0.2	0.4	0.7				0	0	0
8.5	0	—		—	105	72	47	0.4	0.8	1.4				0	0	0.7
9.5	0	—		—	132	95	65	0.6	1.3	2.6				0	0.5	2.4
10.5	1	9.72		— 150	160	120	86	0.8	2.0	4.4	+ 10	— 30	— 64	0.4	0	2.6
11.5	4	0.32		— 135	185	146	111	1.3	3.1	6.9	+ 50	+ 11	— 24	4.8	0.5	0.9
12.5	3	0.20		— 191	200	171	138	2.5	4.8	10.2	+ 09	— 20	— 53	0.3	0.3	5.8
13.5	6	0.50		— 203	205	188	168	5.8	8.5	13.5	+ 02	— 15	— 35	0.1	0.5	6.0
14.5	17	0.95		— 198	205	195	198	14	18	17	+ 07	— 03	— 00	0.2	0.0	0
														10.4	5.0	20.8

log surf 0.66 and 0.28. Abs. screen a $\varrho_1 = 10.5$, $\varepsilon = 2.8$ and 5.0; b $\varrho_1 = 11.5$, $\varepsilon = 2.9$ and 5.0; c $\varrho_1 = 12.5$, $\varepsilon = 3.2$ and ∞.

Table 27. R. Müller, ϱ Oph.ield ($\beta = +16°$) 15.70 sq.d.

m	n	log A^1	log A	Δ log A	Δ log A comp. a	b	c	n comp.			$O-C$			E		
5.5	1	8.80	8.73	+ 07	37	22	11	0.4	0.5	0.7	+ 44	+ 29	+ 18	1.8	1.4	0.7
6.5	1	8.80	9.17	— 37	52	31	18	0.7	1.1	1.6	+ 15	— 06	— 19	0.7	0	0
7.5	4	9.40	9.62	— 22	68	44	27	1.4	2.4	3.6	+ 46	+ 22	+ 05	4.3	1.5	0.2
8.5	6	9.58	0.06	— 48	85	60	40	2.6	4.6	7.2	+ 37	+ 12	— 08	4.1	0.7	0.1
9.5	17	0.03	0.50	— 47	102	77	55	4.8	8.5	14	+ 55	+ 30	+ 08	4.8	2.6	0.3
10.5	17	0.03	0.92	— 89	112	94	73	10	15	25	+ 23	+ 05	— 16	1.7	0.1	1.8
11.5	22	0.14	1.34	— 120	116	107	91	24	30	43	— 04	— 13	— 29	0.1	1.3	8.7
12.5	50	0.50	1.75	— 125	116	113	108	62	66	74	— 09	— 12	— 17	1.0	1.8	3.9
13.5	209	1.12	2.14	— 102	113	113	117	162	162	158	+ 11	+ 11	+ 16	2.2	2.2	4.1
14.5	483	1.48	2.52	— 104	107	110	119	450	420	340	+ 03	+ 06	+ 15	0.2	0.8	4.9
														20.9	12.4	24.7

log surf. 1.20. Abs. screen a $\varrho_1 = 10.5$, $\varepsilon = 2.9$; b $\varrho_1 = 11.5$, $\varepsilon = 3.0$; c $\varrho_1 = 13.5$, $\varepsilon = 3.4$.

Table 28. R. Müller, ξ Oph. field (+ 8°), darkest part *A* 3.09 sq.d., (*B* 3.38 sq.d.).

m	n A	n B	log A^1 A	log A^1 B	log A	Δ log A A	Δ log A B	Δ log A cp a	b	c	n comp· a	b	c	$O-C$			E		
7.0	0	1	—	9.47	9.57	—	—10	49	35	23	0.4	0.5	0.7	—	—	—	0	0	0
8.8	0	2	—	9.77	0.02	—	—25	57	44	31	0.9	1.2	1.6	—	—	—	0	0.4	0.9
9.0	3	3	9.99	9.95	0.46	—47	—51	62	52	40	2.1	2.7	3.6	+ 15	+ 05	— 07	0.7	0.2	0
10.0	6	8	0.29	0.37	0.91	—62	—54	64	58	48	5.8	6.6	8.3	+ 02	— 04	— 14	0.1	0	0.4
11.0	29	58	0.97	1.23	1.34	—37	—11	64	61	55	15	17	19	+ 27	+ 24	+ 18	3.4	3.0	1.8
12.0	78	183	1.40	1.73	1.77	—37	—04	63	62	58	43	44	48	+ 26	+ 25	+ 21	7.0	6.6	4.8
13.0	117	227	1.58	1.83	2.19	—61	—36	61	60	59	117	120	123	00	— 01	— 02	0	0	0.1
14.0	241	497	1.89	2.17	2.60	—71	—43	58	58	58	320	320	320	— 13	— 13	— 13	3.5	3.5	3.5
log surf. 0.49. Abs. screen *a* $\varrho_1 = 10.5$, $\varepsilon = 1.5$; *b* $\varrho_1 = 11.5$, $\varepsilon = 1.5$; *c* $\varrho_1 = 12.5$, $\varepsilon = 1.5$.																	14.7	13.7	11.5

The Cygnus rift.

The galactic rift in Cygnus, which is so conspicuous to the naked eye as a division of the Milky Way into two branches, has been the object of an investigation by HELMUT MÜLLER. [1]) In two small fields, a dark one midway between λ and γ Cygni ($20^h\ 36^m + 38°\ 15'$, $\beta = -3°$) and a bright one near λ Cygni ($20^h\ 45.5^m + 35°\ 15'$), the magnitudes of the stars down to 17^m were determined, and their numbers counted from the catalogue, whilst the colour indices were determined by photovisual plates. Because many plates with different exposure times were taken of each field a careful discussion of the mean errors was possible and the resulting magnitudes seem to have considerable accuracy.

The bright field was intended to be a comparison field, supposed to be free from absorption. The increase of log A with m in this field is more constantly steep than for latitude 0°—5° is normally the case after our Table 12. Table 29 gives a comparison of log A after H. MÜLLER's counts in his area and the normal values of Table 12 based on *Groningen Publ.* **43**. The shortage of bright stars may be due to chance by the smallness of the area; in the dark field there are more. So, in smoothing we adapt

Table 29. H. Müller, Bright Field in Cygnus.

m	n	log A	Normal with Diff.	Smoothed, with Diff.	*Smd—Norm*	Bal-Hase	Miller
10.5	—	—	1.22	1.23	+ .01	1.64 (54)	1.56
11.0	1	1.04	1.45	1.46	.01		
11.5	5	1.74	1.67 44	1.69 46	.02	1.88(97)	1.90
12.0	6	1.82	1.89	1.92	.04		
12.5	6	1.82	2.11 43	2.15 46	.04	2.40(310)	2.30
13.0	20	2.34	2.32	2.38	.06		
13.5	37	2.61	2.53 41	2.61 45	.08	2.57(460)	2.68
14.0	65	2.85	2.73	2.83	.10		
14.5	106	3.06	2.93 39	3.06 46	.13	2.75(690)	2.97
15.0	174	3.28	3.12	3.29	.17		
15.5	320	3.54	3.31 37	3.51 44	.20		
16.0	498	3.74	3.49	3.73	.24		
16.5	786	3.94	3.67 35	3.95 44	.28		
17.0			3.84	4.17	.33		

[1]) Astr. Nachr. **269**, p. 57 (1939).

Table 30. H. Müller, Dark field in the Cygnus rift ($\beta = -3°$) 0.1186 sq.d.

m	n	log A	Δ log A	Δ log A comp. a	b	Number comp.		$O-C$		E		Δ log A''	Comp. c	n cpt.	$O-C$	E
10.5	3	1.41	+ 19	23	13	1.1	1.5	+ 42	+ 32	3.2	2.0	+ 18	15	1.4	+ 33	2.2
11.0	6	1.71	+ 26	28	17	1.7	2.2	+ 54	+ 43	7.8	5.5	+ 25	20	2.1	+ 45	5.8
11.5	4	1.53	— 14	34	21	2.5	3.4	+ 20	+ 07	1.3	0.3	— 16	26	3.2	+ 10	0.5
12.0	3	1.41	— 48	40	26	3.6	5.0	— 08	— 22	0	0.4	— 51	33	4.6	— 18	0.2
12.5	9	1.88	— 23	46	31	5.2	7.4	+ 23	+ 08	2.8	0.5	— 27	41	6.5	+ 14	0.7
13.0	11	1.97	— 35	52	37	7.4	10.5	+ 17	+ 02	1.9	0.0	— 41	50	8.9	+ 09	0.8
13.5	17	2.16	— 37	58	43	10.5	15	+ 21	+ 06	1.8	0.2	— 45	60	12	+ 15	1.0
14.0	22	2.27	— 46	64	50	14	20	+ 18	+ 04	1.7	0.1	— 56	71	16	+ 15	1.3
14.5	22	2.27	— 66	69	57	20	27	+ 03	— 09	0.1	0.8	— 79	82	20	+ 03	0.1
15.0	28	2.38	— 74	73	64	29	36	— 01	— 10	0	1.2	— 91	91	28	00	0
15.5	42	2.55	— 76	75	70	43	48	— 01	— 06	0	0.5	— 96	98	40	+ 02	0.1
16.0	58	2.69	— 80	76	75	63	65	— 04	— 05	0.3	0.5	— 104	104	58	00	0
16.5	89	2.88	— 79	76	79	96	89	— 03	00	0.2	0	— 107	108	74	+ 01	0
17.0	154	3.11	— 73	75	82	145	123	+ 02	+ 09	0.1	2.2	— 106	110	138	+ 04	0.5
										21.2	14.2					13.2

log surf. 9.05. Abs. screen a $\varrho_1 = 15.5$, $\varepsilon = 2.5$; b $\varrho_1 = 16.5$, $\varepsilon = 3.0$; c $\varrho_1 = 16.5$, $\varepsilon = 2.7$.

log $A(m)$ for this area to the normal curve at its bright end ; its surplus of stars increases regularly with m. This increasing surplus of faint stars may be represented by a greater density at distances above 1000 parsecs. The values of MÜLLER's bright region are, however, not in accordance with those of other observers. Among the „normal'' comparison fields of BALANOVSKY and HASE [1]) Field III ($20^h\,42^m + 35.°3$), situated very near to MÜLLER's bright area, has values of log A as given in the 7^{th} column. Three areas counted by F. D. MILLER [2]) in the Cygnus cloud give the values of the 8th column. Both have a greater number of bright stars, but for the fainter magnitudes a more rapid decrease. It may be that in both these cases local absorptions play a part ; but it is not certain that we have to consider the small bright field counted by H. MULLER as the only field, where without absorption we see the normal distribution of stars present in the entire region of the rift between the Milky Way branches. We shall first assume, therefore, that in this case the normal distribution of Table 12 holds. The data for the dark field and the reductions are given in the first part of Table 30. The results as well as the curves in Fig. 18 show that $\varrho_1 = 14.5$ would give too large Δ log A ; only for $\varrho_1 = 15.5$ and 16.5 do the curves fall between the points, and $\varrho_1 = 16.3$ ($r = 1800$ parsecs) fits them in the best, though not entirely satisfactory way. The values of E have been computed with $f = 1{,}20$ $\mu_s^2 = 20$.

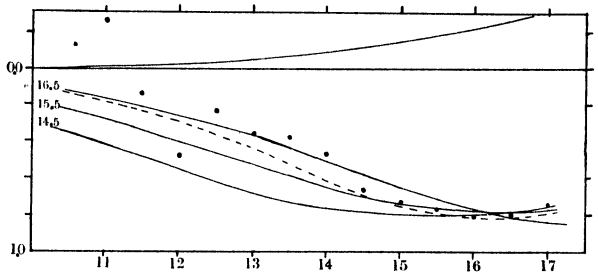

Fig. 18. Δ log A in Cygnus field, H. Müller.

A comparison with the smoothed results of the bright field, on the supposition that they represent a local normal distribution, is given in the second part of the same table. To account for this unobscured distribution an increased density at great distance had to be

[1]) Harvard Annals **105**, p. 304.
[2]) Pulkowo Bulletin **14**, Nr. **2**, p. 5.

assumed, and $\Delta \log A''$ had to be computed on the basis of this density distribution. It appeared that even with $\varrho_1 = 16.5$ the computed $\Delta \log A''$ would be too large for nearly all the brighter magnitudes; so a somewhat greater distance *e.g.* $\varrho_1 = 17$ $r = 2500$ may be estimated. In Fig. 18 the differences between the smoothed local and the normal log A are represented by the line curved upward; the depression of the points below that line represent the $\Delta \log A''$, and the dotted curve represents this case with $\varrho_1 = 16.5$.

These results, however, cannot be considered as proof that the absorbing matter is really situated at that great distance of nearly 2000 parsecs. The result for distance always depends to a large extent on what values of log A are assumed to be the normal ones. Whereas MÜLLER's small bright area showed less bright stars than our table of normals, most investigations give, for the Cygnus region, a greater abundance than is normal for stars of all magnitudes, indicating a greater density than is normal at distances between 300 and 1000 parsecs, and perhaps extending still farther. If the counted log A of a dark area are compared with such greater log A, the $\Delta \log A$ will be larger, and a smaller distance is then found for the absorbing matter. Hence the determination of distance for the dark matter in Cygnus must be preceded by a special examination of the local unobscured distribution.

This line of research has been followed by F. D. MILLER in his „Investigations on Galactic Structure, Part II. The Milky Way from Cygnus to Aquila"[1]) As a part of the Harvard program devised by BOK counts were made on the plates of all stars brighter than the images of an artificial scale standardized by means of S. A. fields and the Polar Sequence. A large number of fields, spread over the Cygnus region, the exact position of which is not given and is only indistinctly indicated on the accompanying map, were counted. To have a sufficient number of stars for the brighter classes without making the number for the fainter classes too large, larger areas were counted for the former, and smaller parts of them for the latter. Since, for the bright magnitudes where the absorption begins, $\Delta \log A$ is nearly independent of ε, this procedure cannot give appreciable systematic errors whereas chance errors due to too small numbers are avoided. The chief purpose of the paper is the distribution of density, which on different assumptions is derived from the counts in apparently unobscured areas. On the basis of this density distribution a number of obscured fields is discussed and their distance determined. Mostly distances above 1000 up to 2500 parsecs are found; W of the America nebula and in the dark parts near ξ Cygni distances 500—600 are given, and farther S, towards Aquila smaller distances indicate an encroachment of outlying parts of the nearby Ophiuchus nebula. Though the original data are not given in sufficient extension to render independent judgment possible, the careful method of discussion applied in this paper make it a valuable and reliable contribution. The dark matter producing the galactic rift in Cygnus is far more remote than the nebulosities of Taurus and Ophiuchus; this is the origin of the fact, already noted by ARGELANDER himself, that this rift is hardly perceptible in the Bonner Durchmusterung stars. Whether less conspicuous nebulosities also occur here at small distances can be coucluded only from star counts, when the distribution of bright stars over large regions is studied.

Still, the structure of the obscuring matter in this region is complicated, as is apparent from the great range of distances derived and the complex structure visible on Milky Way photographs. A great number of specimen gaugings, consisting in combined determinations of magnitude, colour and spectrum, will be necessary to clear up entirely the structure of this part of space.

---

[1]) Harvard Annals **105**, Tercentenary Papers, p. 297 (1937).

III. THE SURFACE DISTRIBUTION OF NEARBY ABSORBING MATTER.

Treatment of surface distributions.

We now know that we are surrounded by absorbing matter distributed irregularly through the central layers of the galactic systerm ; and the problem that faces us is to find the density (*i.e.* absorbing power) of this matter at every point in space. From our point of observation this means determining the density, as a function of distance, for every direction in space. All exsiting investigations have the character of measurements at selected points only; they deal with small areas of the sky and give information about the distance of the chief darkening nebulae in these directions only.

The general problem splits up, just as in the case of the stars, into two parts; that of the lateral distribution, or the surface distribution over the sky, and that of the distribution in depth or distance. As with the stars, the former is an immediate datum of observation. The arrangement in depth, expressed in the case of the stars by the density $D(r)$, has to be deduced from the number of stars as a function of apparent magnitude $A(m)$. In the same way for the dark matter the distribution in depth of the absorption $\varepsilon(r)$ has to be deduced from the deficiency in the number of stars of each magnitude $\Delta \log A(m)$.

For the space density distribution, therefore, we have to proceed from the surface distribution of the stars of different magnitude-classes. In that of the brighter classes the distribution of the nearby absorbing matter is shown. By compering the distribution of fainter star-classes, mainly situated at a greater distance, with that of the brighter stars the regions of more or less strong additional absorption, due to dark matter at a greater distance, are found. By making use, therefore, of consecutively fainter star-classes the distribution of the absorbing matter at incraesing distances may be found; with this restriction, of course that, firstly, just as with the stars, the great dispersion in absolute brightness of the stars smoothes out all the variations with distance and renders their determination difficult. And secondly, as distinct from the case of the stars, that the nearby nebulous matter covers the more remote and obliterates the latter in its effects, so that penetration into greater depth becomes more difficult.

As data of observation only such catalogues and counts can be used that are sufficiently homogeneous and completely cover the sky, or at least those large parts of the sky (the galactic zone) which are to be investigated. Among existing sources these are first, the *Durchmusterung* catalogues, giving the stars to nearly 10^m; then the Harvard Map, going down to $11—12^m$, and the Franklin-Adams maps containing the stars down to $15—16^m$. Perhaps we may insert between these the far less homogeneous and still incomplete ,,Carte du Ciel'', of which the catalogues go down to nearly 12^m and the charts to 14^m.

In the following only the distribution of the Durchmusterung stars will be investigated.

Theoretical computation.

The influence of absorbing matter at different distances upon the number of stars $N(m)$, from the brightest down to a limiting magnitude m can be treated in the same way as its influence on the number $A(m)$ of magnitude m. The stars brighter than m, situated at distance r (with distance modulus ϱ) have an absolute magnitude brighter than $M = m - \varrho$. Their number can be expressed by the same kind of formula as $A(m)$, if we introduce an integral luminosily function

$\Psi(M)$, giving the number of stars from the absolutely brightest down to absolute magnitude M, per cubic parsec near the sun.

$$\Psi(M) = \int_{-\infty}^{M} \Phi(M)dM\,; \quad N(m) = [0.147 - 4]\int_{-\infty}^{+\infty} D(\varrho)\,\Psi(m-\varrho)\,10^{0.6\varrho}\,d\varrho.$$

In the case of an absorbing screen at distance ϱ_1 this integral has to be split into two, separated at ϱ_1, with the argument $m - \varrho$ in one of them replaced by $m - \varrho - \varepsilon$, just as in the expression for $A^1(m)$ p. 8.

Instead of computing these expressions we have made use of the computations already performed of $A(m)$. By simply adding the numbers $A(m)$ or $A^1(m)$, for which $\log A(m)$ and $\Delta \log A(m)$ are given in Table 2, p. 10 (for $\beta = 5°$, vis. magn.) we find $N(m)$ for the cases of absorbing screens at distances $\varrho_1 = 9.5 \ldots 17.5$. In view of the available sources of starcounts the results have been derived for three equally spaced limiting magnitudes 9.5, 12.5, and 15.5. In Table 31 the logarithmic deficiencies $\log N^1(m) - \log N(m)$ are given for the cases $\varepsilon = 1, 2, 3$ magn. and for complete obscuration $\varepsilon = \infty$.

Table 31. Decrease of number of stars $\Delta \log N(m)$ for different ϱ_1 and ε.

ϱ_1	$m = 9.5$				$m = 12.5$				$m = 15.5$			
	$\varepsilon = 1$	2	3	∞	$\varepsilon = 1$	2	3	∞	$\varepsilon = 1$	2	3	∞
9.5	.464	.867	1.125	1.268	.414	.850	1.288	2.143	.341	.708	1.099	3.089
10.5	.419	.717	0.855	0.910	.410	.823	1.196	1.650	.340	.706	1.093	2.516
11.5	.343	.526	.589	.609	.392	.752	1.012	1.208	.339	.699	1.070	1.972
12.5	.243	.339	.365	.372	.352	.616	.758	0.832	.334	.676	0.996	1.481
13.5	.148	.192	.201	.203	.281	.443	.508	.533	.318	.614	.843	1.059
14.5	.077	.095	.098	.099	.196	.281	.308	.316	.282	.504	.635	0.719
15.5	.034	.040	.041	.042	.118	.158	.167	.171	.225	.365	.429	.460
16.5	.013	.015	.015	.015	.060	.076	.080	.080	.156	.232	.259	.270
17.5	.005	.004	.004	.004	.026	.031	.032	.032	.092	.129	.139	.143
	$\log N(m) = 0.963$				$\log N(m) = 2.292$				$\log N(m) = 3.392$			

The results for $\Delta \log N(m)$ as a function of ϱ_1, the distance, and ε, the amount of absorption, are represented in the Figures 19, 20, 21, in the form of a ϱ_1-ε diagram in which curves of equal $\Delta \log N$ are drawn.

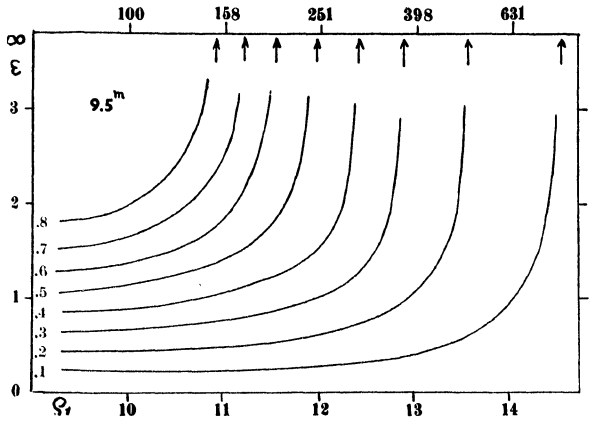

Fig. 19. Lines of constant deficiency in log $N(9.5)$.

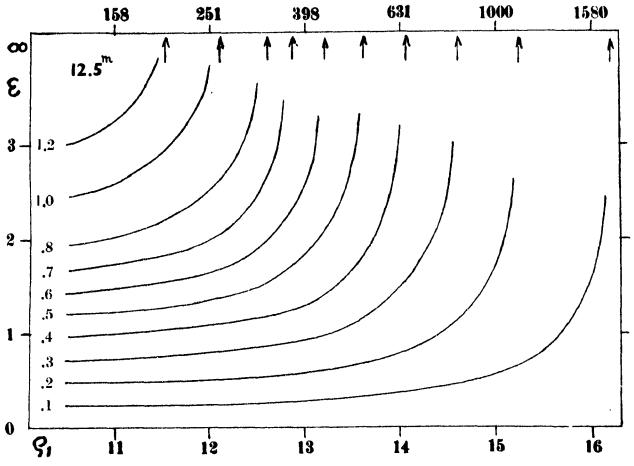

Fig. 20. Lines of constant deficiency in log $N(12.5)$.

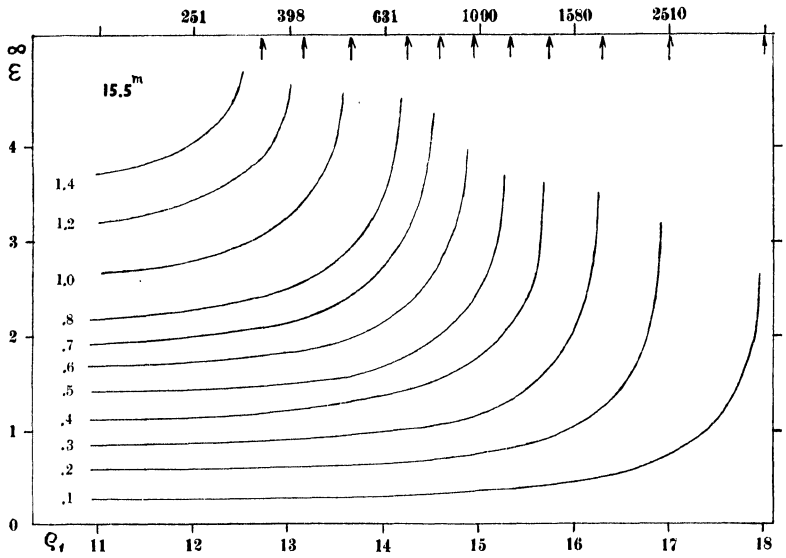

Fig. 21. Lines of constant deficiency in log N(15.5).

These diagrams show at a glance in what way the distribution of the stars down to a certain magnitude (e.g. the Durchmusterung-stars down to photometric 9.5) represents the distribution of absorbing matter within a certain distance. Small deficiencies of stars may be due to more distant absorbing matter obscuring the remote specimens of the stars considered, as well as to weak nearby absorptions. Great deficiencies of stars, however, can only be caused by absorbing matter at a small distance; smaller according as the deficiency is greater. The limit for each Δ log N is given by the distance at which a completely obscuring screen must be placed in order that the remaining foreground stars shall constitute precisely this fraction of the total number. This upper limit of distance is given for each Δ log N in Table 32; first as ϱ, then as r, distance in parsecs.

Table 32. Upper limit of distance of absorbing screen for different Δ log N.

m	0.10	0.20	0.30	0.40	0.50	0.60	0.70	0.80	1.00	1.20	1.50	2.00
	$\varrho_1 =$											
9.5	14.5	13.5	12.9	12.4	11.9	11.5	11.2	10.8	10.2			
12.5	16.2	15.3	14.6	14.1	13.6	13.2	12.9	12.6	12.1	11.6		
15.5		17.0	16.3	15.8	15.3	14.9	14.6	14.2	13.7	13.1	12.5	11.4
	$r =$											
9.5	791	505	377	298	243	203	172	148	112			
12.5	1770	1140	836	652	532	446	380	331	261	207		
15.5		2500	1820	1430	1170	964	824	705	540	425	310	195

This table shows that, when the number of stars brighter than 9.5 is reduced to *e.g.* $^1/_4$ (Δ log $N = 0.60$) the absorbing matter must be nearer than 200 parsecs. So it gives a numerical expression to the qualitative thesis that the irregularities in the surface density of these brighter telescopic stars represent the distribution of the nearby absorbing matter.

The Bonn and Cordoba Durchmusterung Catalogues.

For the surface distribution of the stars down to the 9th magnitude we have to make use of the Durchmusterung Catalogues of Bonn and Cordoba.

It is a very curious thing that, after half a century of rapid development of celestial photography and refinement of photometric methods, we are still compelled, for such a simple matter as the distribution of the brighter telescopic stars, to have recourse to the relatively coarse estimates of the Bonn observers of almost a century ago. Admirable and ingenious tho' their work was

for that time, it cannot be considered adequate for our present needs. It was intended for identifying and mapping purposes, not for magnitude determinations. Surely the technique of photographic photometry during many decades has already been able to provide for good magnitudes (say with no greater p.e. than $0^m.10$) of all stars down to the 9th magnitude, and within a reasonably limited time. It is indeed a remarkable fact that no observatory has as yet undertaken such a program of work. For the present, therefore, we cannot do otherwise than make use of counts of stars in the DM catalogues, with all the errors and uncertainties they contain.

These uncertainties concern not only the large chance errors, but chiefly the reduction of the estimates to photometric scale. The estimates were made on a mental scale, variable from night to night, and even in the same night under variable conditions (stardensity, fatigue), different for different zones, different years, and different observers. The derivation of reductions to photometric scale presupposes a certain constancy; but what we find is an average of which we do not know how far it holds for specific cases.

The reductions can be deduced only by comparison with a limited number of photometrically measured stars, in this case restricted to some narrow zones at 5° interval of declination. Whether they hold, or how they must be interpolated for intermediate zones, remains uncertain. Yet we have to content ourselves with corrections deduced in this way, and we can only hope that the essential features of the distribution will emerge.

An extensive discussion of the corrections to the DM magnitudes was given in *Publ. Amsterdam* **1.** With the exception dealt with in the next paragraph we have used them here as they were given there. For the Bonn DM the stars for every square degree were counted down to 9.0 inclusive, so that the limit of counting is 9.05 DM scale. The photometric equivalent of DM 9.0 was taken from *Publ. Amst.* **1,** Table 26, corrected for Rectascension after Table 30; the result was taken to hold for the middle of each hour of AR in the middle of each zone of 5° width, and was interpolated for separate degrees of declination and areas of 20^m in AR. For the half-width of the decimal 9.0 an amount of 0.08 was added. The reduced magnitudes on the average are about 9.3. So **9.30** was assumed as the exact photometric limit for the reduced counts. If, for a counted area, the computed photometric equivalent of 9.05 is m, then the counted number of stars has to be multiplied by $N(9.30)/N(m)$. Assuming, as sufficient approximation for this case, $\log N(m) = a + bm$ with $b = 0.50$, the logarithm of the correction factor is $0.50\ (9.30—m)$. This factor is combined with the factor sec δ for the reduction of the 4^m AR area into a square degree. From 50° to 70° of declination a width of 8^m, from 70° to 80° a width of 20^m in AR was counted as one area. In this way the surface density of stars down to 9.30 vis. was derived from the counts.

A correction for density was not applied. Since we do not know its exact origin, whether from the differences in glare of the stars influencing the contraction of the pupil, or from the lesser or greater leisure in noting all the stars, we cannot see what average density, of a larger or a smaller field, must be taken as argument, especially in the case of rapid variations. The effect of this correction would be to enhance the great and to diminish still further the small values of density. Then location and form of the dense and the poor regions would not be altered, but solely the amplitude of their difference would be slightly enhanced. The omission of this correction, therefore, can only have the effect of getting the deviations from the mean a fraction or so too small.

The same procedure was followed for the SDM (— 2° to — 23°), where *Publ. Amst.* **1,** Tables 40 and 41 were used, and a half width 0.12 for the decimal 9.0 was assumed. The Cordoba DM in its second part, from — 42° to — 62°, was counted down to 9.2 incl., *i.e.* to the catalogue limit 9.25. The corrections to photometric scale were taken from Table 52 (mean of the corrections for 9.15 and 9.35) and Table 55.

Corrections to the Cordoba DM between —22° and —42°.

A close inspection of the zones of the 1st part of the Cordoba DM showed that the discussion in *Publ. Amsterdam* 1 did not go into details suffciently to represent the rapid and irregular variations in scale. A fresh discussion, therefore, was needed here. Especially in the galactic regions, jumps seemed to occur. A graph, however, of all the separate differences between the Cordoba and the Harvard photometric magnitudes showed that, by taking half hour averages, the rapid changes were well rendered. So here half-hour means, and for the rest of the zones hourly means were taken. They are given in Table 33 (the number of separate stars is added in smaller type) ; first for the stars 8.5 (8.3 to 8.7), and then for 9.0 (8.8 to 9.2).

Table 33. Differences Harvard 34—Cordoba DM for 8.6^m and 9.0^m.

Hour	Zone — 25°	Zone — 30°	Zone — 35°	Zone — 40°
0	+ 41 6 + 55 6	+ 62 3 + 64 6	+ 61 5 + 69 4	
1	+ 29 7 + 52 6	+ 52 10 + 42 4	+ 46 9 + 51 6	+ 36 6 + 50 2
2	+ 27 8 + 59 5	+ 42 4 + 30 6		
3	+ 50 9 + 49 10	+ 51 8 + 23 4	+ 36 13 + 46 7	+ 21 4 + 67 5
4	+ 58 10 + 65 3			
5	+ 39 9 + 50 15	+ 36 11 + 37 5	+ 47 5 + 62 4	+ 29 9 + 18 6
6, 1	+ 44 6 + 56 9	+ 65 5 + 69 5	+ 16 12 + 27 4	+ 59 8 + 47 3
6, 2	+ 48 5 + 58 10	+ 80 5 + 41 4		
7, 1	+ 03 5 + 29 9	+ 36 8 + 46 8	+ 43 6 + 50 11	— 03 7 + 37 3
7, 2	+ 00 4 + 21 9	+ 51 3 + 54 9	+ 05 6 + 59 12	+ 35 7 + 35 4
8, 1	— 09 7 + 15 5	+ 46 5 + 46 9	+ 30 9 — 12 4	+ 13 6 + 20 10
8, 2	+ 54 7 + 37 5	+ 40 5 + 64 8	+ 55 9 + 10 3	— 02 6 + 37 10
9, 1	+ 82 10 + 96 7	+ 61 10 + 48 3	+ 42 4 + 50 9	+ 38 6 + 29 7
9. 2				+ 54 6 + 23 7
10	+ 78 11 + 105 10	+ 61 8 + 67 9	+ 58 6 + 55 6	+ 32 9 + 35 7
11	+ 57 6 + 61 12	+ 29 6 + 68 7	+ 60 5 + 26 5	+ 71 5 + 58 8
12	+ 41 5 + 46 14	+ 74 9 + 54 10	+ 66 6 + 72 8	+ 67 5 + 55 6
13	+ 40 5 + 75 11	+ 65 9 + 66 14	+ 51 9 + 16 7	+ 83 5 + 48 4
14	+ 60 7 + 67 9	+ 66 5 + 81 14	+ 75 7 + 66 3	+ 44 8 + 55 4
15, 1	+ 36 5 + 37 11	+ 31 2 + 52 21	+ 72 11 + 53 3	+ 46 5 + 52 6
15, 2				+ 63 5 + 46 7
16, 1	+ 27 8 + 19 13	+ 69 8 + 71 6	+ 54 6 + 58 5	+ 69 7 + 47 8
16, 2		+ 45 8 + 62 7		
17, 1	— 27 3 + 33 8	— 27 4 + 19 12	+ 33 9 + 64 5	+ 43 6 + 47 8
17, 2	+ 32 3 + 25 8	— 07 5 + 15 12	(— 28 13 — 02 7)	+ 31 7 + 29 7
18, 1	+ 15 4 — 04 8	— 04 4 + 27 8	+ 06 13 + 25 9	+ 12 8 + 25 4
18, 2	+ 15 3 + 47 9	+ 17 3 + 58 8		
19	+ 52 3 + 20 7	+ 45 8 + 54 13	+ 40 13 — 07 4	+ 22 9 + 25 4
20	+ 37 5 + 17 17	+ 68 9 + 54 8	+ 70 5 + 105 2	+ 39 6 + 40 8
21				
22	+ 50 6 + 56 4	+ 42 8 + 61 12	+ 67 8 + 64 5	+ 43 5 + 31 8
23				

It appears that, for these two groups, the values and the variations with AR are almost identical ; so they could be combined in one graph and a common curve drawn through the points. The readings of these curves are given in Table 34.

Table 34. Differences Ha—Cord (curves) in 0.01^m.

AR	25°	30°	35°	40°	*AR*	25°	30°	35°	40°
$0^h\ 0^m$	+ 46	+ 60	+ 62	+ 40	13^h	+ 59	+ 66	+ 57	+ 60
1	48	55	59	41	14	51	68	58	58
2	50	43	56	41	15	42	65	60	55
3	52	37	53	42	16	31	53	57	52
4	55	37	50	41	17 0^m	22	27	47	47
5	55	42	47	40	17 30	19	10	38	37
6	52	56	44	38	18 0	19	09	25	26
7 0	35	51	38	32	18 30	20	25	14	21
7 30	18	48	31	28	19 0	23	41	14	21
8 0	07	48	24	24	19 30	27	50	22	25
8 30	28	50	27	22	20	30	54	36	29
9	60	53	38	26	21	35	58	55	37
10	82	58	52	38	22	41	60	66	40
11	77	60	55	50	23 0	44	60	66	40
12	68	62	56	60					

The corrections to be added to the Cordoba magnitudes are generally so large, that, in order to come near to the photometric magnitude 9.30, the catalogue limit must be taken below 9.0. Therefore the stars to 8.8 incl. were counted here ; only for the denser galactic regions where the corrections, after Table 34, fall to a low value, were they counted to 9.0 incl. (from $7^h\ 0^m$ to $9^h\ 0^m$, and from $16^h\ 20^m$ (for the zones 22° to 31°) or $17^h\ 40^m$ (for the zones 32° to 41°) to $19^h\ 40^m$). The limits in the catalogue scale, 8.85 and (taking the decimal error into account) 9.06 are reduced to photometric scale by taking the corrections for 8.75 from Table 34 and adding to them the mean difference be-

Table 35. Photometric equivalents for Cordoba magnitudes.

	Limit 8.85					Limit 9.06			
AR	I	II	III	IV	*AR*	I	II	III	IV
5 0	9.40	9.24	9.33	9.24	7 0	9.47	9.72	9.50	9.43
6 0	36	43	29	21	20	32	69	43	39
6 30	32	45	27	18	40	11	67	37	35
7 0	14	36	21	14	8 0	09	68	31	32
7 30	8.99	32	12	08	20	29	70	32	30
8 30	9.05	34	07	01	40	54	73	40	31
9 0	47	38	21	06	9 0	86	76	50	35
9 30	73	42	34	12					
10 0	82	45	40	21	16 20	9.37	9.64	9.76	
10 30	78	47	42	29	40	33	52	70	
11 0		48	44	37	17 0	29	37	63	9.64
12 0			45	51	20	26	20	54	55
13 0				51	40	24	12	44	45
14 0	9.35	9.60	9.48	48	18 0	25	13	32	35
15 0	23	55	51	44	20	26	26	21	31
15 30	16	48	49	42	40	28	42	15	26
16 0	08	38	47	40	19 0	31	57	17	28
16 30	02	24	41	37	20	34	66	23	31
17 0	8.97	05	33	33	40	37	73	34	35
17 30		8.84	21	20					

between the correction for these limits and that for 8.75, as well as the corrections for incompleteness of the catalogues after *Publ. Amst.* 1, p. 58—60. So we find the photometric equivalents of the two limits of counting as given in Table 35. They hold for narrow zones along the parallels of 25°, 30°, 35° and 40° and are numbered I—IV.

These comparisons can give no indication as to how the corrections for the consecutive zones change with declination. That there have been gradual changes in the conditions of observation and the mental scale of estimates is shown by the differences between the curves I—IV, of which the second has a larger average amount than the others. It is shown also by the changes in the total number of stars observed in each zone of declination. These numbers, reduced to equal surface by the factor sec δ are shown in Table 36.

Table 36. Reduced number of stars in Cordoba zones.

Zone	log N sec δ	Zone	log N sec δ	Zone	log N sec δ	Zone	log N sec δ
22°	4.253	27°	4.270	32°	4.328	37°	4.291
23	297	28	322	33	308	38	303
24	296	29	338	34	296	39	299
25	270	30	362	35	295	40	304
26	276	31	361	36	303	41	309

We see here, beginning from 28°. a gradual rise to a maximum in the zones 30° and 31°; then a decrease, but not entirely to the low values of the zones North of — 28°. This variation corresponds to the large value in II of Table 35. It appears probable, therefore, that both variations occurring simultaneously are due to the same mental process : at 27—28° a change sets in which, at 30°—31°, attains a maximum, and then returns at 33°—34° to normal values slightly higher than in the first zones. We will assume, therefore, the values I for zones 22° up to 27°, II for 30° and 31°, III for 34°, IV for 40°—41°, and values interpolated from Table 35 according to declination for the other zones. With these photometric equivalents for the limiting magnitudes the reduction to limit 9.30 was performed as explained above.

Corrections to the Cordoba DM between —62° and the South Pole.

In our discussion in *Publ. Amsterdam* 1 we had to omit the part below — 62°, because the Cordoba DM was only completed down to that limit. Since then the last part of this DM was published in 1932 in Vol 21 of the „*Resultados del Obs. Nac. Argentino*". In order to make use of these zones for the present purpose we had to derive systematic corrections to reduce the estimated magnitudes to the photometric scale. Here, however, great difficulties stood in our way.

According to the Introduction by Prof. PERRINE the completion of these zones had met with several impediments spoiling the homogeneity of the work. In 1914 CHAUDET began observing the extreme polar zone — 82° to — 90° with the meridian circle; then in the years 1923—26 he observed the zones — 62°, 63°, 64°. The remaining zones from — 65° to — 81° incl. were observed between1926 and 1930 by Mr. TRETTER. So the different zones have to be discussed separately.

The following sentence in PERRINE's Introduction presented us with another, more serious diffculty :

„The scale of magnitudes adopted was that of Harvard. As a general rule, before commencing the observing, some of the Harvard magnitudes were noted in the telescope, the estimates of magnitude being in most cases the result of memory. For this reason the Harvard magnitudes were adopted where they existed, if there was no reason to suspect variability''.

In *Public. Amsterdam* 1 it was pointed out how every observer gradually acquires a scale of his own, the relation of which to a photometric scale can be ascertained afterwards by comparing the estimated magnitudes with the photometric ones. If he tries to adapt his scale continually to the photometric one, the result usually is great instability without actually reaching conformity with the latter. Matters are worse, however, if for the comparison stars not the estimated, but the foreign photometric magnitude is given in the catalogue. Then, all means of ascertaining the relation of the scales are lacking. So, after the statement in the Introduction, it must, indeed, appear impossible to derive systematic corrections to the magnitude scale of these Cordoba zones.

When finally making the experiment, however, it appeared that this statement must rest on a misunderstanding ; in comparing the DM with the Harvard magnitudes, as measured with the Rumford photometer (Harvard Annals Vol 72 p. 131 sqs) they were found to be generally different. So we have assumed that the printed magnitudes in the DM catalogue represent the observer's estimates and may be used to derive the systematic corrections.

We have of course, to treat the two observers separately ; from the data it will be seen that their methods of observing were different. In CHAUDET's zone — 62° the faintest magnitude recorded is 9.5, in the next zones it is 9.7. TRETTER, in the zones —65° to —81°, notes magnitudes down to 10.2. In accordance with this his number of stars is larger, 16.7 per sq. d., whereas in the first three zones of CHAUDET there are only 9.4, and in the polar cap (which, owing to its greater galactic latitude, is not further discussed here), 7.3. Sudden jumps appear, of course, at the boundaries of these parts. The total number of Harvard comparison stars is small : only 29 for the first three Chaudet zones, and 130 for the Tretter zones. It was not possible, therefore, to derive minor fluctuations with declination or Rectascension. We had to content ourselves with deriving corrections merely as a function of magnitude. The differences Harvard 72 — Cordoba DM are given in Table 37.

Tabje 37. Differences Ha 72—Cordoba.

— 62, 63, 64°			— 65 to — 81°		
m Cord	*H—C*	*n*	*m* Cord	*H—C*	*n*
8.3	— 0.09	7	7.3	+ 0.06	6
9.0	+ .09	5	7.8	— .01	9
9.2	+ .01	5	8.1	+ .17	11
9.5	+ .26	8	8.4	+ .02	10
			8.65	— .04	9
			8.85	+ .14	8
			9.0	+ .08	6
			9.1	— .11	5
			9.2	+ .14	7
			9.3	— .18	8
			9.4	+ .20	5
			9.52	+ .13	13
			9.76	+ .22	13
			10.02	+ .36	20

This table shows at first small, slowly increasing and then for the fainter magnitudes, rapidly increasing corrections to the DM. There must be, moreover, considerable decimal errors, since different decimals occur in very unequal numbers. By counting all the stars including every next tenth magnitude, hence, after reduction to a square degree, finding $N(m + 0.05)$ for consecutive limits and comparing them with tables of $N(m)$, we may find ,,statistical magnitudes'' corresponding to these limits. They are given in Table 38, first part. They are used to derive the extent of each decimal, and decimal corrections to the smoothed results of the photometric comparisons. In this way the finally adopted photometric equivalent for each limit was derived as given in the second part of Table 38.

Table 38. Photometric equivalents of Cordoba limiting magnitudes.

m	Statistical m		Photometric m	
	62°—64°	65°—81°	64°—64°	65°—81°
8.95	8.60	8.99	8.60	9.01
9.05	9.07	9.13	9.15	9.13
9.15	9.09	9.17	9.19	9.16
9.25	9.31	9.40	9.44	9.38
9.35	9.36	9.49	9.51	9.47
9.45	9.41	9.54	9.57	9.52
9.55	9.76	9.76	9.95	9.74
9.65		9.84		9.82
9.75		9.93		9.94
9.85		10.07		10.10
9.95		10.15		10.21
10.05		10.43		10.51

To obtain the numbers for the adopted limit 9.30, the stars in all the separate areas were counted down to 9.2 incl, *i.e.* to 9.25. To account for the remaining corrections — 0.14^m and — 0.08^m we have to multiply the counted numbers by factors whose log is — 0.066 and — 0.037. In the zones — 62° to — 71° areas of 8^m in AR, — 72° to — 81° areas of 20^m in AR were counted.

Results for surface distribution.

Thus, over the entire galactic zone, for areas of nearly a square degree, we have the number of stars (computed with one decimal) per sq. d. down to the limit 9.30^m. These numbers, rounded off to entires, are collected in six schematic representations p. 58—63.

These values of the surface density, as they stood with one decimal, were smoothed into averages of 4 adjacent areas, so that we got densities over 4 square degrees around points situated at consecutive full degrees of declination and rectascension. The logarithms of these smoothed densities were compared with ,,normal'' values of log N (9.30), for which the following values were adopted:

β =	0°	5°	10°	15°	20°	25°	(gal. pole 193° + 27°)
log $N(9,3)$ =	0,88	0.86	0.83	0.79	0.74	0.69	(Publ. Amst. 1, p. 15)
$N(9.3)$ =	7.6	7.3	6.8	6.2	5.5.	4.9	

The differences Δ log $N(9.3)$ were inserted into maps, and isanomales for positive or negative multiples of 0.10 were drawn to represent the areas of surplus or deficient density.

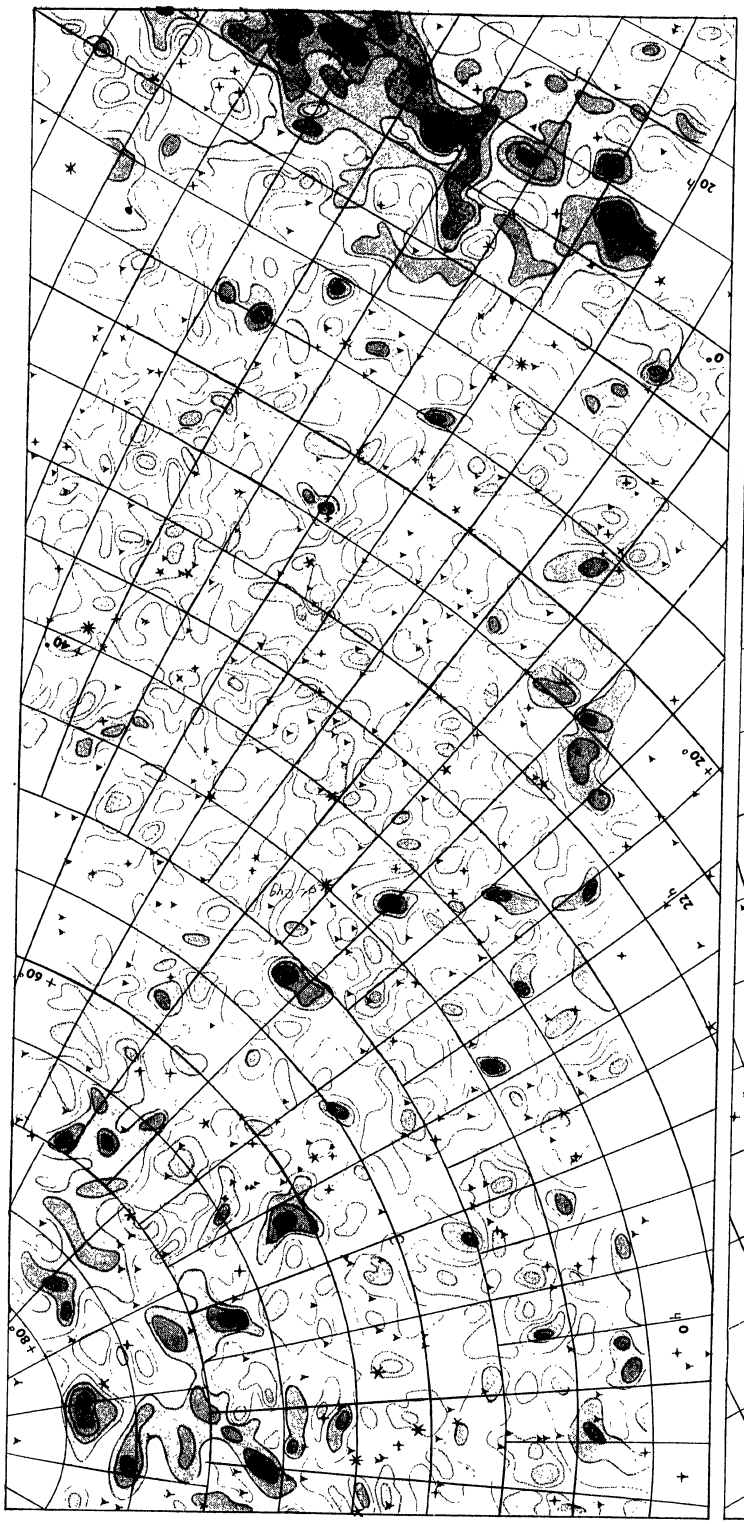

1st Quadrant
352°—95°
of Longitude.

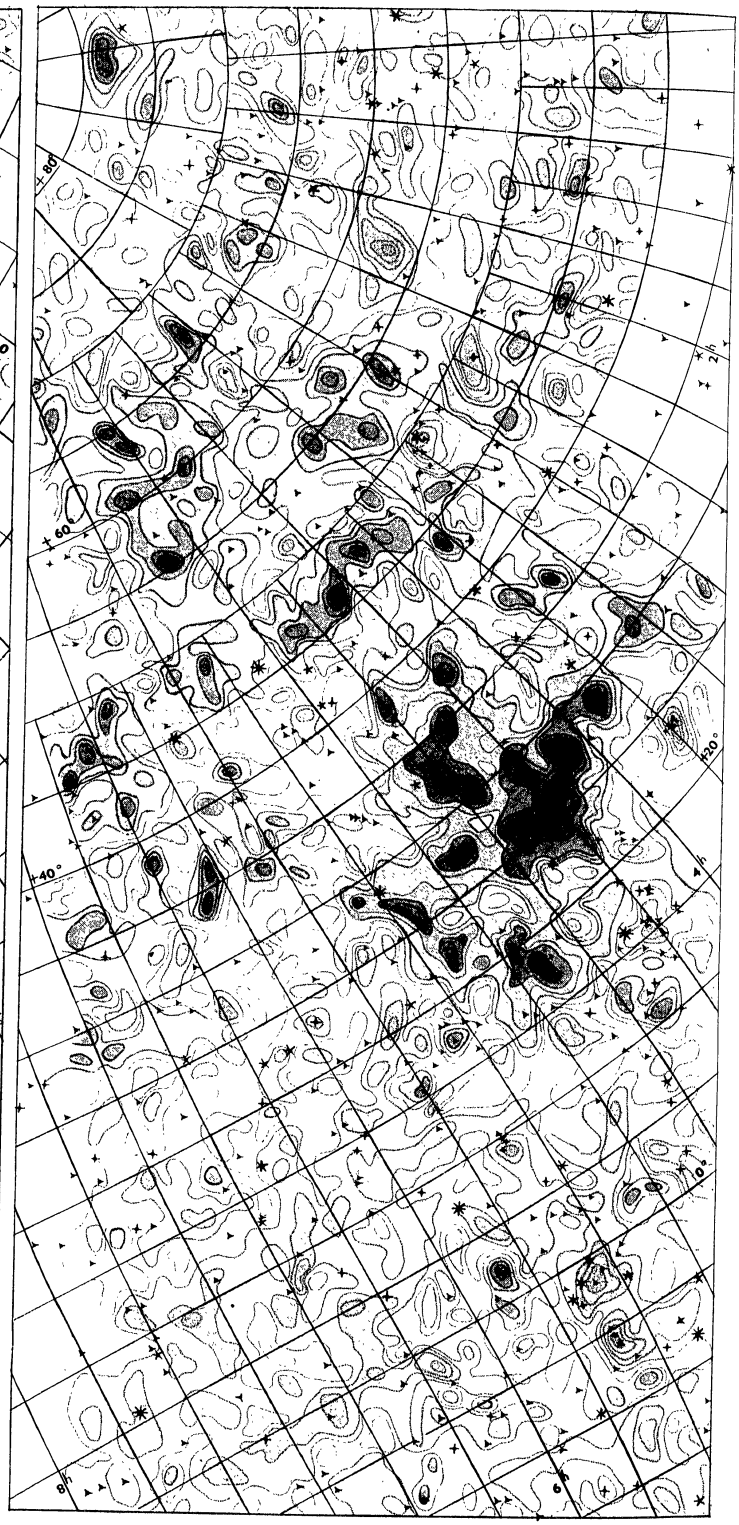

2d Quadrant
85°—188°
of Longitude.

3d Quadrant
172°—275°
of Longitude.

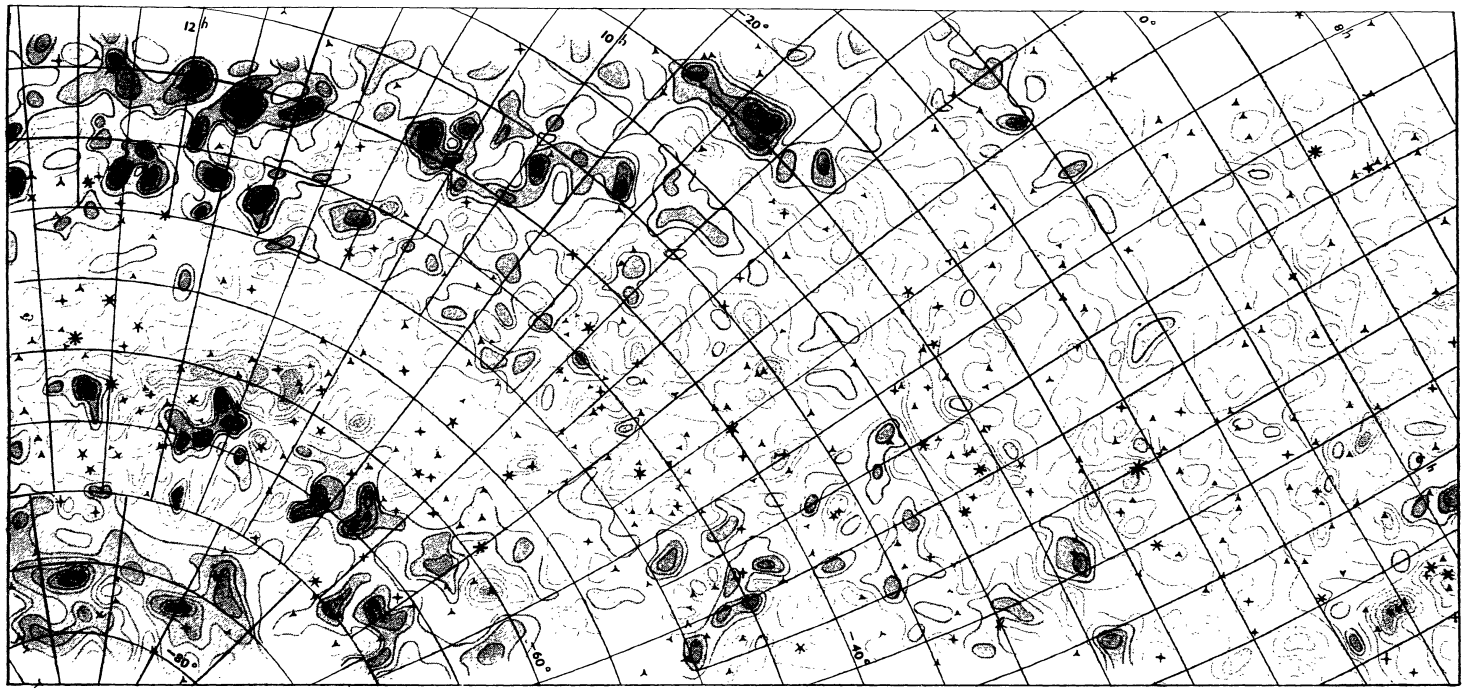

4th Quadrant
265°—8°
of Longitude,

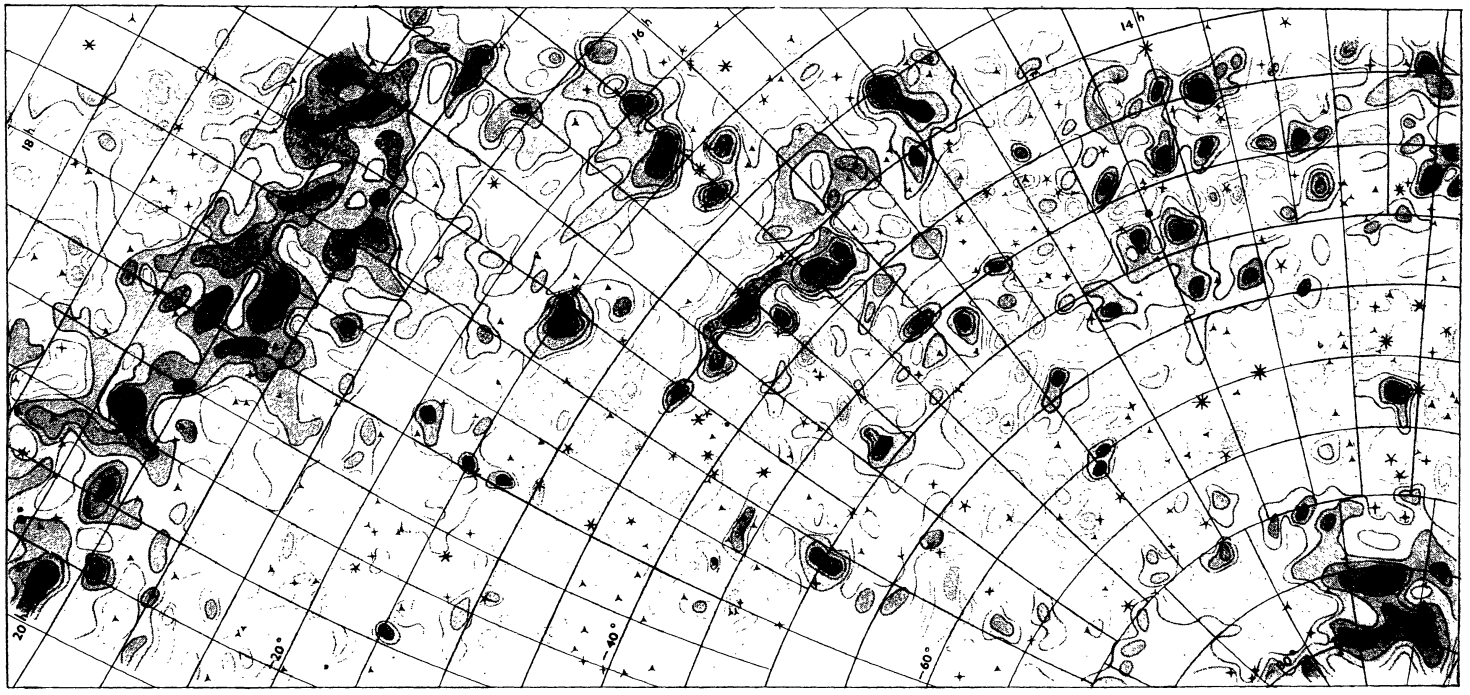

Deviation of density Δ log $N(9.3)$.

These curves still had to be corrected, because in the process of smoothing many of the minor details are deformed. So, if by a N—S elongated poor area two square degrees one above the other show a deficiency, the two 4° fields which are thereby depressed are situated at equal height and suggest an *E—W* elongated depression. Hence it was necessary to compare the course of the isanomales with the original density numbers of the single square degrees. These, of course, exhibit larger fluctuations than the smoothed values. So care was taken not to change the amount of surplus or deficiency, but only the figure of the deviating regions. In this way the extreme values of the logarithmic deficiency, to be compared with the theoretical values of Table 32, with few exceptions — where 2 or 3 concordant deviations would be neutralized by a 4th strongly different value — depend on areas of 4 square degrees, *i.e.* on numbers of stars of normally 30 to 22 (for $\beta = 0°$ and 20°).

The resulting surface distribution of the stellar density anomalies for 9.30^m by these isanomales is represented on the coloured plate in 4 maps, each giving a quadrant of the galactic zone between latitudes of circa 24°. Red indicates a surplus, blue a deficiency of stars. A network of equatorial coordinates and stars down to the 5th magnitude, in black, form the background. It would have been more conform to reality if only the colour shades had been shown gradually varying in intensity. But then it would not be possible to read the amount of logarithmic surplus or deficiency, because it is hardly possible to print the shades in such perfect conformity to the numerical values. Since the maps have to serve as a representation of numerical values, the isanomalous curves had to be inserted as distinct lines. They are red for the values 0, + .10, + .20 .... ; blue for the values — .10, — .20, — .30.... ; the areas included are filled in with gradually intensifying shades, (between 0 and — .10 is left white), in order to indicate clearly the value for each curve. So the aspect of the maps shows at a glance the distribution of the areas of surplus and deficient stellar density. In a way, however, it is delusive and deviates from reality, because the lines of equal anomaly appear here as boundary lines separating distinct regions, and suggesting coherence of regions which, in reality, do not at all belong together.

We may consider these maps as a more perfect representation in minute detail of almost the same distribution given in coarse outlines (based on areas of 5° square) in the 3d Chart of *Publ. Amsterdam* 1 : Deviations of star density for $m = 8.6$. There, attention was directed chiefly to the surplus regions, the condensations of stars, which are now given here in their more precise structure. We here direct our attention chiefly to the regions of deficiency of the stars down to $m = 9.3$, to get information about the surface distribution of nearby absorbing matter. In this discussion we have to bear in mind the weak points in the basic data, the subjective scale and inaccuracy of the DM estimates, and the uncertainty of the photometric reductions. Where we see the curves bounding the regions, in some places (e.g. at longitudes 150°, 210°. 310°) run along the parallels, this strongly suggests that systematic errors depending on declination are still present in the corrected magnitudes. In the last-named case, it is true, the Milky Way photographs show a connected streak of strong absorption running almost exactly along the parallel — 35° ; so here there is no reason for suspicion. But in other cases the suspicion remains ; and so does the desirability of having data other than DM estimates to derive the density distribution of these stars from.

The nearby absorbing nebulae.

From Table 32 we read (neglecting the difference between the practical limit 9.3 and the limit of theoretical computation 9.5) that the maximum distance of the absorbing nebulae corresponding to a logarithmic deficiency of 0.20, 0.40, 0.60, 0.80 is about 500, 300, 200, 150 parsees.

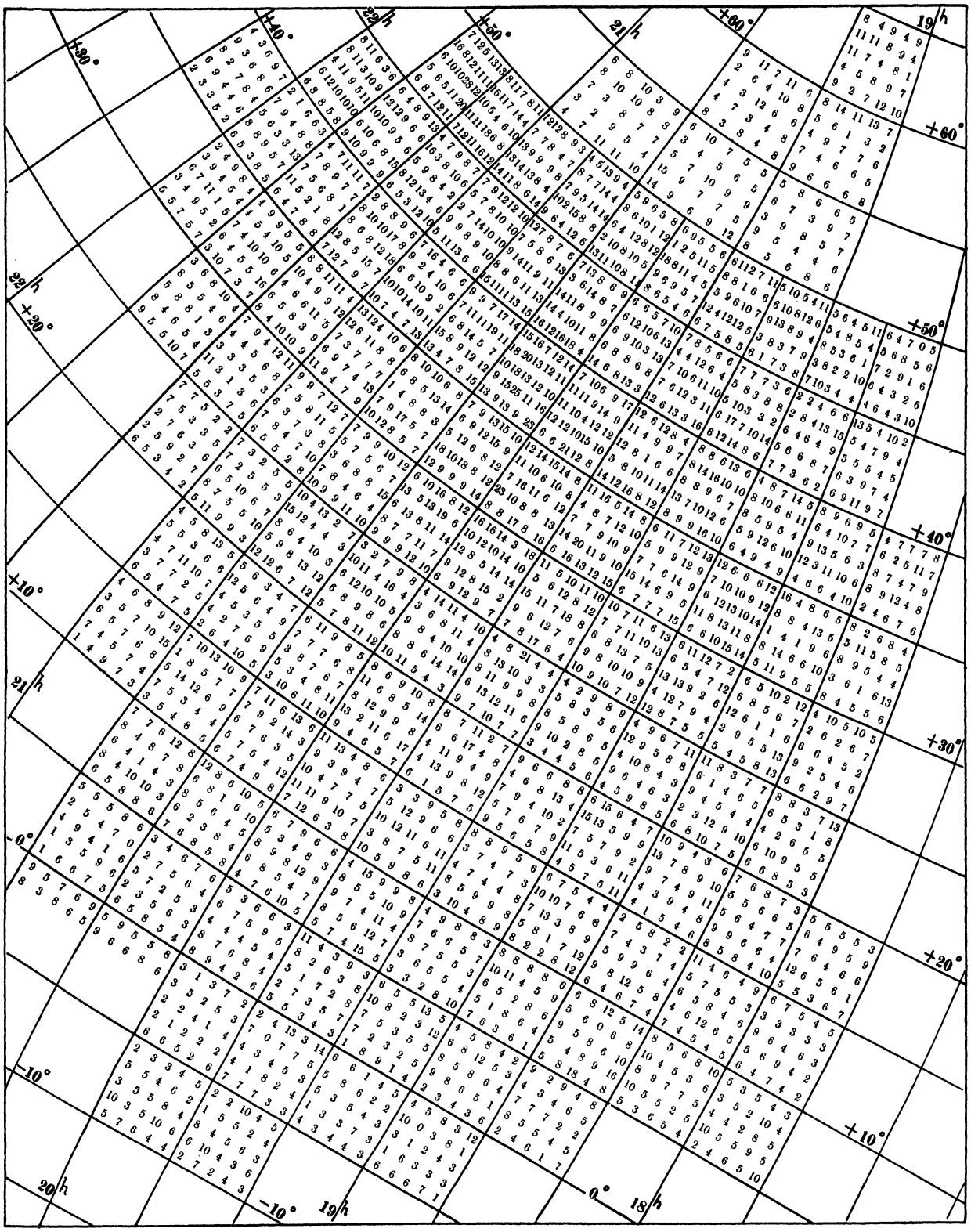

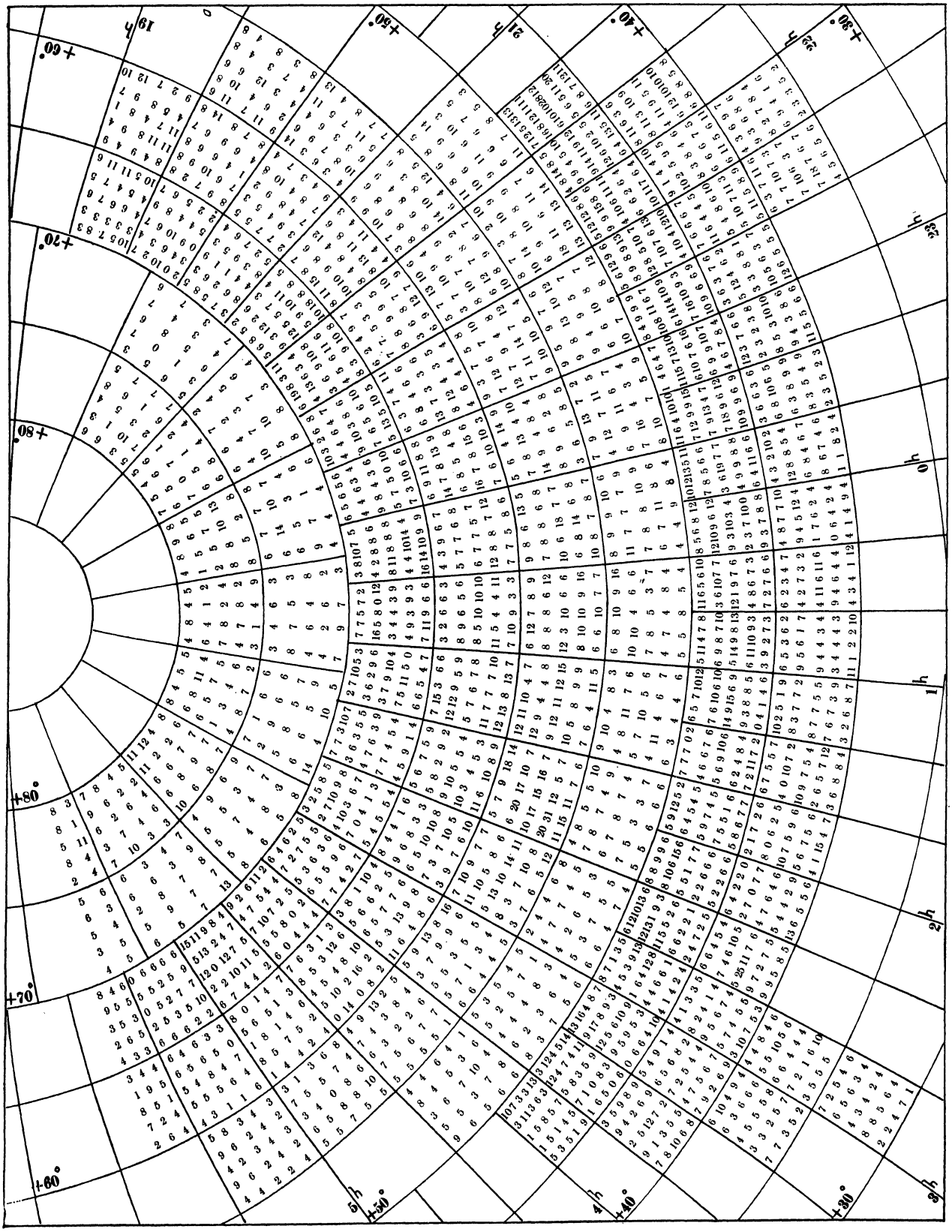

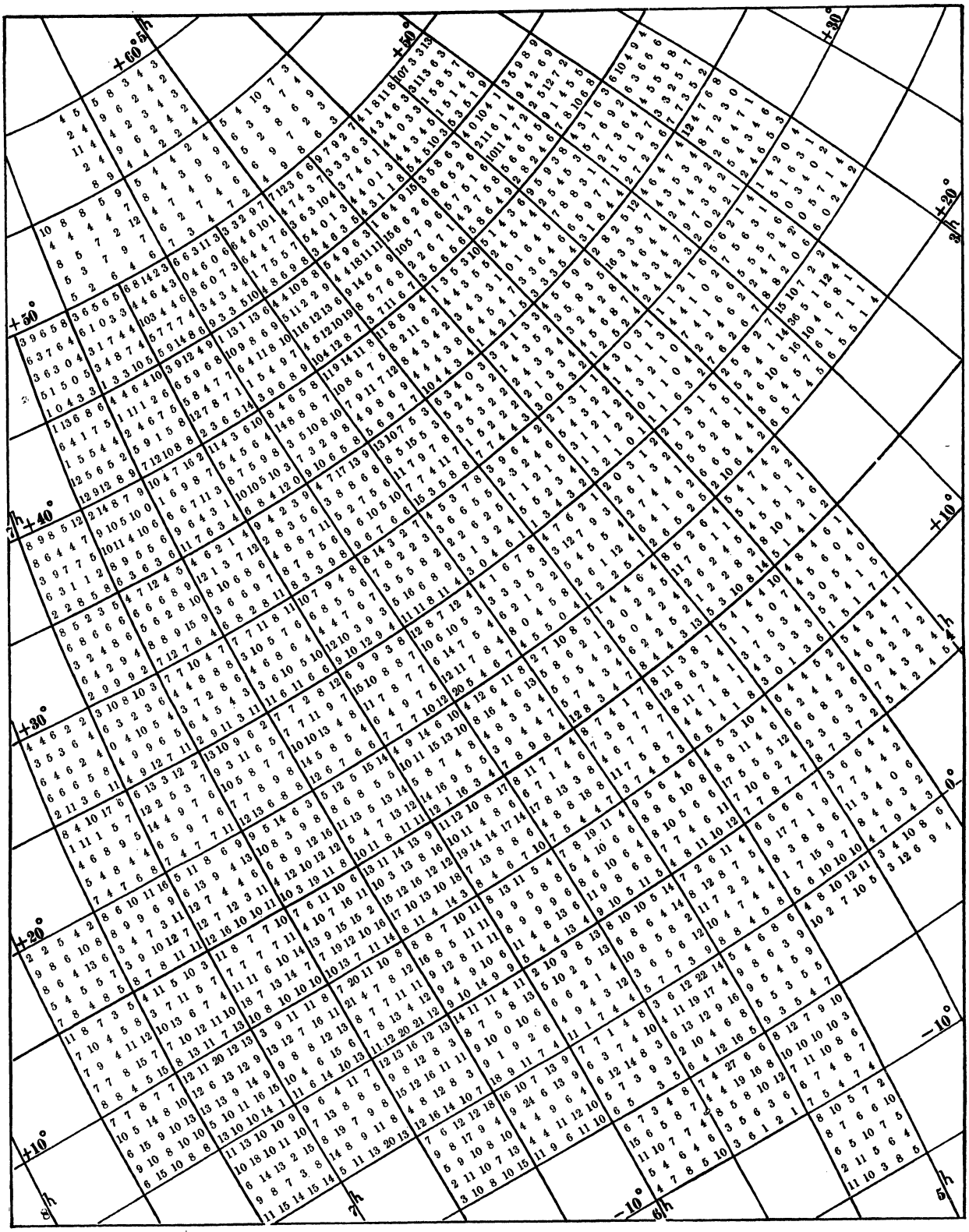

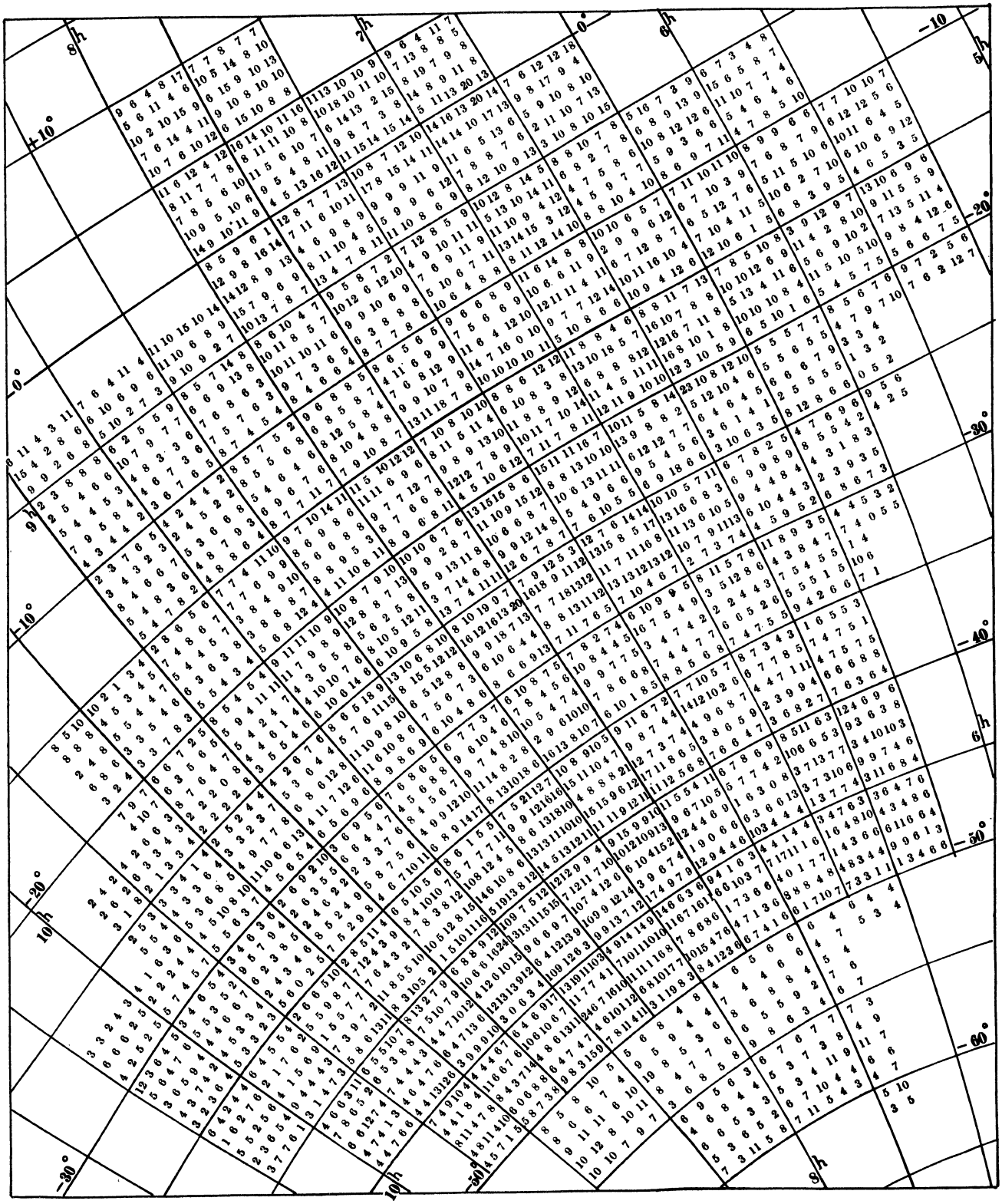

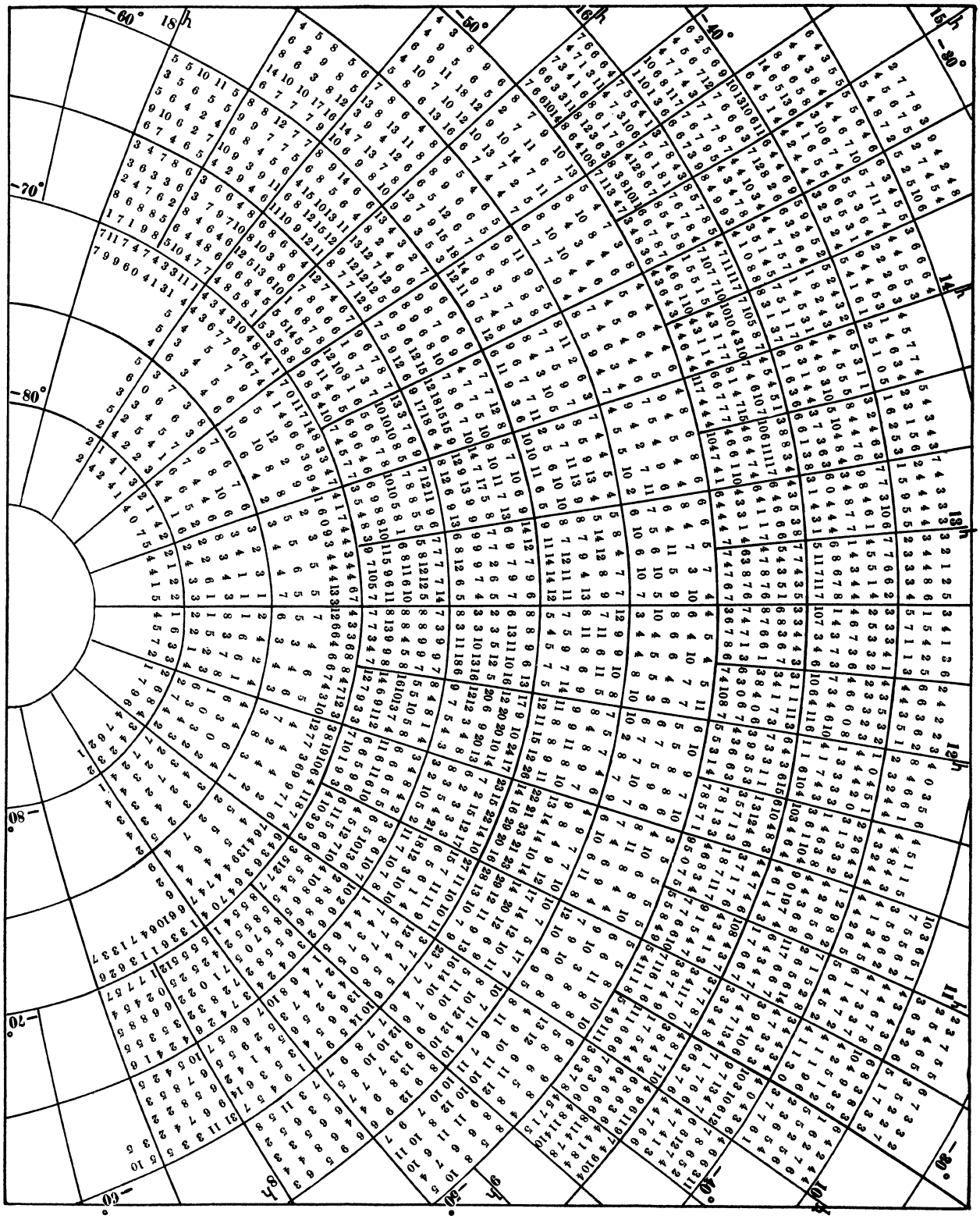

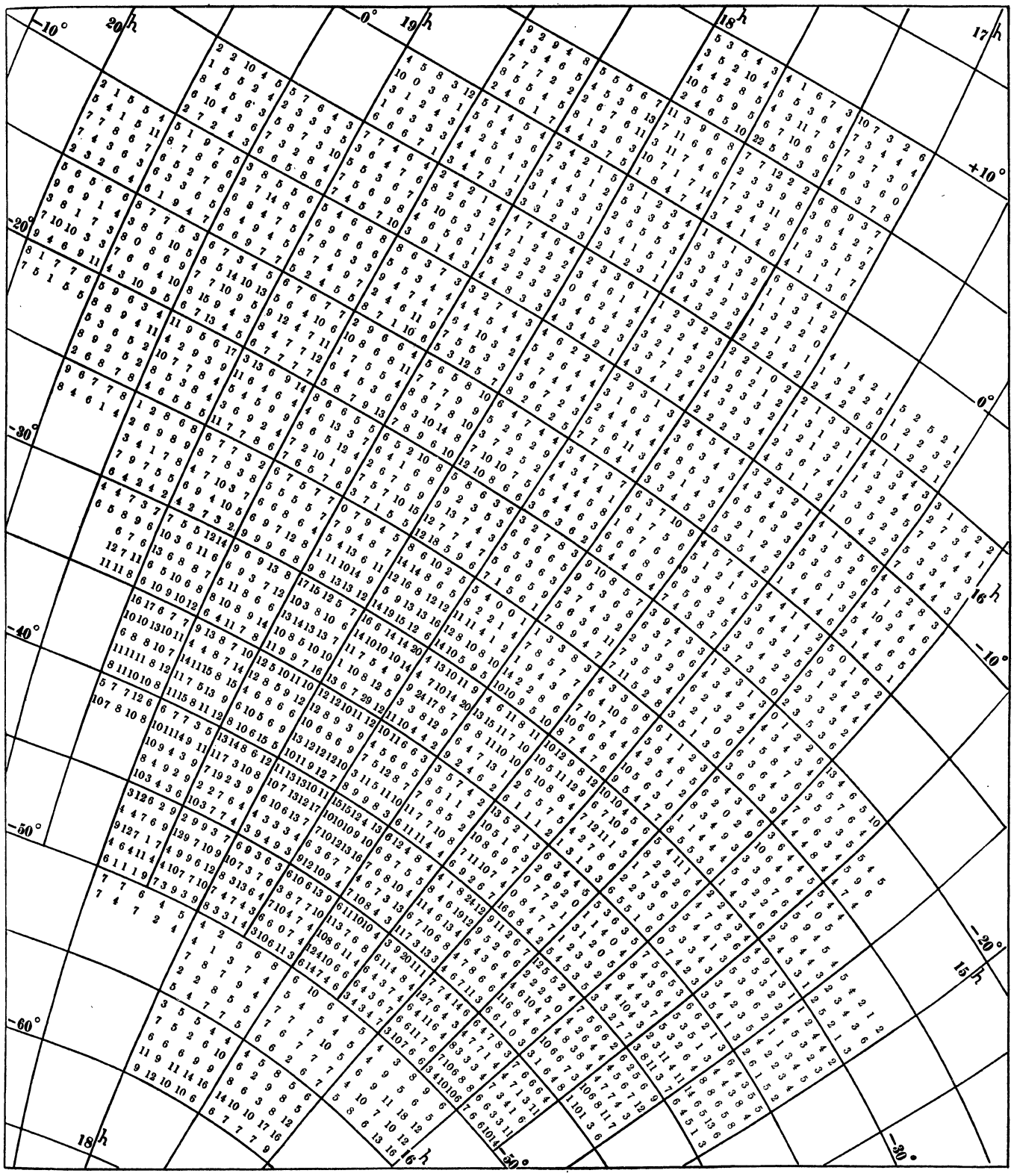

Small values such as 0.20 may fall within the reach of real density differences in different directions ; so their amount and their reality as indications of dark nebulae become doubtful. We have to consider here the amount of chance-error in these values. The number of stars from which they are derived (for 4 sq. d.), normally with $\Delta \log N = 0$ being 30 at $\beta = 0°$ (22 at the border), for $\Delta \log N = -.40, -.60, -.80$ is 12 (9), 7.5 (5.5), 4.8 (3.5). So the natural uncertainty of these $\Delta \log N$ is .13 (.15), .16 (.18), .19 (.22), and the maximum distances 300, 200 and 150 may for this reason be said to mean really : between 420 and 220, between 280 and 150, between 210 and 110.

A list of these nearby dark nebulae (nearer than 300 parsecs) is given in de form of a catalogue of places of deficiency above 0.40. In large coherent absorption regions the maxima have been given as the towering peaks of a mountainous region. The equatorial coordinates give the points where the deficiency in the 4sq.d. averages is largest ; adjoining them are these maximum values themselves. So they may differ slightly from the smoothed curves in the coloured maps. Only in few cases (indicated by *) values derived from 3 sq.d. or from 4 sq.d. arranged otherwise than in a square — used already in the smoothed curves of the maps — are given. Some values below 0.40 have been added, which probably exceed this value relatively to the surplus regions (roughly estimated values in parentheses) around them. The galactic coordinates are deduced from the others by OHLSSON's Tables. The rotating numbers generally follow the order of longitude, but adjacent items in the same region belonging together are kept together. The last column gives the places relative to adjacent stars.

Catalogue of strong deficiencies Δ log $N(9.3) > .40$.

	Galactic coordinates	Equatorial coordinates	Log. Defic. in 0.01	Nearest stars
1	53°— 3°	21^h 0^m + 43°	33 (+ 20)	ξ Cyg
2	70 + 19	20 10 + 69	40	E ε Dra
3	76 + 4	22 32 + 62	39 (+ 10)	δ—ι Cep
4	82 + 6	23 16 + 67	41	S o Cep
5	88 + 16	0 10 + 78	41	NE γ Cep
6	92 + 5	1 0 + 67	42	W Ψ Cas
7	105 — 15	2 0 + 45	45	N γ And
8	110 — 2	3 2 + 54	41	NE γ Per
9	110 + 1	3 18 + 57	42	S 3H Cam
10	114 — 2	3 24 + 52	42*	NE α Per
11	115 + 2	3 48 + 55	44	NW 12H Cam
12	107 + 11	3 48 + 67	51	N 7H Cam
13	111 + 22	5 50 + 70	48	NW 22H Cam
14	114 + 16	5 4 + 65	46	E 9 Cam
15	118 + 15	5 18 + 61	43	E 10 Cam
16	122 + 12	5 18 + 56	53*	SE 11 Cam
17	121 — 7	3 44 + 44	43	δ—ε Per
18	121 — 2	4 0 + 48	49	c—λ Per
19	123 — 2	4 8 + 47	51	S μ Per
20	126 + 0	4 30 + 46	88	ε Aur—μ Per
21	128 + 3	4 48 + 46	47	N ε Aur
22	130 + 10	5 28 + 48	41*	NE α Aur
23	133 + 16	6 12 + 48	41	
24	136 + 18	6 28 + 47	47	Ψ_1 Ψ_4 Ψ_{10} Aur
25	137 + 19	6 36 + 46	48	

	Galactic coordinates	Equatorial coordinates	Log. Defic. in 0.01	Nearest stars
26	124°— 15°	3^h 28^m + 36°	47	ζ—β Per
27	128 — 20	3 28 + 30	46	SW o Per
28	130 — 7	4 16 + 38	58	SW e Per
29	132 — 17	3 48 + 29	70	S ζ Per
30	133 — 3	4 40 + 38	43	N 1 Aur
31	134 — 7	4 28 + 35	60	E 54 Per
32	137 — 16	4 8 + 27	72	W φ Tau
33	138 — 9	4 36 + 31	64	4° SW ι Aur
34	139 — 15	4 16 + 26	87	φ—χ Tau
35	141 — 13	4 28 + 26	74	E χ Tau
36	143 — 7	4 54 + 28	57	5° W β Tau
37	146 — 1	5 28 + 29	49	E β Tau
38	147 — 4	5 16 + 26	56	S β Tau
39	150 — 8	5 12 + 22	57	n Tau
40	151 — 14	4 52 + 18	58	W m Tau
41	154 — 22	4 32 + 11	50	S c Tau
42	156 — 7	5 28 + 17	32 (+ 10)	S ζ Tau
43	144 + 6	5 48 + 34	38 (+ 10)	S ϑ Aur
44	144 + 9	6 4 + 36	48*	
45	146 + 10	6 10 + 34	45*	4° SE ϑ Aur
46	166 — 20	5 4 + 2	20 (+ 20)	SW ϱ Ori
47	171 — 10	5 46 + 3	41	α—ζ Ori
48	180 — 20	5 28 — 9	21 (+ 20)	3° S ι Ori
49	197 — 20	5 56 — 24	36 (+ 10)	SE δ Lep
50	222 — 17	6 54 — 45	32 (+ 10)	ν—τ—L Vel

	Galactic coordinates	Equatorial coordinates	Log. Defic. in 0.01	Nearest stars
51	229°— 14°	7^h 28^m — 49°	41	τ—γ Vel
52	203 + 17	8 24 — 11	33 (+ 10)	5° W 12 Hya
53	220 + 17	9 8 — 24	63	NW ϑ Pyx
54	226 + 21	9 36 — 25	41	N ϑ Ant
55	231 + 13	9 28 — 34	40	W ε Ant
56	237 + 14	9 56 — 37	46	S η Ant
57	244 + 15	10 24 — 40	42	NE r Vel
58	245 + 17	10 32 — 39	70	
59	249 — 17	8 16 — 68	43	S β Vol
60	249 — 9	9 20 — 63	42	i—v Car
61	252 — 16	8 48 — 70	42	W β Car
62	253 + 18	11 16 — 41	40	5° E i Vel
63	257 + 12	11 24 — 48	43	SW C Cen
64	258 + 20	11 40 — 41	55	N B Cen
65	260 + 14	11 42 — 47	50	S B Cen
66	261 + 21	11 56 — 40	53	NE B Cen
67	262 + 18	11 56 — 43	46	
68	259 — 3	11 4 — 63	38 (+ 20)	S x Car
69	262 — 4	11 28 — 65	38 (+ 20)	S λ Cen
70	264 + 14	12 8 — 48	41	
71	265 + 16	12 12 — 46	46	γ δ D Cen
72	267 + 14	12 24 — 48	42*	
73	267 + 23	12 28 — 39	41	W n Cen
74	269 — 1	12 32 — 63	47 (+ 20)	E α Cru
75	260 — 15	10 10 — 74	42	S J Car
76	263 — 17	10 40 — 77	63	N γ Cha
77	270 — 17	12 40 — 79	55	E β Cha
78	271 — 14	12 50 — 76	77	β Cha—ι Mus
79	273 — 18	13 40 — 80	41	W ε Aps
80	275 — 20	15 0 — 81	49	S α Aps
81	275 + 14	13 8 — 48	53	NE ξ Cen
82	284 + 21	13 48 — 40	62	NE ν Cen
83	285 + 11	14 12 — 84	49	S ι Lup
84	286 + 20	14 0 — 39	47	S ϑ Cen
85	286 + 15	14 8 — 44	54	NW ι Lup
86	290 + 14	14 32 — 44	49	N α Lup
87	300 + 4	15 48 — 47	47	NW η Nor
88	304 + 4	16 4 — 44	59*	NE δ Nor
89	305 — 5	16 48 — 50	42	S ε Ara
90	310 — 14	17 48 — 50	50	W ϑ Ara

	Galactic coordinates	Equatorial coordinates	Log. Defic. in 0.01	Nearest stars
91	304°+ 16°	15^h 26^m — 35°	46	W Ψ Lup
92	306 + 20	15 20 — 30	63	W τ Lib
93	306 + 6	16 4 — 41	40	NE λ Nor
94	310 + 9	16 8 — 37	62	E ϑ Lup
95	311 + 7	16 20 — 37	68	S N Sco
96	313 + 3	16 40 — 38	44	W μ Sco
97	316 + 4	16 48 — 35	70	SE ε Sco
98	318 + 1	17 4 — 36	49	4° W λ Sco
99	317 + 15	16 12 — 27	43	S σ Sco
100	319 + 12	16 24 — 28	64	W τ Sco
101	322 + 16	16 24 — 23	72	E ϱ Oph
102	324 + 18	16 20 — 20	62	E Ψ Oph
103	327 + 23	16 12 — 15	53	NW φ Oph
104	329 + 2	17 28 — 26	91	SE ϑ b c Oph
105	332 + 18	16 40 — 14	47	3° SE ζ Oph
106	336 + 20	16 40 — 10	57	E ζ Oph
107	340 + 25	16 36 — 4	66	6° N ζ Oph
108	340 + 21	16 48 — 7	51	S 23 Oph
109	341 + 15	17 12 — 9	47	N ν Ser
110	342 + 11	17 28 — 10	50	S μ Oph
111	343 + 9	17 36 — 11	56	N o Ser
112	343 + 17	17 8 — 6	75	SE 30 Oph
113	344 + 20	17 0 — 4	64	E 30 Oph
114	345 + 8	17 44 — 10	53	W ν Oph
115	346 + 16	17 16 — 4	57	NW 27H Oph
116	346 + 11	17 32 — 7	60	N μ Oph
117	348 + 11	17 40 — 5	65	NE μ Oph
118	348 + 18	17 16 — 2	54	SE 41 Oph
119	349 + 5	18 0 — 7	61	NE τ Oph
120	351 + 3	18 12 — 7	66	NW 1H Sct
121	352 + 0	18 24 — 7	55	NW 3H Sct
122	354 + 7	18 2 — 2	49	NE ζ Ser
123	354 + 2	18 24 — 4	53	SE η Ser
124	356 — 2	18 40 — 5	48	6H Sct
125	358 + 7	18 12 + 1	42	W d Ser
126	0 — 4	18 52 — 2	68	NW λ Aql
127	0 — 6	19 0 — 3	42	N λ Aql
128	1 — 10	19 16 — 4	42	N f Aql
129	2 — 16	19 40 — 6	44	NE $\varkappa$ Agl
130	6 — 18	19 56 — 3	52	SW ϑ Aql

From 10° of longitude onward, the first nearby nebula is the isolated dark fissure in the lesser Cygnus Cloud, at ξ Cygni. In Cepheus and Cassiopeia some few dark patches occur in the Northern border of the galactic zone; they continue in Camelopardalus, growing stronger, and in Perseus begin to reach across the galactic circle. The small distance < 130 of the dark patch 19 (between δ Per and α Aur) indicates that we are here already in the realm of the Taurus-Auriga complex. A large number of condensations (Nr. 26 to 42) belong to this extensive cloud of dark matter; the darkest places, according to our criterion, indicate a maximum distance of 130 parsecs (which,

by the natural uncertainly of numbers, means : probably lower than 190 parsecs). In the third quadrant of the galactic zone a series of dark patches run along the Northern border, through Hydra, Pyxis, Antlia, and continue in the 4th quadrant through Centaurus and Lupus. Some isolated absorbing objects at small distance, known as the dark bay in the southern boundary in Carina and as J. HERSCHEL's Coal Bag, stand conspicuously dark against the Southern part of the bright galactic light. A larger complex of nearby dark matter (59—61, 75—80) is situated at the Southern border, towards the South Pole, in the constellations Volans, Chamaeleon, Apus. (< 160). The northern border nebulosities in Lupus between λ 290° and 310° then descend between ε and λ Sco to the galactic circle. Further on, the dark patch S of ϑ Oph (Nr. 102) at a distance < 125[1]) forms an outlying member of the Ophiuchus complex of nebulosities, to which all the last items (99—130) of the catalogue belong. They descend with increasing longitude from the vicinity of Antares to the galactic circle, and, crossing it, extend to the S. border in Aquila.

Comparison with the Milky Way.

In the absence of analogous counts from other sources with fainter limits of stellar magnitude which are not at present available, a study of the more remote layer of absorbing matter cannot be made in the way indicated above. This shortcoming may be partly compensated by substituting the Milky Way light as a second source. The Milky Way shows, in the form of surface brightness, the integrated light of all the stars, and reveals, by the dimming of this light, the effect of absorbing matter on the totality of stars.

We can compute theoretically the effects of absorbing nebulae on the visible galactic light. For a given volume of space we first integrate the light of all the stars not seen separately, hence from the faintest up to the luminosity which, for this distance, just emerges as a visual star 6.5^m, *i.e.* to $M = 6.5 - \varrho$. This intensity I (ϱ), myltiplied by the volume and the space density, and reduced by the factor r^{-2} to apparent intensity, must be integrated over all the distances to get the total light per square degree, expressed in the unit one star of magnitude 0.

$$I(\varrho) = \int_{6.5-\varrho}^{\infty} \varphi(M)\, 10^{-0.4\,M}\, dM\,;\quad L = [0.147 - 4] \int_{-\infty}^{+\infty} D(\varrho)\, I(\varrho)\, 10^{0.2\varrho}\, d\varrho.$$

In the case of an absorbing screen at distance ϱ_1 this integral extends from $-\infty$ to ϱ_1, whereas for larger ϱ, from ϱ_1 to $+\infty$, the factor $10^{-0.4\varepsilon}$ is added, because all the light of more remote space elements is dimmed by ε magnitudes.

The undimmed galactic light, computed in this way for $\beta = 5°$, with the data for $D(\varrho)$ and $\varphi(M)$ from *Publ. Amsterdam* **1**, was found to be 0.0175, i.e. 175 stars of 10^m per sq.d. For the brighter galactic clouds the intensity measured is larger ; the computed value is based on stellar densities as derived from numbers of stars averaged over all longitudes and, therefore, already affected themselves by absorption. In the case of absorbing screens at different distance ϱ_1 and different absorption ε, the remaining galactic intensity is given in the first part of Table 39. In the second part of this table the weakening of the galactic light by absorption is given in magnitudes ; for comparison the logarithmic decrease of the number of stars $N(9.5)$ from Table 31, but also converted into magnitudes, is given in the 3d part.

We see that, for nearby absorbing matter, both diminutions almost correspond to ε (for the

[1]) The contradiction between this statement and the value 200 pcs derived from R. MÜLLER's counts, is due to the numbers counted for 7^m and 8^m being too large for a small distance, whereas the small number for 9^m in Table 26 fits to it better. The small number of stars (1, 2, 5) makes all quantitative conclusions uncertain.

Table 39. Milky Way brightness in absorption.

ϱ_1	L in $*10^m$ ($\beta = 5°$) (normal 175)				Δ log L in 0.01^m				Δ log $N(9.5)$ in 0.01^m				L for $\beta = 15°$ (normal 116)			
	$\varepsilon = 1$	2	3	∞	$\varepsilon = 1$	2	3	∞	$\varepsilon = 1$	2	3	∞	$\varepsilon = 1$	2	4	∞
9.5	72	30	14	3	97	190	274	434	116	217	281	317	48	21	10	3
10.5	74	34	18	8	93	178	247	342	105	179	214	228	51	25	14	7
11.5	79	41	26	16	86	156	207	261	86	132	147	152	55	31	22	15
12.5	88	53	39	30	75	130	163	192	61	85	91	93	63	42	33	27
13.5	99	69	57	49	61	100	121	137	37	48	50	51	73	55	48	44
14.5	114	89	79	73	47	73	86	95	19	24	25	25	84	71	65	62
15.5	128	110	102	97	34	51	58	63	8	10	10	10	94	85	81	79
16.5	142	129	123	120	23	33	38	36	3	4	4	4	103	97	95	93
17.5	153	144	141	139	14	21	23	25	1	1	1	1	109	106	104	103

galactic light it is less than for the stars, because the naked-eye stars do not contribute to it). With increasing distance of the absorbing nebula the contrast, and therefore its visibility, diminish. Not so rapidly, however, as does the number of stars. Hence a small deficiency in our map of DM deviations at a place where a dark galactic patch shows strong contrast, indicates a great distance of the nebula; whereas nearby nebulae show up strongly in both cases. The results of the same computations for $\beta = 15°$, added in the last part of Table 39, show that, here, the contrast for the same absorptions is smaller, especially for moderate distances. It must be remarked, however, that the contrast observed in galactic light is strongly lessened by atmospheric and zodiacal light, which is added to the galactic light; their effect will be seen if all values L in Table 39 are increased by a constant amount. On the other hand the contrast becomes greater for remote nebulae appearing in front of bright galactic clouds, where the bulk of the surplus light comes from great distances.

For the galactic light, an analogous graph may be constructed, such as Figs 19—21 show for the number of stars, as well as a table, analogous to Table 32, giving a maximum distance for different degrees of obscuration of galactic light (for 1^m and 2^m this distance is 750 and 3000 parsecs.) But the practical use of this criterion is vitiated by different circumstances, such as the difficulty of making exact measurements, the usually great amount of additional illumination, and the uncertainty about the unobscured intensity. So, we must content ourselves for the present with qualitative considerations only.

The drawings of the Milky Way made by observation with the naked eye show, owing to the faintness of the light, only the largest features, and that only in strongly simplified rounded forms. The long-exposure photographic pictures, on the contrary, show a wonderful richness of detail. Whereas former photographs chiefly aimed at representing the most picturesque structures in a conspicuous way, usually within limited fields, we have now, in the beautiful Atlas of Ross and Miss Calvert, a series of excellent maps, each comprising a large area, and together covering the galactic zone, generally to 20° latitude. It is limited, however, to the parts observable at Northern stations, i.e. between 300° and 220° of longitude; so we have, for the most interesting southern parts, only the reproductions of Bailey's photographs (*Harvard Annals* **72**), made in former times with a much inferior instrument. It is to be regretted that the Ross Atlas has not been extended to embrace the entire course of the Milky Way; with our modern means of travel it would be easy to secure, with the same instrument, the additional photographs at some station in the Southern hemisphere. Its completion should be considered as a most important work, and would double its usefulness in all studies of galactic problems.

These photographic pictures can give no quantitative data of surface brightness. Even in the cloudforms with their apparently continuous blackening, the non-correspondence of their crowded mass of stellar images with the total intensity precludes exact numerical results. Here, extrafocal plates, such as made by MAX WOLF in Heidelberg and reduced in *Publ. Amsterdam* **3** to surface intensities, giving photographic surface brightness with more detail than visual drawings do, may serve as a valuable help in interpreting the results of star counts. In the same way less-extrafocal plates, on a larger scale, with smaller stellar discs, could be used to separate remote cloudy masses of stars from the nearer regions represented by separate star images. Analogous computations as to the visual limit 6.5 would then have to be made for their limiting magnitudes. The foreign illumination of the background, however, remains a serious drawback to exact discussions of these data.

The focal photographic pictures, especially where, as in the Ross Atlas, the stars show perfect minute point-like images, though not offering numerical data on intensity, give most valuable qualitative information. They enable us to look into the structure of each region, the abundance of brighter and fainter stars and the blackness of the background; so they facilitate the interpretation of the visual galactic features on the one hand, and of the distribution of the bright stars on the other hand. The presence of remote dark nebulae may be inferred, where, distinct from adjacent cloudforms and owing to the obscuration of more distant starlight, a large number of well-visible stars stand out against an entirely black background. Nearby absorbing matter is recognised as void regions, poor in visible stars ; sometimes (as in Taurus and the Scorpion) there is a faint continuous light due to the nebulous matter reflecting the light of the imbedded stars. Whereas the Milky Way drawings show little concordance with our coloured maps of the $\Delta \log N$ (9.3) — because the visual Milky Way depends to a very small extent on the nearby stars and nebulae — the photographic Atlas may serve as a bridge, explaining them both as simplified expressions of a different characteristic of the spatial structure.

The detailed aspect of the Milky Way.

The following comparison of the details of the Milky Way with our maps of DM star deviations is intended to derive conclusions, as far as possible, concerning the probable distance of absorbing nebulosities in different regions of the sky. At the same time it tries to interpret the observational features of the Milky Way, by tentatively asserting their origin in either near or remote depths of space. In this enumeration MW denotes the visual aspect (for the Northern part after my own and EASTON's drawings, for the Southern part after my Lembang work), R denotes the features on the Ross Atlas; B those of Bailey's plates, A3 data from the photographic photometry of the Heidelberg plates ; whereas, by DM, the appearance (numerically the deficiency) on our maps of $\Delta \log N(9.3)$ is indicated. The abbreviations d.p., d..r, d.f., d.str., d.n. are used for dark patch, dark region, dark fissure, dark streak, dark nebula ; in the approximate location of these often large objects by AR and declinations, the ^{h}, ^{m}, ^{o}, are omitted.

The d.f. S and W of δ Aql (19 20 + 1), in A3 and R consisting of some not very dark spots, in DM 20—30, may be a weak and not very remote nebula. The d.p. 5° W of ε Aql in the N border (18 34 + 14), in A3 clearly visible, in R strongly black, in DM distinct, > 30, indicates a d.n. at 400, too far away to belong to the Ophiuchus complex. In the rift between the two branches, the d.p. N of ϑ Ser (18 48+ 6) and the d.p. at ω Aql (19 12 + 12), in R showing many brighter stars on a black background, and in DM > 10 or 20, must be a d.n. at greater distance (> 600). For the d.rs., interrupting the W branch, one S of 1 Vul (19 16 + 19) and the other between

6—1—9 Vul (19 28 + 22), in R (and also in A3) dark features of complicated structure, in DM > 10 or 20, the same holds. A less conspicuous small d.p. S of ε Sae (19 28 + 15), black in R, distinct in A3, is stronger in DM (> 30), and may be nearer than other nebulae in the rift. The d.p. seen around 16 Vul, in A3 also a darker spot, in R full of stars on a background darker than in the surroundings, and invisible in DM must be very remote. The same holds for the entire region E of the great Cygnus cloud, where R shows an irregular collection of more or less black parts, and DM mostly a surplus of stars. Farther on, the d.r. α—γ—ν Cyg (20 36 + 42) and the adjacent smaller d.p. ξ — 61 Cyg (21 0 + 41), both dark in A3, where R shows, before a black background, a great number of bright telescopic stars producing a faint luminosity, and where DM shows hardly any depression, must be due to very remote dark matter. The small d.p. around η Cyg. (19 52 + 34), the centre of a remarkable dark marking, conspicuous on all photographs in the middle of the Great Cloud, and represented by some slight depressions in DM, indicates dark matter behind the Cygnus agglomeration of stars variously estimated at 300—600 parsecs.

The small d.p. at ξ Cyg (21 2 + 44), is in R a strong d.f. ; the value > 30 in DM (catalogue 1) is certainly too low owing to smoothing and to a surplus in the surroundings. The conspicuous rift crossing the MW in N—S direction E of A Cyg, in R composed of some d.ps, as also shown in MW drawings (21 20 + 40 at the S border, 21 18 + 44, 21 14 + 47) is hardly indicated in DM as a slight depression, hence seems to be due to remote dark matter. It is apparently connected with the large and strong d.p. between Cygnus and Cepheus (20 54 + 53), a most conspicuous object to the eye and called by EASTON the "Northern Coal Bag" ; in R it also stands out as a strongly black region, though covered with many more stars than the barren fields of the Taurus nebulosities. In DM it appears as a deficiency > 30 which may, perhaps be increased for the surroundings ; so the distance cannot greatly exceed 300 parsecs.

What is seen in MW as a d.p. ϱ—π^2 Cyg (21 36 + 47), in A3 as an irregular d.p., and in R as a very irregular long d.str., must be a very remote structure, since in DM there is only a slight depression further to the S. The same holds for the small d.p. E of π^1 Cyg (21 48 + 51). The d.r. on MW drawings W of ζ Cep (21 52 + 57) is, in R, an extremely complicated structure of dark and bright markings (also in A3), which, as nothing is seen of it in DM, must all be remote. The d.p. N of δ Cep (22 30 + 60), extending in a d.f. S along ι and o Cep (23 0 + 65), in R a complicated mass of dark markings, and in A3 a d.p. further N, shows in DM nearly 40 also more N (cat. 3, 4), hence is not more remote than 300 pcs. The faint Cepheus border regions, not well observable visually, show in R numerous black features, partly corresponding to DM deficiencies, and partly not (cat. 5); so part of them must be nearer than 300 pcs. A visual d.p. in the N border, 33 Cyg—ϑ Cep (20 20 + 59), also black in R, > 20 in DM, may be rather weak and nearby. Black markings in R, corresponding to deficiencies in DM, but not visible in MW because of the faintness of the border regions, often occur, e.g. at the S border at 22 12 + 42, DM > 30.

The large d.p. 1H—τ Cas (23 20 + 59), in A3 not very dark, in R darkest at the W side, in DM showing only as a weak depression at that darkest place, is remote. The d.p. γ—$\varkappa$ Cas (0 40 + 61), in R. rather a d.str. to SW, in DM (as in A3) strongest further to the SW, > 20, indicates a d.n. not farther than 500. The d.f. (EW) S of ε Cas (2 0 + 51), in R a group of d. strs EW, in DM not distinct, must be due to remote nebulosities. A d.r. at the S border, SE of ϑ Cas (1 12 + 51), in R a black region, distinct in A3, in DM smaller, > 20, represents a remote d.n. (perhaps 500).

In the faint light of Northern Cassiopeia and Camelopardalus the MW drawings show dark streaks, proceeding from the region about ι Cas. An EW d.f. S along ω—ψ Cas (1 40 to 1 0 + 66) shows in R as two separate d.ps, S of ω Cas and S of 31 Cas, in DM at the same places > 30 and 40 (cat 6) ; hence it is due to dark nebulosities at 300—400 pcs. The NS d.f. E of A Cas (2 4

+ 68 to + 75), in R a d.str. ι—A Cas, is not clearly indicated in DM. The EW d.f. E of ι Cas to 2H — 9 Cam (2 40 to 4 0 + 66), in R a dark streak ι Cas—1H Cam, is in DM broken up in single patches of deficiency, increasing to 30 or 40. Contiguous to these are the faint regions in the N part of Perseus ; the d.r. NE of γ and α Per (about 3 20 + 52), extending to the other side of γ—α, in R broken up in d.ps, shows in DM corresponding maxima > 40 (cat. 8—11); so the absorbing masses come nearer by. The same is seen in the connected further parts of Camelopardalus, where R and A3 both show a complicated dark structure, and DM shows spots of increasing deficiency, mostly more or less corresponding. The sharply traced black structure in R, N of 12 H and 7 Cam (4 8 + 55), is not visible in DM, hence indicates that also remote nebulosities are present here. Then follows the curved d.p. midway δ Per—α Aur (4 20 + 48), in R an irregular dark structure E of c—μ Per, in A3 large and dark, and by its strong deficiency > 70 in DM (cat. 20) showing its nearness < 170. Here we obviously come into the realm of the Taurus nebulosity, where it extends to the galactic circle.

The nearby dark matter in Taurus, situated chiefly in front of the border parts of the galaxy, is shown only where it comes down to a lower latitude, vaguely in the visual MW, as an extensive region of darkness. The MW drawings show a large d.r. from f Per to ι Aur (darkest 4 40 + 34), some darkness SW of ε Per (3 40 + 38), darker streaks E of ψ and χ Tau (4 30 + 29 and + 25), generally confirmed by A3. The Ross Atlas depicts the dark nebulosities — as do all other photographs e.g. of BARNARD and MAX WOLF — in all their intricate structural detail as extensive patches and streaks, almost devoid of stars, and partly filled with faint diffuse light. Our DM chart gives a somewhat smoothed picture of the density variations in this complex of nebulosities ; by its maxima of deficiency (cat 26—42) it determines their distance at 150 parsecs at most, the lower deficiencies between these peaks being due to a smaller density, not to a greater distance. The d.p. S of β Tau (5 16 + 25), in A3 connected with dark regions more E and S, in R separated in a N and a S d.p., corresponding with two maxima (cat 38, 39) > 50 in DM, belongs to the same complex. Also the d.r. W of m Tau (4 52 + 18), in R an irregular sequence of d.n. extending till S of α Tau, in DM a corresponding sequence of dark parts (cat 40, 41) decreasing to the W, are parts of it. The NW—SE d.f. E along β Tau — 1 Gem (5 16 + 31 to 5 50 + 25) shows in R a series of d.p*s* of which the strongest and most northern one (5 28 + 29), in DM > 40 (cat 37) belongs to the Taurus nebulae. Since A3 shows, for the more SE parts, the same decreasing intensity as DM, it is possible that these parts are its weaker extensions.

The d.f. $\varkappa$ Aur—η Gem (6 8 + 28), in R a d.str, visible also in A3, not distinct in DM, is probably remote. The d.f. W of $\xi\nu$ Ori (5 52 + 15), in R a weak irregular d.str. NS and in A3 a weak depression, is not visible in DM. The d.r. W of γ—ξ Gem — 15 Mon (6 30 + 12), in R a conspicuous irregularly curved d. marking, in A3 a distinct depression, is also missing in DM. These objects must be very remote. The d.r. S of α Ori (5 44 + 3), however, dark in A3, in R a mass of dark starless patches with luminous background, in DM a conspicuous spot (cat 45) > 40, hence a nearby d.n., may be either a far-outlying part of the Taurus complex, or is perhaps connected with the Orion nebula.

A d.p. NE of 18 Mon (6 52 + 4), also in A3, a d.p. also in R, shows a depression in DM, which, relative to the surround ings, may amount to 30. Another d.p. between 10—18 Mon (6 28 — 3), the beginning of a d.f., in A3 a d. spot, in R one of many dark patches, shows an analogous depression in DM. Possibly both markings are not more distant than 400. Here the information of A3 ceases. The broad, slightly dark cross-furrow S of 20 Mon (along — 6°), in R a series of weak d.ps, does not clearly show in DM. The d.p. NE of γ C Ma (7 8 — 12), in R a conspicuous streaky d.r., with d. streaks to the N, corresponding to a d.f. in MW (7 4 — 9), showing in DM > 10, *i.e.*,

relative to the surroundings, perhaps 30, may represent a not very remote d.n. (400). The same holds for the d.p. E of Sirius (6 50 — 16), in R visible as adjacent dark regions of a complicated structure, of which the visual MW may represent a strongly smoothed image. At the N border a d.p. N of 4 Pup (7 40 — 11), in R slightly darker than the surroundings, in DM a slight depression, finds its continuation where, along — 10°, the border region shows a darkening represented in DM by values > 20 and 30. The d.p. in the central band S of 107 Pup (7 32 — 18) and more NW, in R also a vague d.r., is hardly discernable in DM. The same holds for the d.p. NE of ϱ Pup (8 12 — 23), which is darker also in R. At the S border of the galactic light stream a d.f. E of τ C Ma (7 16 — 23 to 7 24 — 26), which in R is seen as a tortuous band of dark patches, the darkest at 7 24 — 25, corresponds to a depression > 10 in DM, which may be 30 relative to the surroundings. Another d.f. W of τ C Ma (7 4 — 21 to 7 12 — 25), in R a series of d.ps, shows at one place in DM a depression of the same amount. Since the narrow features may be smoothed in DM, they are probably not very remote. The complicated structure which R depicts SE of η C Ma cannot be followed further on because the Atlas ceases here.

The dark region between ζ and ξ Pup (centre 7 56 — 34) in our MW drawing, with irregular bands, corresponds in its central part to a depression > 10 (rel. perhaps 30) in DM; the darkest S part, a d. str. N along ξ—b—c Pup (7 52 —37), darker also in B, is not visible in DM. Nor do the darker places in the region ζ Pup—γ—λ Vel, though mostly traceable, albeit in different forms, in B, appear in DM; with the exception, however, of the d.p. SW of λ Vel (8 56 — 44), which is > 30 in DM, so this one may be a rather nearby d.n. The broad fissure interrupting the galactic light between γ—c and δ—M Vel, less conspicuous as an outstanding feature in B, appears as a weak and narrower depression in DM. In the MW pictures it is divided into a number of separate d.ps, but they do not correspond to notable deficiencies in DM at the same places. Farther to the E, at the N side of the galactic stream, d.ps N of K Vel (9 4 — 49), W of m Vel (9 32 — 46) and N of ϱ Vel (9 56 — 48), also traceable in the darker streaks in B, correspond to deficiencies > 20 in DM, and so may be not very remote. It is noteworthy that in the N border regions between 10^h and 12^h, — 35° and — 45°, notwithstanding their faintness, the parts most densely occupied by nearby dark nebulae are generally indicated as visually darker.

In the bright Carina region the d.p. E of J Vel (10 24 — 55), faintly discernible in B, is visible in DM as a depression of a reletive amount of 20; another d.p. W of u Car (10 40 — 58), clearly seen as an irregular dark mass in B, does not appear in the coloured map of DM, but is shown in a depression in the star numbers themselves of p. 62 at that place; both must be rather remote obscuring objects. Of the double d.p. E of π Cen (11 30 — 55), in B a faint d.p., and of the d.f. NE of o Cen (11 40 — 58), in B slightly more N, in DM hardly suspected as slight depressions, the same may be said. At the S side the bright Carina light is cut out by a conspicuous dark bay z Car—λ Cen (11 16 — 62), more complicated in B, in DM > 30 (cat 68), probably considerably higher relatively to the surroundings; so here we have a near dark object, not more remote than 200 pcs. Farther S is a d.r. SW of λ Cen (11 20 — 64), in B a group of d.ps, in DM also > 30 (cat. 69); probably connected with the former. Then comes the Coal Bag, S of β Cru (12 44 — 62), irregularly limited on the photographs and less far extending to the N than is shown on the drawings, in DM E of α Cru, still more S, > 40, (cat 74) which, relatively to the bright regions around, may be estimated at 60 — 70; hence the distance is < 150, in accordance with the results of Unsöld and Rolf Müller. A faint d.p. W of α Cru (12 10 — 62) also indicated in B and in DM, may be a weak extension of it. These nearby dark objects obscuring the bright galactic light at its S side may perhaps be considered as outlying parts of the Chamaeleon-Volans complex of nearby dark nebubae; narrow dark streaks visible in B may form a connection. This complex appears in B as black starless

regions, which partially coincide in MW drawings with regions indicated as darker in the faint border light. The indistinct darkness between ε and v Car (centre 8 40 — 62), not certain in B, distinct in DM, 30 — 40, may be a weak extension of it, as well as the large d.r. in the faint border δ Mus—γ Tr A (14 20 — 72), distinct in B, in DM partly coinciding with d.ps > 30. The faint d.ps $\alpha\beta\delta$ Mus (12 48 — 69) and E of η Mus (13 28 — 67), not distinct in B, corresponding in DM with deficiencies > 20, may also belong to it.

The faint fluctuations and patches in the light W and S of β—α Cen, partly recognizable in B, are absent from DM. Nor do the two d.ps SE of α Cen (14 52 — 62) and E of α Cir (14 52 — 64), in B combined into an irregular dark mass, show themselves in DM, so they are all due to remote objects. The weaker SE extension of the former, however, N of β Tr A (15 36 — 61), hardly discernable as a faint blackening in B, is very distinct in DM, > 30 and suggests a near d.n. The great d.p. N.E. of α Cen (14 48 — 58), visually the beginning of the great rift between the branches of the Milky Way, in B a corresponding large d.p. with numerous bright stars, in DM only at a small centre > 10, looks like a remote absorbing mass. Its continuation NE of γ Cir (15 30 — 55), in DM > 30, indicates a closer vicinity. The next d.p. S of η Nor (15 50 — 52), in B a d.p. intruding on the bright Norma cloud from the W, is only just below 0 in DM. The conspicuous cross-fissure bounding the Norma cloud to the N side, from γ Nor to 24 Ara (16 12 — 50 to 16 40 — 50), in B quite as distinct, appears in DM as part of a slightly depressed region > 10, hence must be a fairly remote d. mass. The adjacent small spot of deficiency > 40 in DM (cat 89) is not seen as a MW feature. Further S the d.p. at 16 48 — 47, a d.r. in B, is not shown in DM ; the d.p. N of α Ara (17 8 — 48), faintly indicated in B, is only > 10 in DM ; both may be remote features.

At the N side dark streaks in MW, in B represented by a more complicated system of narrow d. lanes, show better visible nodes SW of ε Cen (13 20 — 56), N of v Cen (14 16 — 53) and SW of ζ Lup (14 52 — 53), which can be recognized in d. features in B ; at nearly the same places DM has deficiencies > 20 or 30. The d.p. SE of ζ Cen (14 4 — 48) nearly coincides with a d.p. > 50 in DM (cat 83). The d.r. α Lup —η Cen (14 30 — 43), in B slightly darker than the surroundings, shows a deficiency > 40 in DM (cat 86). All these are due to d.n. at a small distance. The faintly d.p. π—ε Lup (15 8 — 46), about where B has slightly darker spots, extending farther E, DM has only > 20, but farther E is a spot > 30. The usually uncertain forms of these soft shades of intensity often do not correspond well to the DM features, although both, in a different way, can be identified with the more complicated photographic features. The d.r. E of φ Lup (15 30 — 36), in B an irregular black region extending from φ to χ Lup, is part of an extensive region of deficiency in DM, up to > 40 (cat 91). The weak d.p. on the extreme border near f Lup (15 16 — 31), in DM is > 60 (cat 92). So a complex of nearby nebulosities along the northern border of the galaxy in Centaurus and Lupus is visible here in the, generally faint, MW features.

What appars visually and on photographs as the great dark rift that, inclined to the central line, runs to the N from Lupus to the Scorpion's head, consists of a complicated structure of more or less dark streaks and patches, visually smoothed into mostly different forms. The d.f. from η Nor to the N, W along δ Nor (15 56 — 47 to — 42), in B a broad dark band, and the d.f. E along δ Nor (16 0 — 47 to 16 8 — 43), in B a narrow black streak broken up near δ Nor, appear in DM in a different arrangement, as dark spots > 40 and 50 (cat 87, 88). Here, however, the process of smoothing has played a part, for the original numbers (of p. 63) show that in the oblong d. spot E of δ Nor two places of strong deficiency, corresponding to the two fissures, have been combined under obliteration of the real structure. There can be no doubt that we have to do here with dark nebulosities at a small distance, 200 at most. The same holds for the d.p. E of ϑ Lup (16 8 — 37), part of what is in B a large d.r. extending to H—N Sco, in DM quite as large and > 50 (cat 94).

The d.p. W of ζ Sco (16 32 — 42), a d.p. also in B, is only > 20 in DM ; its less dark continuation S along this star is absent in DM. The two d.ps E of ζ Sco (16 52 — 42) and N of η Sco (17 4 — 41), both conspicuous in B and R, merge into one depression > 20 in DM. So it may seem that these features about the central line are due to more remote dark nebulae ; but the aspect in R, suggesting as it does nearby absorption, poses the question of whether rapid fluctuations in its density may have been smoothed in the star densities. Then comes the d.r. NW of λ Sco (17 24 — 35), in R a strongly black region, in DM divided into two parts > 30 and > 40 (cat 98). It is connected with the d.p. S of ε Sco (16 44 — 36) extending W of μ Sco, very black in R, in DM > 60 (cat 97). The photograph shows them as a broad dark stream, proceeding from the black regions SW of H—N Sco, breaking through the W branch between ε and μ Sco and crossing the central line towards the E branch. The corresponding great deficiencies in DM show this structure to be due to near obscuring matter. The continuation of the d. λ Sco r. as a less d.f. N along λ—$\varkappa$ Sco (17 32 — 37), less dark also in B and R, though in DM only a relative depression 10 — 20, may still belong to it.

A d.str. proceeding from the same d.r. to the N, W along d Oph (17 16 — 31), and the parallel d.f. E of Mess 6 (17 36 — 31), both clearly depicted in R, are missing in DM, where between the parallels of 30° and 33° stretches a surplus band. This discrepancy, although in the original densities two or three low values occur, is partly due, doubtless, to remaining systematic errors in the reduction to photometric scale. The d.p. SE of ϑ Oph (17 24 — 26), visually the blackest part of the Milky Way, as it also is in R, is in DM > 70 (cat 104), revealing the small distance of the d.n. Its extension to the W, strongly marked and black on the photographs, and to the N, into a less d.p. E of ξ Oph (17 20 — 21), continued N of 58 Oph, on the photographs a complicated mixture of dark and bright structures which generally confirms the drawing, appear as moderate deficiencies of 20 or 30 in DM, not always coinciding in place ; this may be no hindrance to considering them as thinner and more mixed absorbing structures at the same distance. The d.ps in the region N of Antares, one E of ϱ Oph (16 24 — 24) and the other E of χ Oph (16 24 — 19), well-known black, almost starless regions on the photographs, are > 60 in DM (cat 101, 102), hence the distance is below 150. The dark lanes emanating from the former towards the E, recorded also in the eye observations, are in the DM results smoothed down to > 20. The regions indicated as somewhat darker an MW drawings in the faint light of Ophiuchus, though highly uncertain, coincide partly with the darkest regions in R, *e.g.* W of σ Oph (17 10 + 5), S of μ Oph (17 28 — 9), W of η Ser (18 4 — 3), S of η Ser (18 10 — 7). The darkest parts in the more minute structure in R usually correspond to the strongest deficiencies in DM.

The dark spots in the Eastern galactic branch present greater difficulties, because owing to their smallness and rapid variations of intensity, which as a rule correspond to the photographic pictures, it cannot be decided whether the smaller deficiencies in DM are due to smoothing or to great distance. In some cases : the d.p. E of μ Sgr (18 12 — 21), a small one N of λ Sgr (18 20 — 25) and a d.p. E of cluster 9 Sgr intruding into the Large Cloud (18 4 — 25), DM shows values > 30 or 20. By projecting all the original density values of p. 63 upon the Ross photographs, some doubt may arise whether chance deviations do not play a rôle here, since the smallest values often occur outside the blackest parts which themselves show greater densities. At the W side of the central line, in the region of 58 Oph we find a general concordance as to detail ; here we are certainly in the realm of the nearby Ophiuchus nebulosities. The d.ps forming here the narrow separation of the two branches, are not shown in DM; only with the d.p. 18 0 — 13, in DM nearly 40, do we arrive in the Ophiuchus realm. The rich variety of galactic detail in the Eastern branch, not represented in DM, points to more remote nebulosities, say, beyond 500, which also single out some of the bright clouds as indicated by the greater values of the DM densities.

The d.p. S of the Scutum cloud (18 36 — 13), which separates it from the small 2H Sct cloud, in R a group of parallel black streaks, is only > 20 in DM ; still, it may be an offshoot though perhaps more remote, of the Ophiuchus nebulosities, since the darkest places coincide with streaks devoid of stars (10—11^m) on SCHÖNFELD'S map of the S. B. DM. The small d.p. about 4H Sct (18 36 — 9) intruding from the W into the Scutum cloud, and the narrow d.str. E of 3H Sct (18 31 — 8), not visible in the smoothed DM chart features, appear distinctly in the original numbers of p. 63. North of the Scutum cloud the DM indicates, by large deficiencies nearby absorptions. The small d.p. E of 6H Sct (18 44 — 5) is represented in DM by a darkness > 40 around this star (cat. 124). Its extension to the N, in R an irregular large d.p. (18 44 — 3), also clearly shown in A3, is not represented by small density values in DM, whereas the strong deficiency further E (cat 126) corresponds in R to a complicated structure of bright and slightly dark features, apparently full of stars, and not appearing dark to the eye. This discrepancy may be partly due to the transition from the N to the S part of the Bonn Durchmusterung at — 2°, with different systems of corrections. The d.ps S of *d* Aql (19 10 — 2) and around *e* Aql (19 24 — 4), in R a band of d.ps, in DM > 40 (cat 128), belong to the most Eastern parts of the Ophiuchus nebulae.